

People's Democratic Republic of Algeria
Ministry of Higher Education and Scientific Research
University 8 Mai 1945 Guelma



Faculty of Sciences and Technology
Department of Mechanical Engineering
Laboratory of Mechanics and Structures (LMS)

Thesis

Submitted in Candidacy for the Degree of *Doctorate in Third Cycle*

Field: Sciences and Technology **Stream:** Mechanical Engineering
Option: Mechanical Construction

Presented by

OUELAA Zakarya

Titled

***APPLICATION OF OBJECTIVE AND SUBJECTIVE METHODS FOR
THE DIAGNOSIS OF ROTATING MACHINE FAULTS: CONSTANT
AND VARIABLE REGIME***

Defended on: : 07 January 2024

In front of the Jury composed of

Name and first name	Position		
Mr. DJAMAA Mohamed Cherif	Pr	University 8 Mai 1945 Guelma	President
Mr. DJEBALA Abderrazek	Pr	University 8 Mai 1945 Guelma	Supervisor
Mr. YOUNES Ramdane	MC/A	University Larbi Tebessi Tebessa	Co-supervisor
Mr. CHAOUI Kamel	Pr	University Badji Mokhtar Annaba	Examiner
Mr. MOUSSAOUI Abdelkrim	Pr	University 8 Mai 1945 Guelma	Examiner
Mr. OUELAA Nouredine	Pr	University 8 Mai 1945 Guelma	Guest

Academic year: 2023/2024

«لا تحاول أن تصبح رجلا ناجحا

حاول أن تصبح رجلا ذا قيمة»

«Do not try to become a successful man.

Try to become a man of value ».

« N'essayez pas de devenir un homme qui a du succès.

Essayez de devenir un homme qui a de la valeur ».

Albert Einstein

Dedication

Dedication

I would like to dedicate this thesis:

To my beloved parents, for their unwavering dedication, support, and sacrifices throughout my studies. Your love and encouragement have been my pillars of strength.

To my inspiring siblings, extended family, and dear friends who have been a constant source of support and motivation.

To everyone who has shown unwavering support and belief in my abilities, thank you for being there every step of the way.

Acknowledgments/Gratitude

I would like to express my heartfelt gratitude to the following individuals and institutions for their invaluable support and contributions throughout the completion of this thesis:

First and foremost, I would like to extend my deepest appreciation to my supervisor **Pr. DJEBALA Abderrazek**, co-supervisor **Dr. YOUNES Ramdane** and **Pr. OUELAA Nouredine** for their guidance, expertise, and unwavering support. Their insightful feedback and encouragement have been instrumental in shaping the outcome of this research.

I would like to express my appreciation to all the members of jury: **Pr. CHAOUI Kamel** from the university of Annaba, **Pr. DJAMAA Mohamed Cherif** and **Pr. MOUSSAOUI Abdelkrim** from the university of Guelma.

I would also like to acknowledge the assistance and support provided by my colleagues and friends who have stood by me during this journey. Their discussions, feedback, and encouragement have been invaluable in overcoming challenges and reaching new heights.

Furthermore, I extend my thanks to the LMS staff, particularly **Mr. OURFELLA Rabah**, for the valuable insights, advice, and academic mentorship. Their contributions have greatly enriched my understanding of the subject matter.

I am deeply grateful to **Dr. BOUACHA Khaider** and **Pr. Charles PEZERAT** for providing the necessary resources, access to facilities, and research opportunities in the University of SoukAhras, Algeria and ENSIM, le Mans, France, that have enabled the successful completion of this thesis.

Lastly, I would like to express my appreciation to all the participants and individuals who generously volunteered their time and shared their expertise for the purpose of this study. Their contributions have been essential in gathering the necessary data and insights.

In conclusion, I am truly indebted to everyone who has supported me throughout this thesis journey. Your contributions, encouragement, and belief in my work have been invaluable, and I am immensely grateful for your presence in my life.

Résumé

L'objectif principal de cette thèse est le développement d'une démarche pour le diagnostic des défauts d'engrenages, tant en régime stationnaire qu'en celui variable. La méthodologie proposée est basée sur deux approches différentes mais complémentaires : une approche subjective basée sur la perception sonore et une approche objective basée sur l'analyse vibratoire. En effet, cette analyse permet de détecter les défauts et les anomalies en interprétant les signaux vibratoires, indépendamment des fluctuations de vitesse de rotation. L'analyse perceptive, quant à elle, se concentre sur l'identification des sons anormaux liés aux défauts des engrenages dans des conditions de fonctionnement en régime stationnaire et en régime variable. En combinant ces deux approches analytiques, nous pouvons obtenir des informations précieuses sur l'état de santé des machines tournantes afin de mettre en place des stratégies de maintenance efficaces permettant d'améliorer la fiabilité de ces machines dans divers scénarios opérationnels.

Après une revue et synthèse des références bibliographiques, le travail porte en premier lieu sur une étude comparative entre les méthodes objectives et subjectives pour identifier la gravité des défauts simples et multiples des engrenages à partir de signaux mesurés dans un environnement bruité. Cette analyse approfondie permet de mieux comprendre les forces et les faiblesses de chaque méthode et d'en proposer des recommandations pour leur application dans des situations réelles où les signaux sont bruités. De ce fait, cette contribution conduit à l'élargissement des connaissances sur les approches objectives et subjectives pour l'analyse des défauts d'engrenages. En deuxième lieu, une méthode hybride optimisée pour détecter les défauts d'engrenages dans des conditions non stationnaires a été proposée. Cette approche combine la méthode ICEEMDAN, le débruitage par ondelettes et l'analyse d'ordre. Les résultats démontrent l'efficacité de cette méthode pour détecter divers types de défauts d'engrenages dans différents modes de variation de vitesse de rotation.

Enfin, des tests perceptifs ont été réalisés à l'ENSIM, Le Mans, France, dans une chambre semi-anéchoïque pour simuler différents types de défauts d'engrenages. La particularité de ces tests est que les mesures ont été effectuées avec un régime de vitesse variable, comprenant des phases d'accélération, de maintien et de décélération. Cette approche permet d'évaluer la perception des défauts d'engrenages dans des conditions réalistes de fonctionnement. Les résultats de ces tests fournissent des informations précieuses sur la détection subjective des défauts d'engrenages dans des environnements dynamiques.

Mots clés : Approche objective, approche subjective, Perception sonore, Analyse multirésolution par ondelettes, Cyclostationnarité, ICEEMDAN, Analyse d'ordre.

Abstract

The main objective of this thesis is the development of an approach for diagnosing gear faults, both in steady-state and variable operating conditions. The proposed methodology is based on two different but complementary approaches: a subjective approach based on auditory perception and an objective approach based on vibration analysis. Indeed, this analysis allows for the detection of faults and anomalies by interpreting vibrational signals, independently of rotational speed fluctuations. The perceptual analysis, on the other hand, focuses on the identification of abnormal sounds related to gear faults in both steady-state and variable operating conditions. By combining these two analytical approaches, we can obtain valuable information about the health status of rotating machinery in order to implement effective maintenance strategies to improve the reliability of these machines in various operational scenarios.

After conducting a literature review and synthesis, the research primarily focuses on a comparative study between objective and subjective methods to identify the severity of single and multiple gear faults based on measured signals in a noisy environment. This in-depth analysis helps to better understand the strengths and weaknesses of each method and provides recommendations for their application in real scenarios with noisy signals. Consequently, this contribution leads to the expansion of knowledge regarding objective and subjective approaches for gear fault analysis.

Secondly, an optimized hybrid method for detecting gear faults under non-stationary conditions has been proposed. This approach combines the Improved Complete Ensemble Empirical Mode Decomposition with Adaptive Noise (ICEEMDAN), wavelet denoising, and order analysis. The results demonstrate the effectiveness of this method in detecting various types of gear faults under different rotational speed variation modes.

Finally, perceptual tests were conducted at ENSIM, Le Mans, France, in a semi-anechoic chamber to simulate various types of gear faults. What makes these tests unique is that measurements were taken under variable-speed conditions, including phases of acceleration, steady-state, and deceleration. This approach allows for the assessment of gear fault perception under realistic operating conditions. The results of these tests provide valuable insights into the subjective detection of gear faults in dynamic environments.

Keywords: Objective approach, subjective approach, Auditory perception, Wavelet multiresolution analysis, Cyclostationarity, ICEEMDAN, Order analysis.

ملخص

تهدف هذه الأطروحة أساساً إلى تطوير منهجية لتشخيص عيوب التروس، سواء في حالة سرعة دوران ثابتة أو متغيرة. وتعتمد المنهجية المقترحة على اتباع نهجين مختلفين ولكن متكاملين: نهج ذاتي أو شخصي يقوم على الإدراك الصوتي ونهج موضوعي يقوم على تحليل الاهتزازات. في الواقع، يمكن لهذا النوع من التحليل اكتشاف العيوب والأعطاب من خلال تفسير إشارات الاهتزاز بصورة مستقلة عن تقلبات سرعة الدوران بينما يركز التحليل الذاتي على تحديد الأصوات غير العادية المرتبطة بعيوب التروس في ظروف التشغيل الثابتة والمتغيرة. من خلال الجمع بين هذين النهجين التحليليين، يمكننا الحصول على معلومات قيمة حول الحالة الصحية للآلات الدوارة لتنفيذ استراتيجيات الصيانة الفعالة وتحسين موثوقية هذه الآلات في سيناريوهات تشغيل متنوعة.

بعد استعراض وتلخيص المراجع الببليوغرافية، يركز العمل في المقام الأول على دراسة مقارنة بين الأساليب الموضوعية والأساليب الذاتية لتحديد مدى خطورة العيوب البسيطة والمتعددة في التروس من خلال تحليل الإشارات المقاسة في بيئة ذات ضجيج (صاخبة). يتيح لنا هذا التحليل المعمق فهم نقاط القوة والضعف في كل طريقة وتقديم توصيات لتطبيقها في مواقع حقيقية حيث تكون الإشارات ذات ضجيج، مما يساهم في توسيع دائرة المعرفة بشأن النهج الموضوعي والنهج الذاتي في تحليل عيوب التروس.

في المرحلة الثانية، تم اقتراح طريقة هجينة محسنة للكشف عن عيوب التروس في ظروف عمل أين تكون سرعة الدوران غير ثابتة. تجمع هذه المنهجية بين تقنية تحليل الوضع التجريبي الكامل المحسنة بالتخلص من الضوضاء (ICEEMDAN)، وتقنية تقليل الضوضاء باستخدام الموجات فوق الصوتية، وتقنية تحليل الترتيب. تظهر النتائج فعالية هذه الطريقة في الكشف عن أنواع مختلفة من عيوب التروس في إوضاع مختلفة للتعديل في السرعة.

أخيراً، تم إجراء اختبارات الإدراك السمعي داخل غرفة شبه عازلة لتحكي مختلف أنواع عيوب التروس في المدرسة الوطنية العليا للمهندسين (ENSIM) المتواجدة في مدينة لومان بفرنسا. ما يميز هذه الاختبارات هو أن الأصوات التي تم الاستماع إليها تم إنتاجها على أساس الإشارات المقاسة تحت نظام سرعة متغير، يشمل فترات التسارع والاستقرار والتباطؤ. تسمح هذه المنهجية بتقييم كيفية إدراك عيوب التروس في ظروف تشغيل واقعية حيث أن نتائج هذه الاختبارات ستوفر معلومات قيمة حول الكشف الذاتي لعيوب التروس في بيئات ديناميكية.

الكلمات الرئيسية: النهج الموضوعي، النهج المحسوس، الإدراك السمعي، تحليل متعدد القرار باستخدام الموجات، التردد الدوري، ICEEMDAN، تحليل الترتيب.

List of figures

Chapter One

Figure 1.1. Different types of maintenance depending on time.....	5
Figure 1.2. Different analysis methods used in conditional maintenance.....	6
Figure 1.3. The three principles of vibration analysis.....	6
Figure 1.4. The different stages of industrial diagnosis.....	8
Figure 1.5. Vibratory response of a machine.....	9
Figure 1.6. Defect on the outer ring.....	10
Figure 1.7. The failure frequencies of bearing components.....	10
Figure 1.8. Worn gear.....	11
Figure 1.9. Extracted tooth.....	11
Figure 1.10. Deformation of teeth under overload.....	12
Figure 1.11. Corrosion.....	13
Figure 1.12. Scales of absolute evaluation.....	17

Chapter Two

Figure 2.1. Waterfall decomposition in three levels.....	39
Figure 2.2. Signal sum + its components (left).The IMF's representing mode mixing (right).....	42
Figure 2.3. Comparison between EMD (left) and EEMD (right).....	43
Figure 2.4. Comparison between EEMD (left) and CEEMDAN (right).....	44
Figure 2.5. Comparison between the number of iterations of EEMD (left) and CEEMDAN (right).....	44
Figure 2.6. Number of iterations obtained by the ICEEMDAN.....	45
Figure 2.7. Experimental setup.....	46
Figure 2.8. Simulated defects for three severities (a) Small defect, (b) Average defect, (c) Critical defect.....	48
Figure 2.9. The outlined methodology for the subjective approach.....	49
Figure 2.10. The outlined methodology for the objective approach.....	50
Figure 2.11. Perceptual space.....	53
Figure 2.12. Detail D2 and its corresponding envelope spectrum of the healthy case signal (S1) obtained after the application of OWMRA.....	53
Figure 2.13. Dispersion between the dimension (DIM1) and the scalar indicators.....	54
Figure 2.14. Dispersion between the dimension (DIM2) and the scalar indicators.....	55
Figure 2.15. Dimension 1 values for the 6 sounds.....	56

Figure 2.16. Dispersion between the dimension (DIM1) and the scalar indicators.....	57
Figure 2.17. Dimension DIM1 values for the 6 sounds.....	58
Figure 2.18. Perceptual space, S(i) obtained by sound perception and M(i) obtained by the mathematical model.....	58
Figure 2.19. Vibratory signals measured for different severity of gear defects (a) SDG2,(b)ADG2,(c)CDG2,(d)CDG2+SDG4,(e)CDG2+ADG4and,(f)CDG2+CDG4.....	59
Figure 2.20. Envelope spectra obtained from Optimized WMRA (a) SDG2, (b) ADG2, (c) CDG2, (d) CDG2+SDG4, (e) CDG2+ADG4 and (f) CDG2+CDG4.....	60
Figure 2.21. IMID spectra obtained by cyclostationary analysis (a) SDG2, (b) ADG2, (c) CDG2, (d) CDG2+SDG4, (e) CDG2+ADG4 and (f) CDG2+CDG4.....	62
Figure 2.22. Envelope spectra obtained from the ICEEMDAN-MVD hybrid method for (a) SDG2, (b) ADG2, (c) CDG2, (d) CDG2+SDG4, (e) CDG2+ADG4 and (f) CDG2+CDG4.....	63
 Chapter Three 	
Figure 3.1. Typical spectrum of an undamaged pair of gears.....	69
Figure 3.2. Spectrum in the case of small defect located on the gear turning at Fr2= 50 Hz.....	69
Figure 3.3. Signal of extracted tooth defect.....	70
Figure 3.4. Spectrum of an extracted tooth defect.....	71
Figure 3.5. Cepstrum in the case of extracted tooth defect.....	71
Figure 3.6. Envelope spectrum in the case of extracted tooth defect.....	72
Figure 3.7. Signal of extracted tooth defect measured in acceleration regime: (a) Pure signal and (b) rpm signal.....	72
Figure 3.8. Spectrum of the signal in the case of variable regime.....	73
Figure 3.9. (a) Cepstrum and (b) Envelope spectrum of the signal in the case of extracted tooth defect in variable regime.....	73
Figure 3.10. Global flowchart of the proposed method.....	76
Figure 3.11. Experimental setup.....	77
Figure 3.12. (a) Half-extracted tooth defect, (b) Extracted tooth defect, (c) Generalized defect.....	77
Figure 3.13. Kurtogam of the signal of extracted tooth defect.....	78
Figure 3.14. IMFs and corresponding spectra obtained after the application of ICEEMDAN.....	79
Figure 3.15. (a) Optimal IMF, (b) Denoised IMF, (c) Order envelope spectrum.....	80
Figure 3.16. Order envelope spectrum with the rpm signal of output shaft.....	81
Figure 3.17. (a) IMF7 signal, (b) Denoised IMF7, (c) Order envelope spectrum.....	82
Figure 3.18. (a) Signal of the extracted tooth in the case of deceleration mode (b) rpm	83

signal (c) Order envelope spectrum.....

Figure 3.19. (a) Original signal of extracted tooth defect (b) rpm signal (c) denoised IMF (d) Order envelope spectrum in combined mode..... 84

Figure 3.20. (a) Original signal of generalized defect (b) rpm signal (c) Denoised IMF (d) Order envelope spectrum in combined mode..... 85

Figure 3.21. (a) Original signal (b) rpm signal (c) order envelope spectrum in the case of half-extracted tooth in combined mode..... 86

Chapter Four

Figure 4.1. 3D accelerometer (B&K 4524B 33569) and the Pulse 16.1 vibration analyzer software..... 92

Figure 4.2. Sound Listening Tests in a Semi-Anechoic chamber 93

Figure 4.3. Learning Phase Interface..... 94

Figure 4.4. Scatter plot between measured and reconstructed similarities..... 94

Figure 4.5. Proximity space..... 95

Figure 4.6. Explanation of the proximity space 97

Figure 4.7. New representation of DIM2..... 98

Figure 4.8. Scatterplot between DIM1 and vibratory indicators..... 99

Figure 4.9. Scatter plot between DIM2 and vibration indicators..... 99

Figure 4.10. Sounds classified by the listeners (Si) and those calculated by the mathematical models (Mi)..... 100

Figure 4.11. Values of DIM1 for the 4 sounds..... 101

Figure 4.12. Spectrum of a healthy gear measured in the band [0-6400] Hz..... 103

Figure 4.13. Spectrum of a half-tooth spalling defect measured in the band [0-6400] Hz..... 105

Figure 4.14. Spectrum of gear showing generalized wear measured in the band [0-6400] Hz..... 106

Figure 4.15. Spectrum of a gear with a completely broken tooth measured in the band [0-6400] Hz..... 107

List of tables

Chapter Two

Table 2.1. Used gears and characteristic frequencies.....	47
Table 2.2. Experimental plan.....	47
Table 2.3. Mathematical expressions of the used scalar indicators.....	51
Table 2.4. Scalar indicators' values.....	52

Chapter Three

Table 3.1. Experimental plan.....	77
--	----

Chapter Four

Table 4.1. Various gear defects.....	93
Table 4.2. The various computed indicators for the four sounds, arranged in the order of personal pre-judgment.....	96
Table 4.3. The various computed indicators for the four sounds, arranged according to the judgments of the listeners (DIM1).....	97
Table 4.4. Belts characteristic.....	103

Table of contents

Dedication.....	iii
Acknowledgments.....	iv
Résumé.....	v
Abstract.....	vi
ملخص.....	vii
List of figure.....	viii
List of table.....	xi
Table of contents.....	xii
General introduction.....	1

Chapter One

General concepts and bibliographic synthesis

1. Introduction.....	3
2. Overview of Maintenance.....	4
3. Tools for Monitoring Faults in Rotating Machinery.....	5
3.1. Vibration Analysis.....	6
3.2. Thermal Monitoring.....	7
3.3. Oil Monitoring.....	7
3.4. Acoustic Monitoring Systems.....	7
4. The diagnosis and monitoring through vibration analysis.....	7
5. Common elements of different rotating machines.....	9
5.1. Relationship between the physical phenomenon and measurement.....	9
5.2. Bearings.....	9
5.2.1. Generation of vibrations in a defective bearing.....	9
5.3. Gears.....	11
6. Common causes of gear defects.....	12
7. Impact of a defect on the performance of a gear transmission system.....	13
8. Objective approach based on vibration analysis for the detection of gear defects.....	14
9. Subjective approach based on perceptive method for the evaluation gear defects.....	16
9.1. Estimation of magnitude.....	16
9.2. Absolute evaluation.....	16
9.3. Comparative evaluation.....	17
9.4. Categorization.....	17
9.5. Similarity measurement.....	17
9.6. Pairwise comparison.....	18
9.7. Dissimilarity experiment.....	18
10. Bibliographic synthesis.....	19

- 10.1. Objective approaches for the detection of gear defects in constant regime..... 19
- 10.2. Objective methods for variable-speed gear fault detection..... 23
- 10.3. Subjective methods for detecting gear defects..... 26
- 11. References..... 28

Chapter Two

Detecting gear defects in a noisy environment using objective and subjective approaches: case of steady-state regime

1.	Introduction.....	35
2.	Mathematical foundations of the subjective approach.....	35
2.1.	Sound perception tests.....	36
2.1.1.	Multi-dimensional scaling method.....	36
2.1.2.	The Bravais-Pearson correlation coefficient.....	36
2.1.3.	Determination of the number of dimensions.....	37
3.	Mathematical foundations of the objective approach.....	38
3.1.	Wavelet Multi-Resolution Analysis (WMRA)	38
3.2.	Cyclostationary analysis.....	39
3.3.	Improved CEEMDAN.....	40
4.	Experimental procedure.....	46
5.	Proposed methodology.....	48
6.	Results and discussion.....	50
6.1.	Analysis of the scalar indicators.....	50
6.2.	Results obtained by sound perception approach.....	52
6.2.1	Comparison of DIM1 obtained by sound perception and mathematical model.....	55
6.2.2	Improvement of the DIM1 mathematical model.....	56
6.3.	Results obtained by vibratory analysis.....	59
6.3.1	Results obtained by OWMRA.....	59
6.3.2.	Results obtained by cyclostationary analysis.....	61
6.3.3.	Results obtained by ICEEMDAN-MVD.....	62
7.	Conclusion.....	64
8.	References.....	65

Chapter Three

Detection of gear defects in variable regime using a new hybrid objective approach

1. Introduction.....	68
2. Gear faults detection in variable regime.....	68
3. Theoretical background.....	74
3.1 Multivariate denoising using wavelet and PCA analysis.....	74
3.2 Order tracking analysis.....	74
4. Proposed approach.....	75
5. Experimental procedure.....	76
6. Results and discussion.....	78
6.1. Case of extracted tooth in acceleration mode.....	78
6.1.1. Choice of the optimal frequency range.....	78
6.1.2 Improved CEEMDAN decomposition and selection of the relevant IMF....	78
6.1.3. Wavelet denoising and order tracking analysis.....	79
6.1.4. Case of non-appropriate rpm signal.....	80
6.1.5. Case of non-appropriate selection of the relevant IMF.....	81
6.2. Case of extracted tooth in deceleration mode.....	82
6.3. Case of extracted tooth in combined mode (Acceleration-steady state regime- deceleration).....	83
6.4. Case of generalized defect in combined mode.....	84
6.5. Case of half-extracted tooth in combined mode.....	85
6.6. Comments on the obtained results.....	86
7. Conclusion.....	87
8. References.....	88

Chapter Four

Application of the perceptive method for the identification of gear fault severities operating under variable conditions

1. Introduction.....	90
2. Experimental study.....	91

2.1. Introduction	91
2.2. Vibration measurements.....	91
2.3. Structure of the Listening System.....	93
2.4. Interface and test subjects.....	93
3. Results and Discussions	94
3.1. Analysis of results obtained by the perceptual method in variable operating conditions.....	95
3.2. Scalar indicators analysis.....	98
3.3. Correlations between scalar indicators and the two dimensions.....	98
4. Verification of DIM1 and DIM2 mathematical models.....	100
5. Faults diagnosis using ICEEMDAN.....	101
5.1. Introduction.....	101
5.2. Signal processing for the healthy state.....	101
5.3. Signal Processing for half-tooth spalling defect.....	104
5.4. Signal processing for generalized wear defect.....	105
5.5. Signal processing for a broken tooth defect.....	107
6. Conclusion.....	107
7. References.....	109
Chapter Five	111
General conclusion	

General introduction

Modern machines and industrial facilities are subject to increasingly diverse operational demands, varying in terms of rotation speed, duration, and efficiency. However, this heightened operational versatility comes with a significant drawback: these machines are constantly exposed to the risk of damage and unexpected failures, leading to costly and unplanned downtime. The economic implications of preventing such machine damage cannot be overstated for today's companies.

Human perception plays a crucial role in assessing the health of these machines. Humans rely on their five senses and memory to perceive and understand the world around them. When it comes to machines, these senses not only detect vibrations but also interpret the sounds generated during their operation. These sounds can serve as early fault indicators. Moreover, the field of vibration analysis has emerged as a fundamental tool in condition-based maintenance, with its effectiveness relying on the expertise of individuals who draw upon technical knowledge and professional experience.

Condition-based maintenance comprises two essential steps: monitoring and diagnosis. Monitoring involves periodic tracking of degradation indicators, while diagnosis employs advanced investigative techniques to determine the precise nature, severity, and urgency of any detected fault. However, traditional diagnostic methods pose a significant challenge when machines operate under variable conditions, requiring either the adaptation of existing techniques or the development of innovative approaches. Among these advancements, vibro-acoustics emerges as a promising discipline, exploring the perceptual impact of machine-generated sounds and their correlation with structural characteristics. Order analysis, which efficiently identifies faults in rotating machinery operating under variable conditions, is also a significant breakthrough in this context.

This thesis was developed with this intention, namely the development of both subjective and objective approaches for gear fault detection, a crucial element in several industrial systems.

The thesis is structured around five chapters:

The first chapter is dedicated to a literature review concerning various types of maintenance used by facilities for industrial machinery. This chapter explores fault detection methods in rotating

machines, with a focus on gears, by examining both objective approaches such as vibration signal analysis and subjective ones using sound perception. It highlights an emerging trend of combining these two approaches to enhance fault detection accuracy, thereby providing a more comprehensive understanding of the machine's health and maintenance strategies, while emphasizing the importance of introducing general concepts before delving into these topics.

The second chapter is dedicated to comparing two approaches for detecting gear faults in a highly noisy environment: a subjective approach based on sound perception through paired comparison tests, and an objective approach based on vibration analysis using three advanced signal processing methods. The work carried out in this chapter is purely experimental and was conducted on a test bench at the Mechanics and Structures Laboratory of the University of Guelma. The first part of the work aims to establish a correlation between the auditory perception of listeners and scalar indicators for different degrees of gear faults. The second part attempts to analyze the same signals using three well-known methods of vibration signal processing.

In the third chapter, a vibrational study is presented for identifying the severity of gear faults under variable operating conditions. These conditions are simulated on a test bench located at the University of Souk Ahras. To this end, an optimized hybrid method for gear fault detection is employed. This method combines ICEEMDAN to decompose the signals into Intrinsic Mode Functions (IMFs), identifies the fault signatures, and then applies multivariate wavelet denoising and Principal Component Analysis (PCA) to improve the signal-to-noise ratio. Subsequently, order tracking analysis eliminates speed variations and reveals an envelope order spectrum highlighting gear faults. This method is applied on various types of gear faults under multiple speed variation conditions, including acceleration, deceleration, and combinations thereof, surpassing conventional fault detection methods.

In the fourth chapter, we utilize a paired comparison sound technique by applying auditory perception to evaluate the severity levels of gear faults in changing operational scenarios. These simulated faults encompass both minor and major gear problems. After conducting listening tests in the semi-anechoic chamber at LAUM, Le Mans, France, we analyze the results to determine whether the auditory perception method can effectively distinguish between different degrees of gear faults under variable operation conditions.

Finally, the fifth chapter contains a general conclusion of the thesis as well as prospects for our future work.

Chapter one

General concepts and bibliographic synthesis

1. Introduction

The maintenance of industrial machinery and installations has become a key concern, both for companies' productivity and for the overall national economy. The role of the maintenance engineer is no longer limited to the detection of unexpected breakdowns but must also focus on proactive measures to anticipate them. This task is particularly critical in certain industrial sectors such as energy production (e.g., wind power) or in high-risk industries such as hydrocarbon and chemical facilities. In such sectors, an unexpected failure can result in significant material damage, environmental harm, and, most importantly, loss of human lives.

Monitoring and prediction are indeed the best means to anticipate such failures or at least reduce the probability of their occurrence. This can only be achieved through the use of reliable tools. In this regard, vibration monitoring and diagnostics have been the most widely used tool in the industry for several decades. Taking advantage of signal processing advancements, this field continues to evolve day by day.

Over the years, researchers have developed diagnostic methods, often tailored for specific faults in rotating machinery such as bearings and gears, enabling detection in the time domain, frequency domain, time-frequency domain, and so on. However, the majority of these methods were developed for steady-state operating conditions. In reality, we encounter machines and installations on a daily basis that operate under variable conditions. Under such operating conditions, monitoring and diagnosing such machines and installations using conventional methods is practically impossible.

In recent years, the necessity of monitoring this type of machinery has prompted researchers to work on two fronts: either adapting conventional methods to make them applicable in variable operating conditions, or designing new methods.

This chapter presents a comprehensive literature review on the utilization of both objective and subjective methods for detecting faults in rotating machinery, with a specific focus on

gears. In the objective approach, recent signal processing methods have been explored, particularly those employing time-frequency analysis techniques such as ICEEMDAN for steady-state operation and order analysis for variable operating conditions. These methods aim to extract relevant fault signatures from vibration signals and provide quantitative measurements for fault detection and diagnosis.

In addition to the objective methods, the subjective approach has gained attention, specifically in leveraging sound perception for fault detection. Although still in its nascent stage, this approach shows promising potential for detecting gear faults. By capturing and analyzing acoustic signals generated by the machinery, researchers have explored the use of sound-based indicators and perceptual features to identify the presence of defects.

Furthermore, the integration of objective and subjective approaches has emerged as a trend in fault detection research. By combining vibration analysis with sound perception, researchers aim to improve the accuracy and reliability of fault detection systems. This hybrid approach harnesses the strengths of both methods, providing a more comprehensive understanding of the machine's health condition and enabling effective early fault detection.

Overall, this chapter highlights the recent advancements in objective and subjective methods for fault detection in rotating machinery, shedding light on the potential of these approaches in improving the reliability and maintenance strategies of gear systems. Before all of this, general concepts about the field of maintenance, vibration analysis, and the different methods used should be presented first to facilitate understanding of the different parts of the thesis.

2. Overview of Maintenance

Maintenance is a crucial aspect in ensuring the reliability and lifespan of industrial equipment. It involves regular monitoring and repair of machinery to prevent unexpected breakdowns and enhance their performance. In general, maintenance is an important element in ensuring the proper functioning of industrial equipment and extending their lifespan. It can also help minimize unforeseen downtime costs and improve overall productivity. There are several types of maintenance: preventive maintenance that involves performing regular tasks to prevent failures and breakdowns. This can include regular inspections, performance testing, planned replacement of worn-out parts, corrective Maintenance is used to address issues that have already occurred. This can involve repairs following failures, replacement of damaged parts, and finally predictive Maintenance utilizes tools such as vibration analysis, thermal monitoring, oil analysis, etc., to detect potential problems before they cause significant damage or breakdowns.

These different types of maintenance can be used individually or in combination to ensure the reliability and lifespan of industrial equipment. The selection of the appropriate maintenance type depends on the specificities of each equipment and work environment (see figure 1.1).

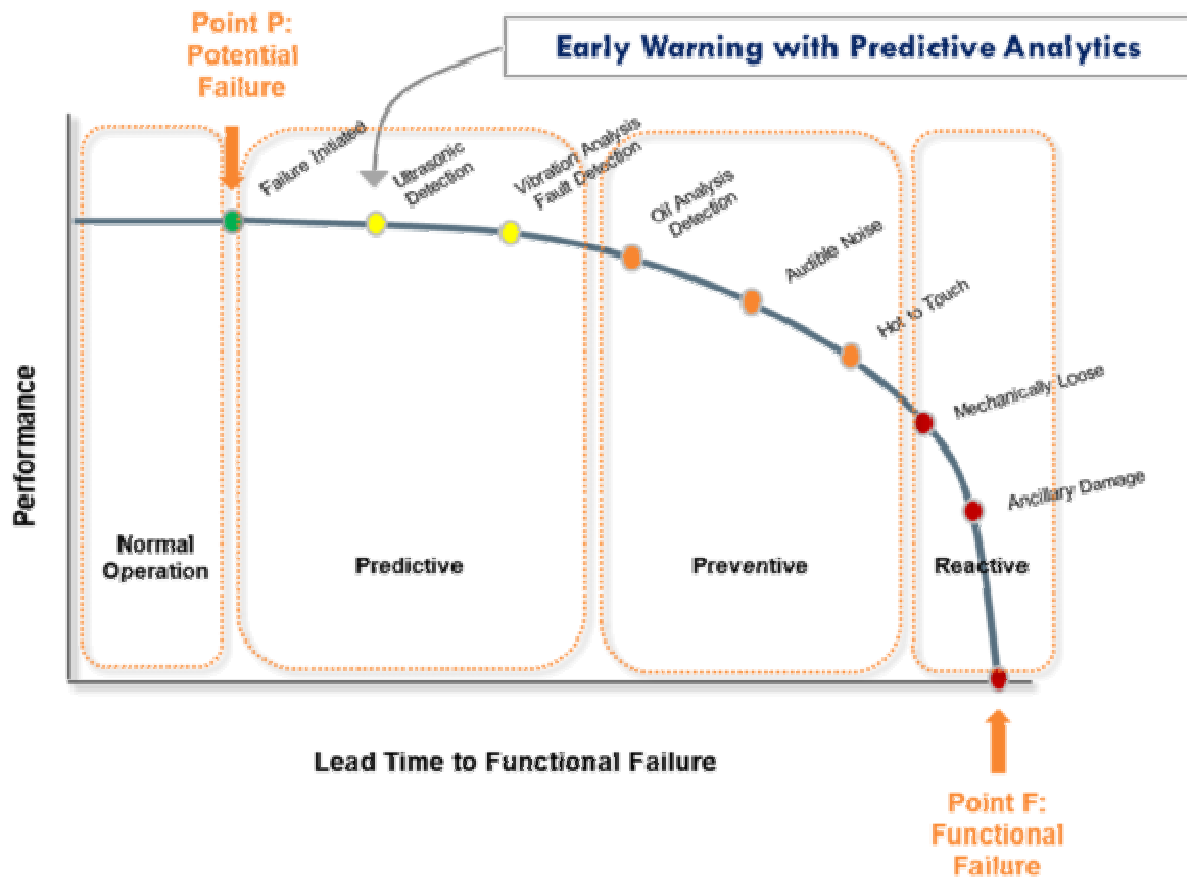


Figure 1.1. Different types of maintenance depending on time [1].

3. Tools for Monitoring Faults in Rotating Machinery

There are different analysis techniques used to monitor the degradation status or performance of machine components such as gears and bearings. These techniques include vibration analysis, acoustic emission, thermography, oil and lubricant analysis, variation in resistance in an electrical circuit, etc. Monitoring these indicators is performed periodically to ensure optimal equipment operation and prevent potential failures [2]. The figure (1.2) shows the utilization rate of these different techniques in the industrial environment.

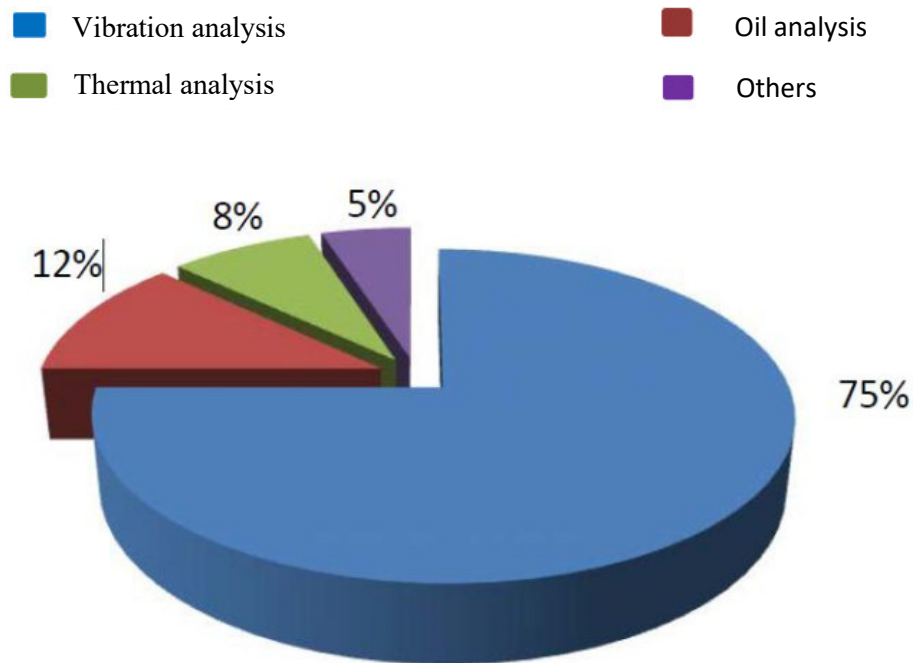


Figure 1.2. Different analysis methods used in conditional maintenance [2].

3.1. Vibration Analysis

Vibration analysis is a technique that measures and analyzes the vibrations produced by the movements of rotating machinery. It can help detect abnormalities in machine operation and prevent failures. The three principles of vibration analysis are summarized in figure (1.3).

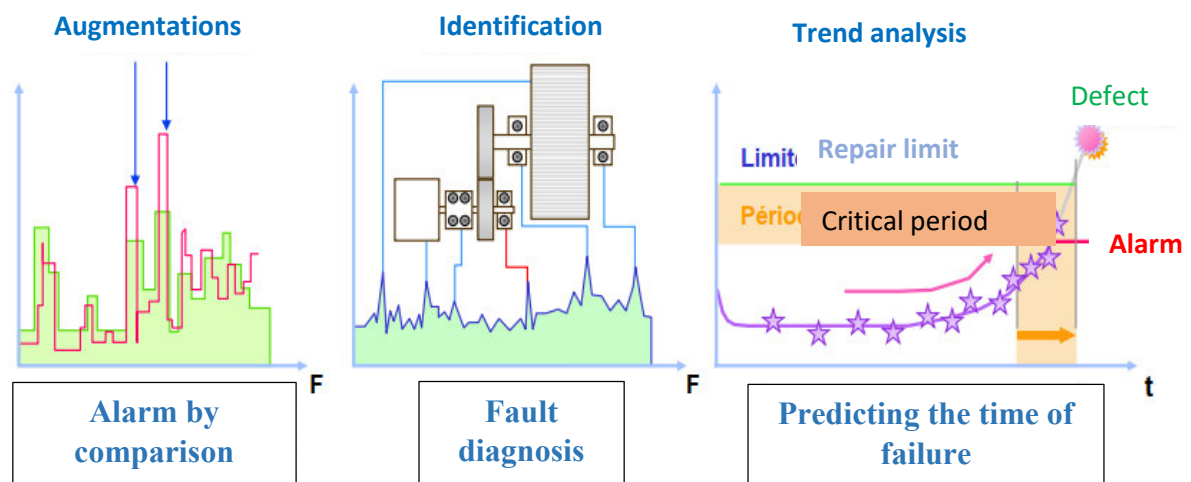


Figure 1.3. The three principles of vibration analysis [3].

The choice of the indicator used for monitoring the degradation status of a machine depends on the type of machine and the type of failure one wants to detect. For rotating machinery, vibration-based indicators are commonly used as they can detect most faults. A trend curve of

the indicator over time is established, and different thresholds corresponding to an alert level, an alarm level, and a failure level are defined. These thresholds are determined either through experience or by applying a standard. Vibration severity charts are used to define the different thresholds [2].

3.2. Thermal Monitoring

Thermal monitoring utilizes temperature sensors to measure the temperature of rotating equipment. It can help detect anomalies in machine operation, such as overheating, which may indicate potential failures.

3.3. Oil Monitoring

Oil monitoring utilizes oil analyzers to measure the properties of lubricating oil in rotating machinery. It can help detect anomalies in machine operation, such as contamination or oil equipment failures, which may indicate potential failures.

3.4. Acoustic Monitoring Systems

Acoustic monitoring systems use microphones to measure the sound level produced by rotating machinery. They can help detect anomalies in machine operation, such as abnormal noises, which may indicate potential failures. The use of these monitoring tools can help detect failures in rotating machinery at an early stage, allowing for timely repairs to be planned before a failure occurs and potentially damages the machine or causes production downtime.

4. The diagnosis and monitoring through vibration analysis

Vibration analysis is a technique used to diagnose and monitor the health status of machines. It involves measuring and analyzing the vibrations produced by the machine's movements. The interest of failure diagnosis in the industrial field lies in productivity gains and competitiveness of the sector, which depend on the essential control of production tool availability and the quality of goods or services provided. There are two essential tasks in diagnosis: observing failure symptoms and identifying the cause of failure using logical reasoning based on observations. The various technical stages of industrial diagnosis necessary for the design, development, and operation of diagnostic aid systems are summarized in figure (1.4).

The extraction of necessary information to form the characteristics associated with normal and abnormal operations is done through appropriate measurement means or observations conducted by surveillance personnel. There are two ways to estimate the physical quantity: either through direct measurement using sensors or through indirect measurement based on state estimators. The development of features and signatures associated with indicative symptoms of failures and degradation is carried out for the purpose of dysfunction detection. This decision-making process may lead to a shutdown of the installation if the consequences are significant. When dysfunction is detected, pre-alarm and alarm thresholds need to be set based on the measured deviation between the nominal signature and the measured one. To determine these thresholds, decision tests need to be defined.

Vibration analysis is an important tool for maintaining the health of machines and preventing breakdowns. Regular monitoring of machine vibrations is crucial for detecting anomalies and taking corrective measures before they cause significant damage.

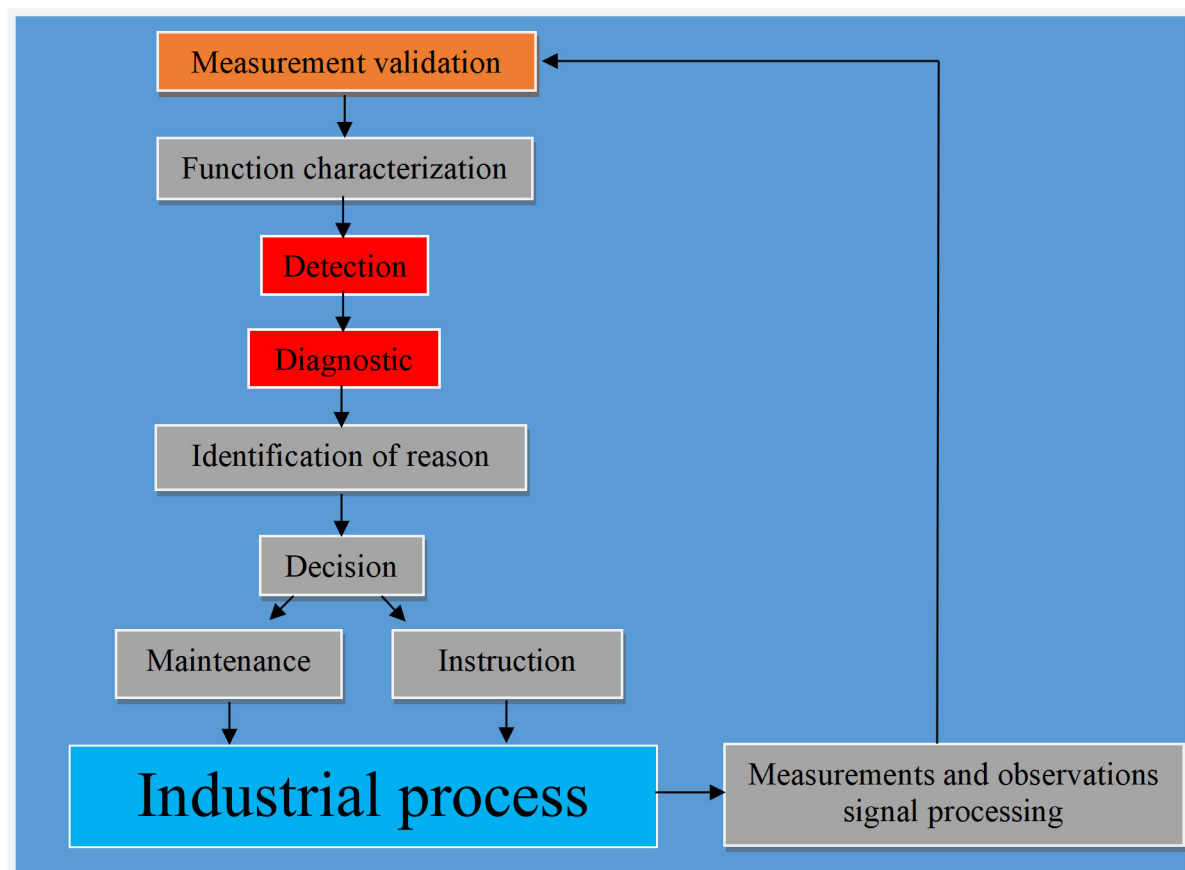


Figure 1.4. The different stages of industrial diagnosis.

5. Common elements of different rotating machines

5.1. Relationship between the physical phenomenon and measurement

The vibrations felt or measured on a machine are, in fact, the response of the structure to the sum of internal or external excitations (See Figure 1.5).

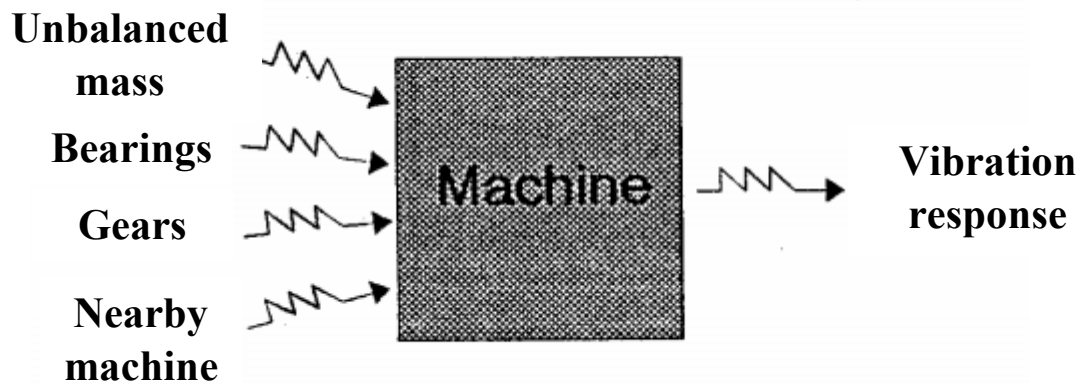


Figure 1.5. Vibratory response of a machine [4].

The measured signal is complex and rich in information. To simplify, we will focus on showing a few examples of diagnostics through vibrational analysis.

5.2. Bearings

Bearings and rolling elements have an estimated lifespan provided by the manufacturer, but this estimation is based on ideal load conditions. Factors such as contamination, misalignment, lubrication or mounting errors, and random overloads can alter the bearing's lifespan and cause unpredictable damage.

5.2.1. Generation of vibrations in a defective bearing

Let's consider an example of a defect on the outer ring of a bearing, which generates an impact when the ball passes over it. This impact creates a vibration that propagates through the bearing's outer ring and cage, which is referred to as an impulse. The phenomenon is illustrated in figure (1.6).

Impulses in machines are characterized by their steep rise and short duration. The typical frequencies of damage depend on the repetition of these impulses, while their amplitude depends on the rotational speed, mechanical clearances, the defect itself, and the load condition. The typical frequency of damage is influenced by the bearing's geometry and the shaft's rotation speed. The relationships between these different variables are depicted in

figure (1.7). Depending on the type of defect, there can be four typical impulse frequencies, with rise and pulse times in the range of a few tens of microseconds.

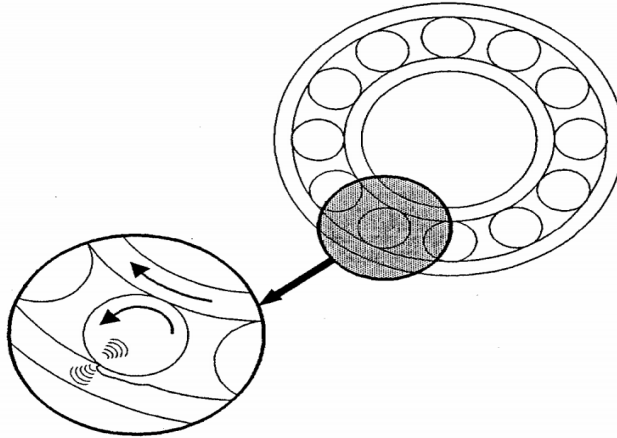
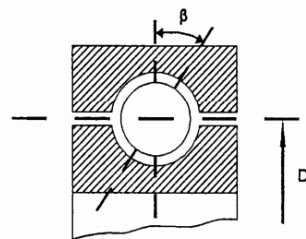


Figure 1.6. Defect on the outer ring.



β = Angle de contact
 d = Diamètre des billes
 D = Diamètre moyen du roulement
 n = Nombre de billes (ou de rouleaux)
 N = Vitesse de rotation de l'arbre

$$\text{Défaut sur bague externe} \quad f_e = \frac{n \cdot N}{2 \cdot 60} \cdot \left(1 - \frac{d}{D} \cdot \cos \beta\right)$$

$$\text{Défaut sur bague interne} \quad f_i = \frac{n \cdot N}{2 \cdot 60} \cdot \left(1 + \frac{d}{D} \cdot \cos \beta\right)$$

$$\text{Défaut sur bille} \quad f_b = \frac{D \cdot N}{d \cdot 60} \cdot \left(1 - \frac{d^2}{D^2} \cdot \cos^2 \beta\right)$$

$$\text{Défaut sur cage} \quad f_c = \frac{N}{2 \cdot 60} \cdot \left(1 - \frac{d}{D} \cdot \cos \beta\right)$$

Figure 1.7. The failure frequencies of bearing components [4].

In the case of multiple defects, there will be harmonics of the previously calculated frequencies. To determine these frequencies, it is necessary to have precise knowledge of the dimensional characteristics of the bearing.

5.3. Gears

Gears are mechanical components commonly used to transmit power and motion between parallel or intersecting axes. Gears typically consist of two toothed wheels, one called the "pinion" and the other the "gear," which mesh together to transfer force. During the initial operation of machines, gear running-in is an important process to eliminate surface imperfections and establish an optimal contact surface between the gear teeth. This process ensures efficient and smooth operation of gears with minimal noise and vibrations. However, other factors such as material quality, lubrication, alignment, etc., can also impact gear operation. Therefore, regular maintenance of gears is crucial to ensure their long-term proper functioning. Gears can have defects that can affect their operation. Common gear defects include:

- **Wear:** Gear teeth can wear over time, leading to poor engagement between the teeth. (See figure 1.8).



Figure 1.8. Worn gear.

- **Extracted Tooth:** Gear teeth can break due to impact or overload. (See figure 1.9).



Figure 1.9. Extracted tooth.

- **Deformation:** Gears can deform due to heat, overload, or torsion, leading to defects in tooth engagement. (See figure 1.10).



Figure 1.10. Deformation of teeth under overload.

- **Excessive backlash:** Excessive backlash between gear teeth can lead to premature wear and poor engagement.
- **Poor alignment:** If gears are not properly aligned, it can result in excessive wear, overheating, and premature failure. Therefore, it is important to take care of gears and maintain them regularly to avoid these defects.

6. Common causes of gear defects

Gear defects can be caused by various factors, including:

- **Overload:** Is one of the most common causes of gear defects. It occurs when the load applied to the gear exceeds its power transmission capacity. Overload can lead to the formation of cracks, pitting, or other types of defects.
- **Corrosion:** Is another common factor that can cause gear defects. It occurs when gears are exposed to corrosive environments, such as acids, bases, salts, or high humidity. Corrosion can lead to the formation of cracks, pitting, or other types of defects (See figure 1.11).



Figure 1.11. Corrosion.

- **Poor design:** Can also cause gear defects. This can include errors in geometric specifications, inappropriate material selection, or improper selection of operating conditions.
- **Fatigue:** Can also cause gear defects. It occurs when gears are subjected to repeated cyclic loads and can result in the formation of cracks.
- **Improper assembly:** This can include misalignment of shafts, inappropriate mounting tensions, or incorrect installation of gears.

7. Impact of a defect on the performance of a gear transmission system

Gear defects can have serious consequences for the operation of mechanical systems, including:

- **Reduction in gear lifespan:** Gear defects can significantly reduce the lifespan of gears. They can lead to the formation of cracks that can propagate over time and result in gear failure.
- **Deterioration of power transmission quality:** Gear defects can also lead to a deterioration in the quality of power transmission. This can result in vibrations, noise, or improper movements, which can cause damage to other components of the mechanical system.
- **Increase in energy consumption:** This can occur when gears are subjected to additional loads to compensate for the defects, which can result in overheating and increased energy consumption.
- **Reduction in reliability :** Gear defects can also reduce the reliability of mechanical systems. This can lead to unexpected downtime, additional costs for repairs, and a decrease in productivity.
- **Damage to adjacent components:** Such as bearings, shafts, and housings.

8. Objective approach based on vibration analysis for the detection of gear defects

Vibration analysis is a widely used monitoring technique for mechanical components and industrial machines in operation. It can detect most faults that may occur in rotating machinery, such as misalignments, imbalances, cracks, bearing defects and lubrication problems. Sensors are used to measure the vibration and resonance frequencies of the machine to detect anomalies and changes in vibration levels. The collected data is then analyzed to determine the health of the machine and plan necessary maintenance. Vibration analysis is widely used in many industries to optimize equipment availability and reliability. [2]. Indeed, various calculated parameters are used in either the time domain, frequency domain, or both, for this purpose.

There are several signal processing techniques that can be utilized to diagnose gear faults. Here are some examples:

- **Fourier Transform:** Is a commonly used technique to convert a time-domain signal into a frequency-domain signal. This allows for the analysis of the distribution of vibrational energy in the frequency domain and the determination of predominant frequencies associated with gear faults.
- **Frequency Response Function (FRF) Analysis:** Measures the vibratory responses of gears at different excitation frequencies and helps determine resonance frequencies associated with gear faults.
- **Spectral Envelope Analysis (SEA):** Allows for visualizing the distribution of vibrational energy over time and can be used to identify gear faults.
- **Cepstral Analysis:** Utilizes an inverse Fourier transformation to convert a frequency-domain signal into a time-domain signal. By employing these signal processing techniques, it is possible to accurately diagnose gear faults and take the necessary measures to address them.

There are other highly effective signal processing techniques for diagnosing gear defects.

Here are a few more examples :

- **Wavelet Analysis:** It is a time-frequency method that separates a time-domain signal into different frequency components. Two versions of wavelet analysis have been widely used for the detection gear defects, the Continuous Wavelet Transform (CWT) and Discrete Wavelet Transform (DWT) still called Wavelet Multi-Resolution Analysis (WMRA).

- **Impact Frequency Analysis (IF):** Measures the vibrations caused by impacts between gear teeth and can be used to detect defects such as shape defects and surface defects.
- **Structural Defect Models (SDA):** Are based on numerical simulation of gear vibrations and can be used to diagnose gear defects by comparing simulation results with actual vibration measurements.
- **Correlation Analysis:** Measures the similarity between vibrational signals measured at different positions on gears and can be used to detect gear defects such as excessive backlash and surface defects.
- **EMD and its derivatives:** Its family are indeed signal processing techniques that can be used to diagnose gear faults. EMD is a non-linear decomposition technique that separates a signal into several empirical modes, each representing a specific component of the signal. The EMD family also includes techniques such as EEMD (Ensemble Empirical Mode Decomposition Improved), CEEMD (Complete Ensemble Empirical Mode Decomposition), and DEEMD (Detrended Empirical Mode Decomposition). These techniques are based on EMD and are designed to handle noisy data and trends present in vibrational signals.

CEEMDAN (Complete Ensemble Empirical Mode Decomposition with Adaptive Noise) and ICEEMDAN (Improved Complete Ensemble Empirical Mode Decomposition with Adaptive Noise) are also signal processing techniques that can be used to diagnose gear faults. CEEMDAN and ICEEMDAN employ an ensemble approach to decompose the signal into multiple empirical modes, with adaptive noise estimation to enhance the quality of the decomposition. CEEMDAN utilizes a multi-modal decomposition approach to produce a series of empirical modes, while ICEEMDAN employs an iterative approach to improve the quality of the decomposition.

EMD and its derivatives can be used to diagnose gear faults by isolating the frequency components associated with the faults and comparing them to vibration standards for gears in good working condition. The results from CEEMDAN and ICEEMDAN can also be used to visualize vibrations over time and identify periods of abnormal vibrations that may be associated with gear faults.

By using a combination of these signal processing techniques, it is possible to obtain a comprehensive picture of gear faults and take the necessary measures to correct them.

9. Subjective approach based on perceptive method for the evaluation gear defects

Perceptive tests are used to evaluate the sound quality of a prototype, compare it to competing models, or generally identify the sound dimensions (such as aspects of timbre) involved in the perception of noise produced by a specific object type. Several methods are available, each characterized by its own implementation methodology and providing specific results.

The use of paired comparison tests allows for assessing preferences or annoyance levels related to a particular noise. Additionally, dissimilarity tests compare different sounds to establish a perceptual space with one or multiple dimensions through principal component analysis (PCA). The connection with physics is then established by seeking correlations between the test results and a scalar indicator or a combination of scalar indicators calculated from these signals.

9.1. Estimation of magnitude

This method has been widely used for estimating the level of noise. Its principle is to directly ask the listener to assign a value proportional to their sensation. It is possible to present the listener with a reference stimulus to which an imposed reference value is assigned. This results in a scale of sensation ratios. However, this method is rarely used for real sounds.

9.2. Absolute evaluation

The listener is required to provide an evaluation of the sound characteristics, and responses to specific questions are performed on a MATLAB interface, as shown in figure (1.12). The response for each sound, represented by numbers on a scale from 0 to 1, depends on the judgment of the listeners, ranging from very similar to very dissimilar, respectively. Analysis of variance methods are then used to assess the significance of differences between the average values of each sound [5].

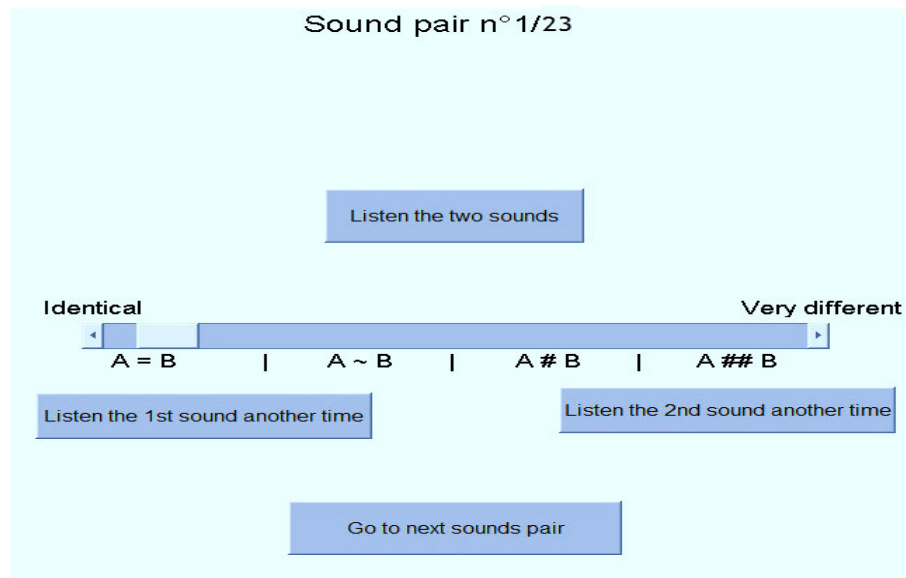


Figure 1.12 Scales of absolute evaluation.

9.3. Comparative evaluation

This method combines both the principles of evaluation and comparison. The listener must listen to the sounds as many times as they want before providing a response. This method is faster than pairwise comparison and more precise than absolute evaluation. However, the results of this method may correspond to an ordering of the sounds rather than a direct comparison.

9.4. Categorization

The principle consists of asking the listener to group the sounds into categories based on their perceived similarities in relation to the tested characteristic. If two sounds are classified in the same category, they are assigned a 1; if they have never been classified together, they are assigned a 0. This allows us to create a matrix called "pseudo-distances" that helps determine groups of sounds with similar characteristics. The great advantage of this method is that it allows us to select a few sounds that best represent the entire set of stimuli on which more detailed studies can be conducted.

9.5. Similarity measurement

Multidimensional Proximity Analysis, also known as similarity measurement, aims to represent estimated dissimilarities (similarities) between stimuli by distances between these stimuli represented as points in a multidimensional space. These points will be further apart in the space if the corresponding stimuli were perceived as more dissimilar [6]. This space

allows for exploring the number and nature of the dimensions underlying the estimations of dissimilarities.

9.6. Pairwise comparison

This method involves comparing two stimuli and indicating which one is preferred, which is easier than evaluating each of them separately due to the limited capacity of auditory memory. Initially, the listener must listen to all the sounds under study. In practice, for N sounds, the number of pairs corresponding to the upper triangular matrix is $N*(N-1)/2$. Generally, listeners perform their task with seriousness, which reduces the extent of this risk. Therefore, it is preferable to allow the response "the two sounds are equivalent," making the test more comfortable for the listener [7].

The order of presentation of pairs should ensure that two consecutive appearances of the same sound are as far apart as possible. This is because if all the sounds were successively compared to one of them, specific characteristics of that sound could gain excessive importance and influence the responses. Techniques exist to construct sequences of pairs that satisfy these conditions. The idea is to randomly permute the order of sounds for each listener before constructing the sequence of pairs.

The responses of the listeners are coded numerically as either 0 or 1. The first step of analysis involves calculating the number of circular errors made by each listener. One limitation of the pairwise comparison method is the number of stimuli, as N sounds result in a minimum of $N*(N-1)/2$ pairs. For example, with 15 sounds, this represents 105 pairs. If each sample has a duration of six seconds, the minimum listening duration would exceed 35 minutes, which is very long for a listener and carries the risk of lower quality responses [6].

9.7. Dissimilarity experiment

The proximity data collected can be obtained from different types of judgments. We distinguish direct judgments, ordered judgments [8], triadic judgments [9-10], and tetradic judgments [11]. Here, we will only focus on the direct judgments used in our experiments. The listener must judge the degree of dissimilarity for each pair in a set of stimuli. The term "dissimilarity experiment" is generally used for this type of protocol. In these types of studies, the listener typically has no other task than to evaluate the dissimilarity between pairs of objects. Specifically, no instructions are given to pay attention to specific attributes that may characterize the stimuli, except, for example, in cases of comparisons between countries,

which can be judged based on a large number of criteria. The data is then collected and organized into a matrix, which can be triangular if only proximities are considered, or complete if both symmetrical proximities are also collected. In the latter case, since the values provided by the subjects will generally differ from each other, these differences will be treated as noise in the data, which can be ignored by averaging the proximities and . This dissimilarity matrix will then serve as input for multidimensional analysis programs [12].

10. Bibliographic synthesis

10.1. Objective approaches for the detection of gear defects in constant regime

Gearbox is a vital element in any power transmission system on rotating machine especially for important torque. It is used to transfer the motion by increasing or decreasing the rotation speed in several systems, such as vehicles, machine-tools, wind turbines, etc.

Vibratory analysis using several signal processing methods is the most popular approach widely used in condition monitoring and diagnosis procedures. In literature, there are many works in this respect where authors used different signal processing methods, online or offline, on rotating machines to identify specific mechanical defects generating mainly impulsive forces. To avoid unscheduled shutdown of the gearbox, there is always continues need for a reliable diagnosis method to detect the defect in its early stage. The classical methods are mainly based on spectrum or cepstrum analyses.

In the frequency domain, spectrum analysis is known as the basic and oldest method. When the defect size grows, the amplitude of the meshing frequency increases. Moreover, in this case a modulation phenomenon occurs, characterized by sidebands around the meshing frequency spaced by the rotation frequency of the shaft carrying the defective gear [13]. In some cases, these sidebands are not clearly visible on the spectrum, using cepstrum analysis is then necessary. This method consists of calculating a vector, named the cepstrum, which represents the inverse Fourier transform of the spectrum logarithm. Many applications of this approach have been widely used [14-16].

Cousinard et al. [15] conducted a study to evaluate two diagnostic methods, namely cepstral analysis and envelope analysis, to detect damage on the teeth of gears operating at low speeds. They used an accelerometer placed on the housing of a gear reducer in a paper mill consisting of four sets of 91-tooth cylindrical wheels with a diameter of 1.5 m, driven by a gear train of 51 teeth each one. By comparing the cepstra and the envelope spectra measured in the radial, horizontal and axial directions for different measurement points, they were able to identify

the origin of the failure. The results show that the two methods are effective for the detection of this type of defect, providing a finesse of analysis which makes it possible to obtain an accurate diagnosis. In addition, envelope analysis has proven to be a complementary technique to cepstral analysis, which is penalized by its high sensitivity to noise and random speed fluctuations.

Since these methods are limited and not adaptable to analyze transient phenomena, time-frequency approaches are developed and favored to use in gear defect detection. The wavelet analysis is undoubtedly the most popular time-frequency method applied in rotating machine faults detection, especially rolling bearing and gear defects. Djebala et al. [17] presented a study based on the parametric optimization of Wavelet Multi-Resolution Analysis (WMRA) to identify rolling bearing defects. The kurtosis was used as an optimization and evaluation criterion. The experimental results show the reliability of this method in the detection of different types of bearing defects. Also, it was used in the literature for gear defects diagnosis in its continuous or discrete versions [18-21]. Moreover, the authors found that the application of the WMRA on pass-band filtered signals gives better results than its application on wide-band or the use of simple pass-band filtered signals. This optimized WMRA was successfully applied to detect simple and combined gear defects in [16]. Chiementin et al. [22] proposed a new wavelet shape adapted to shock signals, with a methodology of reducing the computing time, which is demodulation by a semi-wavelet. The importance of this semi-wavelet lies in a better representation of the signal and its instantaneous use. Three methods are applied, two classical wavelet methods and half-wavelet demodulation. The latter has a particularity that could detect multiple defects on the same ring thanks to its better resolution due to its shape and reduced computing time. On the other hand, the classical methods can only detect one defect with a significant computation time.

In more recent work [23], the kurtosis and the entropy were compared to a new index to detect rolling bearing and gear defects. Theoretical and experimental results show that the proposed index is less affected by impulsive noise, can detect incipient defects, and provide monotonic trending for bearing and gear degradation assessment much better than kurtosis and negative entropy.

Bouzouane et al. have developed a method for monitoring and diagnosing faults in rotating machines that can be integrated into a maintenance program. They used two types of wavelet transformation, namely discrete by Daubechies wavelet and continuous by Morlet wavelet, to

implement this method in real cases. The signals were measured on a test bench on which two types of fault were simulated: the first caused by an imbalance and the second by a fault in meshing. The results obtained indicate that the multi-resolution method (using Daubechies wavelet) is more appropriate for the identification and tracking of unbalance, while the continuous transform (using Morlet wavelet) is better suited to the analysis of non-stationary signals, such as those generated by a defect on the gear tooth [24].

A significant advance in the vibration diagnosis of rotating machines is undoubtedly using reliable periodic methods based on cyclostationarity and separating the cyclic component from the signal [25-26]. Among these methods, the cyclostationarity formulation has several advantages for analyzing such signals compared to conventional approaches. It allows understanding a wide range of behaviors with the same tools, from simple deterministic periodicity to non-stationary randomness [27-28]. Second, it explicitly integrates a temporal dimension that allows following non-stationarity in the systems under study. Third, this analysis enables discovering the amplitude modulations present in the vibration signals [29-30]. This modulation varies depending on the signal components, which can often provide valuable data.

Urbanek et al. [31-32] reported that the Modulation Intensity Distribution (MID) returns information similar to spectral correlation density. The authors proved that the Integration of the Modulation Intensity Distribution (IMID) is the optimal method for detecting the secondary component of cyclostationarity in the vibration signal. Recently, Kebabsa et al. [33-34] used the cyclostationarity method to diagnose a turboalternator and a turbofan in an industrial environment, respectively. Their study highlighted, with great efficiency, various defects such as friction and oil swirl defects in the plain bearings, blade defects, and generalized wear on the reducer's gears. It was also possible to highlight all the modulations in the signals measured in low and high frequencies based on the MID and IMID.

Babouri et al. [35] also used cyclostationarity in a comparative study with other signal processing methods on vibratory signals measured either on an experimental setup or in an industrial environment. Statistical analysis, FFT, envelope analysis, and some time-frequency methods such as Wavelet Multi-Resolution Analysis (WMRA) were used in this work. The results show that these methods have significant limitations when analyzing non-stationary and non-linear signals and confirm the ability of cyclostationarity to diagnose real mechanical defects in an industrial environment. Assaad et al. [36] used a technique to process a cyclostationary signal from a planetary motion transmission gearbox composed of multi-stage

gears. The authors used the first-order cyclostationarity to synchronize the average of the vibration signal, which allows defect location. A combination of cyclostationarity and autoregressive modeling is used to increase the detection and diagnostic capability.

Huang et al. [37] proposed a new method under the name of Empirical Mode Decomposition (EMD). Contrary to wavelet analysis, the EMD does not need analyzing wavelet mother, the signal is decomposed by itself using an adaptive decomposition method. The EMD has been widely used for rolling bearing and gear fault detection [38-40]. It has been also combined with other signal processing tools to provide robust hybrid methods as the wavelet multi-resolution analysis in [41].

Note that EMD and AMRO have proven their effectiveness in other applications, besides fault diagnosis. Babouri et al. combined AMRO and EMD to track and monitor cutting tool wear during the turning of a steel part without lubrication. These vibrational signals were measured under different cutting speed, depth of cut, and feed configurations using a carbide tool (TiCN/Al₂O₃/TiN). The results obtained demonstrate that the proposed hybrid method allows for optimization and meaningful evaluation of the cutting tool's wear condition, surpassing what can be achieved by applying AMRO and EMD separately. [42].

Even with its reliability in fault detection, this method has faced the mode mixing problem, where different scales may be consisted in one Intrinsic Mode Function (IMF), which could lead to false diagnostics. To solve this problem a new version of the EMD is proposed, the Ensemble Empirical Mode Decomposition (EEMD) [43]. The EEMD is a noise-assisted data analysis, it consists in adding a white noise to the signal and calculating an ensemble of trials using the original EMD, and the mean of the result of each ensemble represents the true IMF. Unfortunately, the provided solution causes more computing time. Even with that, the EEMD has been used for the detection of rolling bearing defects [44-46], and gear defects [47-49]. The EEMD has also another limitation concerning the residue of the added white noise that still exists in the new reconstructed components from the IMFs even after applying the averaging process.

To overcome this limitation, a new algorithm called Complete Ensemble EMD with Adaptive Noise (CEEMDAN) was presented by Torres et al. [50]. It provides a complete decomposition with numerically negligible error. This proposed method is a very recent signal decomposition technique that has been applied on the first time on biomedical signal (ECG), where the results gave better spectral separation of mode function. Many authors have discovered that the CEEMDAN could be successfully implemented in monitoring and

machine fault diagnosis [51-54]. Xiao et al. [55] show the efficiency of combining CEEMDAN with Teager Energy Operator for bearing fault diagnosis. CEEMDAN is used to decompose the signal and reduce the noise, and according to the correlation coefficient criterion the most sensitive component is selected and its Teager energy operator is calculated to extract the fault. In the same context, an energy weighting method based on time-frequency spectrum analysis is proposed to extract weak impact features under strong noise background [56]. Sometimes, combining two methods may give us more information about the defect, as in the work of Dong et al. [57] to extract rolling bearing defects using the CEEMDAN and Multi-scale Fuzzy Entropy (MFE).

Trying to improve the CEEMDAN and recover its shortcomings, Colominas et al. [58] proposed the improved version of the complete ensemble EMD with adaptive noise (ICEEMDAN). Several real biomedical signals are treated, the results show that the obtained components have less noise and more physical meaning. However, the ICEEMDAN is only in its first applications in the field of fault detection in rotating machines [59-61].

10.2. Objective methods for variable-speed gear fault detection

Unfortunately, most of these methods are not useful to analyze variable signals. The need to monitor machines working in variable condition (speed, load) leads researchers to adapt classical methods to the variable regime or developing new ones. Several researches have been made for rolling bearing and gear defects in variable regime [62-65], however their number remains far lower than that of the constant regime.

The article proposed by Nguyen Trong Du [66], based on a new method for detecting gear faults in gearboxes operated in non-stationary conditions without the need for a tachometer. The method is based on variable sideband analysis (VSA) of the gearbox vibration signals. The VSA method involves extracting the sidebands of the gearbox vibration signal using the Hilbert transform and then analyzing their amplitude and frequency variations over time.

The proposed method is evaluated using simulation data and experimental data collected from a gearbox operated in non-stationary conditions. The results show that the method can effectively detect gear faults even in the absence of a tachometer. The method is also shown to be robust to changes in operating conditions, such as changes in load and speed. The authors conclude that the proposed method has the potential to improve gear fault detection in gearboxes operated in non-stationary conditions, which can lead to more effective maintenance and increased machine reliability.

The article proposes a new method for diagnosing planetary gearbox faults under variable speed conditions. The method is based on the scaling operator demodulation spectrum (SODS), which is used to analyze the vibration signals of the gearbox. The SODS method involves decomposing the vibration signals into different frequency bands using the continuous wavelet transform (CWT), and then calculating the SODS of each band.

Dezun Zhao et al. [67] are introduced a new method to diagnose faults in planetary gearboxes that operate under varying speeds. The method relies on the scaling operator demodulation spectrum (SODS) to analyze the gearbox's vibration signals. This involves decomposing the signals into various frequency bands using continuous wavelet transform (CWT) and computing SODS for each band.

To evaluate the method's effectiveness, the authors used both simulated and experimental data from a planetary gearbox operating under variable speed conditions. Results indicate that the proposed method can detect different types of gearbox faults, including gear tooth breakage and wear, with a high degree of accuracy. Moreover, the method shows resilience to changes in load and speed. Based on these findings, the authors suggest that the proposed approach can significantly enhance the diagnosis of planetary gearbox faults under variable speed conditions. This, in turn, can lead to more efficient maintenance practices and improved machine reliability.

Farhat et al. [68] presents a numerical model developed to analyze the behavior of a single stage gearbox operating under variable operating conditions. The study focuses on capturing the effects of changing speeds and loads on the gearbox performance.

They start by providing an overview of the importance of studying gearboxes operating in variable regimes, highlighting the challenges and the need for accurate modeling and analysis techniques. They emphasize that conventional models and methods designed for steady-state conditions may not be suitable for capturing the dynamic behavior of gearboxes under variable regimes.

The numerical model presented in the article is based on mathematical equations and algorithms that account for the dynamic behavior of the gearbox components, including gears, bearings, and shafts. The model incorporates parameters such as gear mesh stiffness, damping, and contact forces to accurately simulate the interaction between the gearbox components.

To validate the model, the researchers compare the numerical results with experimental data obtained from a test rig. The comparison demonstrates the model's capability to accurately

predict the gearbox behavior under variable operating conditions. The article concludes by highlighting the significance of the developed numerical model in understanding the performance and reliability of gearboxes operating in variable regimes. The model can be used for further studies, such as optimizing gear design, analyzing the effects of different operating parameters, and assessing the gearbox's response to varying loads and speeds. Overall, the article contributes to the field of gearbox analysis by providing a numerical model that can effectively simulate and analyze the behavior of single stage gearboxes under variable operating conditions.

Merzoug et al. [64] highlights the need for adapted monitoring techniques to detect gear faults in gear transmissions operating under variable regimes. The study presents a specialized vibratory monitoring approach that combines signal processing and machine learning to analyze vibration signals from the gear system. Experimental validation demonstrates the approach's effectiveness in accurately detecting gear faults and assessing overall gear health. The article emphasizes the significance of vibratory monitoring in improving reliability and maintenance strategies for gear transmissions in variable regimes, offering early fault detection and reducing the risk of unexpected failures. Overall, the study contributes to the field of gear transmission monitoring by introducing a tailored vibratory monitoring approach for variable operating conditions.

Hammami et al. [69] explores the use of the CEEMDAN method to analyze the dynamic behavior of a defective spur gearbox operating under an acyclic regime. The study emphasizes the need for advanced analysis techniques for gearboxes under such conditions. The article focuses on applying CEEMDAN, a signal processing method that decomposes vibration signals into intrinsic mode functions (IMFs), to analyze the gearbox vibrations. Experimental tests on a defected spur gearbox were conducted, and CEEMDAN was found effective in capturing the gearbox's dynamic behavior. The method enables accurate fault detection and diagnosis by revealing distinct fault-related frequency components and their time-varying characteristics. This research contributes to improving the understanding and maintenance strategies for gear systems operating in acyclic regimes.

In the article of Chaabi et al. [62] a new method is performed to improve monitoring rolling bearing defects in variable regime using ICEEMDAN, multivariate denoising, and order analysis. The proposed method has been successfully applied on simulated and experimental signals measured in variable regime. For several years intelligent systems have been used to provide automatic detection of defects in industrial systems.

10.3. Subjective methods for detecting gear defects

Several works have been carried out in diagnosing and evaluating the severity of defects, mainly in gears and bearings, using a subjective method. Among the subjective methods found in the literature, sound perception is simple to use and does not require prior knowledge of signal processing. It uses sounds generated by defects and listening tests in which any listener can participate provided they have healthy audibility. In addition, several researchers have been studying and refining the perceptual impact of sounds and seeking to correlate them with the most appropriate scalar indicators calculated from the measured signals.

The sound perceptive approach has been used in several fields, including the work carried out by Parizet et al. [70], where it was used to study the noise in a high-speed train at different locations. The authors carried out a study concerning the usual physical or psycho-acoustic parameters. The test results indicate that the first factor influencing the perception of noise in a high-speed train is the intensity, which the overall weighted signal level can correctly describe. On the other hand, the influence of loudness is practically the same for all listeners. The use of sound perception in the diagnosis of defects in rotating machines is very recent. In the study carried out by Younes et al. [5-71-72], the authors applied the sound perception method to several types of defects. In [5], the authors used this method to classify real gear defects based on signals measured every two hours over several days. The authors also used the same method for experimentally simulated gear defects on several wheels in a test bench. In [71], the authors applied it to single and double gear and bearing defects. The results show that despite the difference between the two types of defects, the sound perception gives acceptable results where listeners distinguish bearing defects from gear defects. However, the correlation ratios obtained remain relatively low. To improve them, the authors proposed in another paper [72] the equalization of the sound pressure levels of the different sounds to help listeners focus on the content of the sounds and not on their pressure levels, which considerably improved the correlation ratios. In all their work, the authors show the possibility of ranking the defects of single and double gear and bearing defects in ascending order of degradation, according to the type and size of the defect, in a two-dimensional perception space. The correlation of the sound perception results, obtained by the pairwise comparison method, with the scalar indicators of the measured signals has resulted in mathematical models with good coefficients of determination, which can be effectively used in the monitoring of the evolution of the defect size in rotating machines.

Despite its efficiency in constant regime, the sound perception approach has never been applied to detect rolling bearing or gear defects in variable regime. This is perhaps due to the difficulty for the auditors to distinguish the different sounds in acceleration or deceleration rates.

11. References

1. Ben Saci M.M., Belkhir T. La maintenance des équipements par l'analyse vibratoire: University Kasdi merbah ouargla; 2016, Master thesis.
2. Preventive maintenance research available on : <https://www.hanarasoft.com/preventive-maintenance-vs-predictive-maintenance/>.
3. Présentation des analyses vibratoires. Bruel & Kjaer. Novembre 2005.
4. Medjadi D., Tachi F. Diagnostic par Analyse Vibratoire pour Machines Tournantes. Présentation technique. Centre DP – Hassi R'mel, 15-20 Mai 2006.
5. Younes R., Ouelaa N., Hamzaoui N., Djebala A. Experimental study of real gear transmission defects using sound perception. The International Journal of Advanced Manufacturing Technology. 2015;76(5-8):927-40.
6. Kanzari. T. M., "Diagnostic vibro-acoustique des défauts d'engrenage : Analyse d'une démarche de perception sonore. Thesis," INSA de Lyon (2009).
7. David H.A. , The method of paired comparison. Oxford University Press, New-York (1988).
8. Stevens S.S. A Metric for the Social Consensus: Methods of sensory psychophysics have been used to gauge the intensity of opinions and attitudes. Science. 1966;151(3710):530-41.
9. Roskam E. The method of triads for nonmetric multidimensional scaling. Psychologia; 1970.
10. Burton M.L., Nerlove S.B. Balanced designs for triads tests: Two examples from English. Social Science Research. 1976;5(3):247-67.
11. Yoshida A., Ohue Y., Ishikawa H. Diagnosis of tooth surface failure by wavelet transform of dynamic characteristics. Tribology international. 2000;33(3-4):273-9.
12. Michaud P-Y., Meunier S., Herzog P., d'Aubigny G.D., Lavandier M. Méthode de test adaptée à l'évaluation perceptive d'un grand nombre de stimuli audio: Application aux enceintes acoustiques. 10^{ème} Congrès Français d'Acoustique, Lyon, France ; 2010.
13. Sidahmed M. Détection précoce de défauts dans les engrenages par analyse vibratoire. Revue Française de Mécanique. 1990(4):243-54.
14. Capdessus C., Sidahmed M. Analyse des vibrations d'un engrenage: cepstre, corrélation, spectre. TS Traitement du signal. 1992;8(5):365-72.
15. Cousinard O., Rousseau P., Bolaers F., Marconnet P. Paramétrage, utilisation et apport de l'analyse cepstrale en maintenance prévisionnelle. Mécanique & Industries. 2004;5(4):393-406.
16. Djebala A., Ouelaa N., Benchaabane C., Laefer D. Application of the wavelet multi-resolution analysis and Hilbert transform for the prediction of gear tooth defects. Meccanica. 2012;47(7):1601-12.
17. Djebala A., Ouelaa N., Hamzaoui N. Optimisation de l'analyse multirésolution en ondelettes des signaux de choc. Application aux signaux engendrés par des roulements défectueux. Mécanique & Industries. 2007;8(4):379-89.

18. Moumene I., Ouelaa N. Application of the wavelets multiresolution analysis and the high-frequency resonance technique for gears and bearings faults diagnosis. *The International Journal of Advanced Manufacturing Technology*. 2016;83(5):1315-39.
19. Tayachi H., Gabzili H., Lachiri Z. A New Approach for Detection of Gear Defects using a Discrete Wavelet Transform and Fast Empirical Mode Decomposition. *International Journal of Computer Science and Network Security*. 2022;22:123-30.
20. Inturi V., Pratyush A, Sabareesh G. Detection of local gear tooth defects on a multistage gearbox operating under fluctuating speeds using DWT and EMD analysis. *Arabian Journal for Science and Engineering*. 2021;46(12):11999-2008.
21. Kumar A., Gandhi C., Zhou Y., Kumar R., Xiang J. Latest developments in gear defect diagnosis and prognosis: A review. *Measurement*. 2020;158:107735.
22. Chiementin X, Rasolofondraibe L, Bolaers F, Pottier B, Dron J-P. Detection precoce de défaut de roulement par adaptation d'ondelette aux signaux de type choc.
23. Mendieta D.R.C, Li C., Zhenzhong S., Wang D., Ju'E G. Theoretical Investigations on Kurtosis and Entropy and Their Improvements for System Health Monitoring.2020, *Transactions on Instrumentation and Measurement*.
24. Bouzouane B., Miloudi A., Hamzaoui N., Benchaala A. Détection de défauts de machines tournantes par la méthode des ondelettes.
25. Antoni J. Cyclostationarity by examples. *Mechanical Systems and Signal Processing*. 2009;23(4):987-1036.
26. Boustany R., Antoni J. A subspace method for the blind extraction of a cyclostationary source: Application to rolling element bearing diagnostics. *Mechanical Systems and Signal Processing*. 2005;19(6):1245-59.
27. Bonnardot F., Randall R., Guillet F. Extraction of second-order cyclostationary sources—application to vibration analysis. *Mechanical Systems and Signal Processing*. 2005;19(6):1230-44.
28. Urbanek J., Barszcz T., Zimroz R., Antoni J. Application of averaged instantaneous power spectrum for diagnostics of machinery operating under non-stationary operational conditions. *Measurement*. 2012;45(7):1782-91.
29. Urbanek J., Barszcz T., Sawalhi N., Randall R.B. Comparison of amplitude-based and phase-based method for speed tracking in application to wind turbines. *Metrology and measurement systems*. 2011;18(2):295-303.
30. Gellermann T., Walter G. Requirements for condition monitoring systems for wind turbines. *AZT Expertentage*. 2003;10(11.11).
31. Urbanek J., Barszcz T., Antoni J. A two-step procedure for estimation of instantaneous rotational speed with large fluctuations. *Mechanical Systems and Signal Processing*. 2013;38(1):96-102.
32. Urbanek J., Barszcz T., Antoni J. Integrated modulation intensity distribution as a practical tool for condition monitoring. *Applied acoustics*. 2014;77:184-94.

33. Kebabsa T., Ouelaa N., Antoni J., Djamaa M.C., Khettabi R., Djebala A. Experimental study of a turbo-alternator in industrial environment using cyclostationarity analysis. *The International Journal of Advanced Manufacturing Technology*. 2015;81(1-4):537-52.
34. Kebabsa T., Ouelaa N., Antoni J., Djamaa M.C., Khettabi R., Djebala A. Fault Diagnosis Through the Application of Cyclostationarity to Signals Measured. *Applied Mechanics, Behavior of Materials, and Engineering Systems: Springer*; 2017. p. 251-66.
35. Babouri M.K., Ouelaa N., Kebabsa T., Djebala A. Application of the cyclostationarity analysis in the detection of mechanical defects: comparative study. *The International Journal of Advanced Manufacturing Technology*. 2019;103(5-8):1681-99.
36. Assaad B., Eltabach M., Antoni J. Vibration based condition monitoring of a multistage epicyclic gearbox in lifting cranes. *Mechanical Systems and Signal Processing*. 2014;42(1-2):351-67.
37. Huang N.E., Shen Z., Long S.R., Wu M.C., Shih H.H., Zheng Q., et al. The empirical mode decomposition and the Hilbert spectrum for nonlinear and non-stationary time series analysis. *Proceedings of the Royal Society of London Series A: mathematical, physical and engineering sciences*. 1998;454(1971):903-95.
38. Du Q, Yang S. Application of the EMD method in the vibration analysis of ball bearings. *Mechanical systems and Signal processing*. 2007;21(6):2634-44.
39. Gao Q, Duan C, Fan H, Meng Q. Rotating machine fault diagnosis using empirical mode decomposition. *Mechanical systems and Signal processing*. 2008;22(5):1072-81.
40. Kebabsa T., Djebala A., Babouri M.K., Djamaa M.C., Chaabi L., Ouelaa N. Comparative study between cyclostationary analysis, EMD, and CEEMDAN for the vibratory diagnosis of rotating machines in industrial environment. *The International Journal of Advanced Manufacturing Technology*. 2020;109(9):2747-75.
41. Djebala A., Babouri M.K., Ouelaa N. Rolling bearing fault detection using a hybrid method based on empirical mode decomposition and optimized wavelet multi-resolution analysis. *The International Journal of Advanced Manufacturing Technology*. 2015;79(9):2093-105.
42. Babouri M.K., Ouelaa N., Djebala A. Experimental study of tool life transition and wear monitoring in turning operation using a hybrid method based on wavelet multi-resolution analysis and empirical mode decomposition. *The International Journal of Advanced Manufacturing Technology*. 2016;82(9-12):2017-28.
43. Wu Z., Huang N.E. Ensemble empirical mode decomposition: a noise-assisted data analysis method. *Advances in adaptive data analysis*. 2009;1(01):1-41.
44. Jiang Y., Tang C., Zhang X., Jiao W., Li G., Huang T. A novel rolling bearing defect detection method based on bispectrum analysis and cloud model-improved EEMD. *IEEE Access*. 2020;8:24323-33.
45. Yang J., Huang D., Zhou D., Liu H. Optimal IMF selection and unknown fault feature extraction for rolling bearings with different defect modes. *Measurement*. 2020;157:107660.
46. Zhang M., Jiang Z., Feng K. Research on variational mode decomposition in rolling bearings fault diagnosis of the multistage centrifugal pump. *Mechanical systems and Signal processing*. 2017;93:460-93.

47. Mahgoun H., Chaari F., Felkaoui A., Haddar M. Early detection of gear faults in variable load and local defect size using ensemble empirical mode decomposition (EEMD). *Advances in Acoustics and Vibration*: Springer; 2017. p. 13-22.
48. Akram M.A., Khushnood S., Tariq S.L., Ali H.M., Nizam L.A. Vibration based gear fault diagnosis under empirical mode decomposition and power spectrum density analysis. *Advances in Science and Technology Research Journal*. 2019;13(3).
49. Chen H., Chen P., Chen W., Wu C., Li J., Wu J. Wind turbine gearbox fault diagnosis based on improved EEMD and Hilbert square demodulation. *Applied Sciences*. 2017;7(2):128.
50. Torres M.E., Colominas M.A., Schlotthauer G., Flandrin P. A complete ensemble empirical mode decomposition with adaptive noise. 2011 IEEE international conference on acoustics, speech and signal processing (ICASSP); 2011: IEEE.
51. Vanraj, Dharmi, S.S., Pabla, B.S. Non-contact incipient fault diagnosis method of fixed-axis gearbox based on CEEMDAN. *Royal Society open science*. 2017;4(8):170616.
52. Lei Y., Liu Z., Ouazri J., Lin J. A fault diagnosis method of rolling element bearings based on CEEMDAN. *Proceedings of the Institution of Mechanical Engineers, Part C: Journal of Mechanical Engineering Science*. 2017;231(10):1804-15.
53. Babouri M.K., Ouelaa N., Kebabsa T., Djebala A. Diagnosis of mechanical defects using a hybrid method based on complete ensemble empirical mode decomposition with adaptive noise (CEEMDAN) and optimized wavelet multi-resolution analysis (OWMRA): experimental study. *The International Journal of Advanced Manufacturing Technology*. 2021;112(9):2657-81.
54. Lingli J., Liman C., Hongchuang T., Xuejun L. Fault diagnosis of spiral bevel gears based on CEEMDAN permutation entropy. *Advances in Asset Management and Condition Monitoring*: Springer; 2020. p. 695-704.
55. Jing X., Jianmin M., Zhiqiang Z., Chun C. Bearing fault diagnosis based on CEEMDAN and Teager energy operator. *Journal of Physics: Conference Series*; 2019: IOP Publishing.
56. Hu, R.-q., Y.-r. Zhou, et al. Bearing Fault Diagnosis Based on CEMDAN Energy Weighting Method. 2nd International Conference on Informatics, Control and Automation, 2019, ISBN: 978-1-60595-637-4.
57. An D., Xu B., Shao M., Li H-D, Wang L-Y. CEEMDAN-MFE method for fault extraction of rolling bearing. *Journal of Physics: Conference Series*; 2019: IOP Publishing.
58. Colominas M.A., Schlotthauer G., Torres M.E. Improved complete ensemble EMD: A suitable tool for biomedical signal processing. *Biomedical Signal Processing and Control*. 2014;14:19-29.
59. Ding F., Li X., Qu J. Fault diagnosis of rolling bearing based on improved CEEMDAN and distance evaluation technique. *Journal of Vibroengineering*. 2017;19(1):260-75.
60. Tiboni M., Remino C., Bussola R., Amici C. A Review on Vibration-Based Condition Monitoring of Rotating Machinery. *Applied Sciences*. 2022;12(3):972.
61. Ouelaa Z., Younes R., Djebala A., Hamzaoui N., Ouelaa N. Comparative study between objective and subjective methods for identifying the gravity of single and multiple gear defects in case of noisy signals. *Applied Acoustics*. 2022;185:108432.

62. Chaabi L., Lemzadmi A., Djebala A., Bouhalais M.L., Ouelaa N. Fault diagnosis of rolling bearings in non-stationary running conditions using improved CEEMDAN and multivariate denoising based on wavelet and principal component analyses. *The International Journal of Advanced Manufacturing Technology*. 2020;107(9):3859-73.
63. Mahgoun H., Chaari F., Felkaoui A., Haddar M. L-Kurtosis and Improved Complete Ensemble EMD in Early Fault Detection Under Variable Load and Speed. *Advances in Acoustics and Vibration II*, Springer, 2019:3-15
64. Merzoug M., Sghir K.A., Miloudi A., Dron J.P. Vibratory monitoring of gear transmissions in variable regime. *Mechanics & Industry*. 2014;15(5):377-82.
65. Bouhalais M.L., Djebala A., Ouelaa N., Babouri M.K. CEEMDAN and OWMRA as a hybrid method for rolling bearing fault diagnosis under variable speed. *The International Journal of Advanced Manufacturing Technology*. 2018;94(5):2475-89.
66. Dien, N.P. and N.T. Du. Fault detection for rotating machines in non-stationary operations using order tracking and cepstrum. *Advances in Engineering Research and Application: Proceedings of the International Conference on Engineering Research and Applications*, 2019, Springer.
67. Zhao D., Wang T., Chu F. Deep convolutional neural network based planet bearing fault classification. *Computers in Industry*. 2019 ;107:59-66.
68. Farhat M.H., Hentati T., Chimentin X, Bolaers F, Chaari F, Haddar M. Numerical model of a single stage gearbox under variable regime. *Mechanics Based Design of Structures and Machines*. 2023;51(2):1054-81.
69. Hammami A., Hmida A., Khabou M., Chaari F., Haddar M, Felkaoui A. Applications of Ceemdan in Dynamic Behavior of Defected Spur Gearbox Running Under Acyclism Regime. *Journal of Mechanics*. 2020;36(6):825-39.
70. Parizet E., Hamzaoui N., Jacquemoud J. Noise assessment in a high-speed train. *Applied acoustics*. 2002;63(10):1109-24.
71. Younes R., Ouelaa N., Hamzaoui N., Djebala A. Experimental study of combined gear and bearing faults by sound perception. *Advances in Acoustics and Vibration: Springer*; 2017. p. 145-51.
72. Younes R., Ouelaa N., Hamzaoui N., Djamaa M.C., Djebala A. The Influence of the Sound Pressure Level on the Identification of the Defects Severity in Gear Transmission by the Sound Perception. *Acoustics Australia*. 2019;47(3):239-46.

Chapter Two

Detecting gear defects in a noisy environment using objective and subjective approaches: case of steady-state regime

1. Introduction

In light of the substantial global technological advancements, there exists a pressing need to ensure the safety of workers who are exposed to exceptionally high noise levels originating from rotating machinery. This elevated use of rotating machinery is primarily driven by their increasingly high rotational speeds and prolonged operational periods. It's important to note that these machines are susceptible to damage and unexpected breakdowns, leading to unscheduled downtime. The expenses associated with production stoppages significantly outweigh those incurred in repair activities. Consequently, the prevention of machinery damage holds paramount economic significance for all companies. Moreover, the noise levels produced by machine operations, exacerbated by defects within various mechanisms, can surpass international standards governing noise levels within workshops, as stipulated by ISO (1999).

The objective of this chapter is to formulate and establish two methods for detecting defects in gears. These methods are grounded in both subjective and objective approaches. The efficacy of the proposed methods is put to the test and validated using defective gears operating within a noisy environment under steady-state conditions.

2. Mathematical foundations of the subjective approach

The approach employed in this thesis that relies on subjective assessment primarily centers around the sound perception method, the theoretical framework of which was introduced in chapter 1. In the subsequent sections, we will expound upon its mathematical underpinnings in a clear and explicit manner.

2.1. Sound perception tests

Perceptual assessments serve to dissect various sound attributes and uncover the perceptual dimensions that listeners employ to discriminate among audio stimuli. Utilizing relative difference metrics, we are able to construct a matrix that captures the perceived disparities among these stimuli. The dimensions themselves are unveiled through the application of the Multi-Dimensional Scaling (MDS) method [1]. In multidimensional space, the MDS represents the dissimilarities of stimuli perceived by the listeners.

2.1.1. Multi-dimensional scaling method

This technique enables the representation of objects within a spatial framework by leveraging the proximity relationships between each pair of objects. In this space, it becomes possible to represent each individual object. Various algorithms have been developed to determine the coordinates of objects in this space based on the distances between them. Some of these algorithms can account for the unique characteristics of different subjects or groups of subjects exposed to different stimuli, and in some cases, they can consider both aspects simultaneously. In this study, the multi-dimensional scaling analysis algorithm employed is the INDSCAL model, which stands for Individual Differences SCALing. Originally introduced by Carroll and Chang [2-3], the INDSCAL algorithm is based on the assumption that despite that the auditors use the same dimension, they don't attribute them the same weight. Equation (2.1) takes into account the different weights attributed by the listener as W_{kr} :

$$d_{ij} = \left[\sum_{r=1}^R W_{kr} (X_{ir} - X_{jr})^2 \right]^{1/2} \quad (2.1)$$

where, d_{ijk} is the distance between objects i and j according to the subject k . X_{ir} and X_{jr} are the coordinates of these objects on the dimension r of the perceptive space.

2.1.2. The Bravais-Pearson correlation coefficient

The Bravais-Pearson correlation coefficient is a statistical measure that expresses the strength and direction (positive or negative) of the linear relationship between two quantitative variables. It is a measure of linear association, which assesses the ability to predict one variable (x) based on another variable (y) using a linear model [3].

It allows measuring the strength of the relationship between two quantitative variables. Therefore, it is an important parameter in the analysis of linear regressions (simple or multiple). However, this coefficient is zero ($r=0$) when there is no linear relationship between

the variables (although it does not exclude the existence of a non-linear relationship). Additionally, the coefficient is positive if the relationship is positive (direct, increasing) and negative if the relationship is negative (inverse, decreasing). This coefficient ranges between -1 and +1; the stronger the linear relationship, the closer the coefficient is to +1 or -1, while a coefficient closer to 0 indicates a weaker relationship.

A value close to +1 indicates a strong relationship between the two variables. The linear relationship is positive (meaning the variables vary in the same direction). A value close to -1 also indicates a strong relationship, but the linear relationship between the two variables is negative (the variables vary in opposite directions). A value close to 0 indicates an absence of a linear relationship between the two variables.

The calculation:

The Bravais-Pearson correlation coefficient (r) between two variables X and Y is computed using the covariance and standard deviations by applying the following formula (eq 2.2):

$$r = (X, Y) = \frac{\text{Cov}(X, Y)}{\sigma_X \sigma_Y} \quad (2.2)$$

2.1.3. Determination of the number of dimensions

Experimenters have the prerogative to select the number of dimensions in which they wish to represent the data. There are various criteria at their disposal to guide this decision. Initially, the experimenter can compare the minimum constraint values obtained for different dimensional settings:

$$\text{Stress} = \frac{\sqrt{\sum_{(i,j) \in \Omega} (\delta_{ij,k} - d_{ij,k})^2}}{\sqrt{\sum_{(i,j) \in \Omega} d_{ij,k}^2}} \quad (2.3)$$

$d_{ij,k}$ represents the Euclidean distances, $\delta_{ij,k}$ is the dissimilarity measures between conditions i and j for subject k . The experimental procedures employed to assess discomfort or any other perceptual attribute can be categorized into two main types: absolute evaluations and paired comparisons of sounds. In absolute evaluations, each sound is independently evaluated by the listener, irrespective of the other sounds. However, for a smaller set of sounds, the second method is generally preferred. In this approach, known as paired comparisons, listeners compare two sounds, which tends to be more manageable for non-specialist individuals than performing an absolute evaluation. The Ross series is frequently utilized to construct sequences of sound pairs for the comparison task. Listener responses are digitally coded on a

scale ranging from 0 to 1. For further elaboration on sound perception, additional information can be found in [4-5].

3. Mathematical foundations of the objective approach

3.1. Wavelet Multi-Resolution Analysis (WMRA)

WMRA is a very strong time-frequency method used in several domains to analyze transitory phenomena. Instead of cosine functions used by Fourier transform, wavelet analysis is a mathematical transform that uses analyzing functions named wavelet derived from a wavelet mother after translation and scaling. The wavelets can be expressed in the following form:

$$\psi_{a,b}(t) = \frac{1}{\sqrt{a}} \psi\left(\frac{t-b}{a}\right) \quad (2.4)$$

with, a scaling or expansion parameter and b translation parameter.

In its continuous form, wavelet analysis is given by

$$CWT(a, b) = \frac{1}{\sqrt{a}} \int_{-\infty}^{+\infty} S(t) * \psi^*\left(\frac{t-b}{a}\right) dt \quad (2.5)$$

Where ψ^* is the conjugate of ψ .

The discrete version of the wavelet analysis was developed by attributing constant values, 2^m and $n2^m$, for parameters a and b , respectively (n and m integers) as follows:

$$DWT(m, n) = 2^{\frac{-m}{2}} \int_{-\infty}^{+\infty} S(t) * \psi^*(2^{-m}t - n) dt \quad (2.6)$$

In 1989, Mallat [6] proposed a practical algorithm for the DWT called Wavelet Multi-Resolution Analysis (WMRA). In the proposed algorithm, the analyzed signal passes through a waterfall decomposition using a pair of filters. The low-pass filter allows to isolate the low-frequency components of the signal, called approximation coefficients cA_j . The high-pass filter allows obtaining the detail coefficients cD_j corresponding to high-frequency components.

Throughout the decomposition, these vectors undergo down-sampling, which necessitates their passage through two additional reconstruction filters. These filters facilitate the retrieval of approximations A_j and details D_j . Consequently, the original signal can be reconstructed using the derived sub-signals as follows:

$$A_{j-1} = A_j + D_j$$

$$s = A_j + \sum_{i \leq j}^n D_i \quad (2.7)$$

Djebala et al. [7-8] proposed an optimized version of the WMRA especially adapted for defects inducing periodical shocks. Using the kurtosis as main criterion, a parametric study has been carried out for the selection of several parameters. In this study, the optimized Wavelet Multi-Resolution Analysis (WMRA) is employed for the analysis of vibratory signals that have been measured. Figure (2.1) serves as an illustrative example, demonstrating the decomposition process for the case when $n=3$.

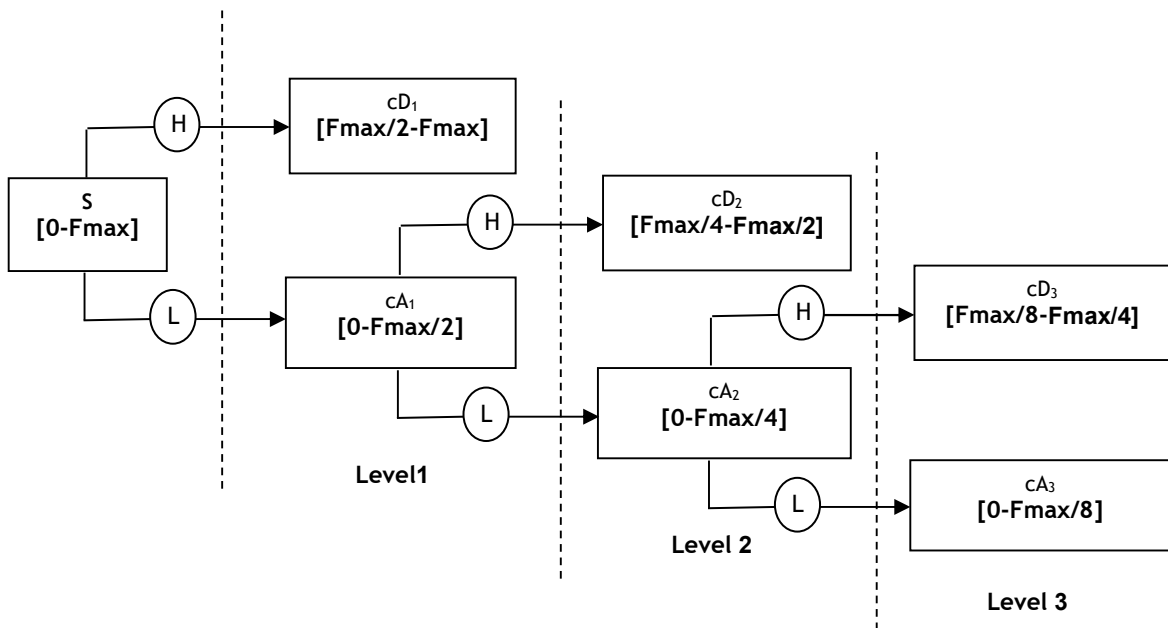


Figure 2.1. Waterfall decomposition in three levels. (6)

3.2. Cyclostationary analysis

Cyclostationarity is a technique primarily centered around the Modulation Intensity Distribution function (MID), which serves as a method for detecting and identifying modulations within a signal. Originally, the MID technique was developed for diagnosing defects in gears, rolling, and journal bearings. The spectral correlation density plays a crucial role in identifying amplitude modulations characterized by symmetrically spaced sidebands in the spectra. It enables the representation of modulation indicator values on a frequency spectrum plot, with respect to both the carrier frequency f and the modulation frequency α . Within the realm of mechanical signal analysis based on cyclostationary properties, two primary methods for detecting modulations are employed: spectral correlation (IMID) and spectral coherence (MID). The core algorithm of the MID utilizes a sideband filter,

facilitating the extraction of signals that may contain the corresponding modulation components. The formulation of functions f and α for a given Δf is referred to as the Modulation Intensity Distribution (MID), and it can be expressed as follows [9]:

$$MID_{\Delta f}^{PSC} = SC_x^\alpha \left(f + \frac{\alpha}{2} \right) SC_x^\alpha \left(f - \frac{\alpha}{2} \right) \quad (2.8)$$

The upper index PSC is the product of the spectral correlation. The degree of cyclostationarity proposed in [10] represents the ratio between the energy $\alpha \neq 0$ and $\alpha = 0$ for a stationary signal; its mathematical expression is given by:

$$DSC^\alpha = \int |R_x^\alpha(\alpha)|^2 d\alpha / \int |R_x^0(\alpha)|^2 d\alpha \quad (2.9)$$

Equation (2.9) can be rewritten using spectral correlation:

$$DSC^\alpha = \int |SC_x^\alpha(\alpha)|^2 df / \int |SC_x^0(\alpha)|^2 df \quad (2.10)$$

The Modulation Intensity Distribution (MID) is inherently a function of both the carrier frequency f and the modulation frequency α . However, presenting it in three-dimensional form can lead to challenges in interpretation and the automated decision-making process, especially in industrial monitoring systems [11]. As a practical solution, it may be more convenient to represent the MID not as a surface but as a curve that depends solely on the frequency modulation after integrating it over a range of carrier frequencies. This integration results in the creation of the IMID (Integrated Modulation Intensity Distribution), which becomes a function solely of the cyclic frequency. This approach allows us to effectively showcase the periodicity within the signal while simultaneously reducing the complexity of the analysis. An added advantage of IMID is its applicability in selecting the carrier frequency for the entire frequency band [12].

$$IMID_{f_1}^{f_2}(\alpha, \Delta f) = \int_{f_1}^{f_2} MID_{\Delta f}(f, \alpha) df \quad (2.11)$$

where, $MID_{\Delta f}(f, \alpha)$ is a vector calculated in the carrier frequency band from f_1 to f_2 .

3.3. Improved CEEMDAN

The EMD (Empirical Mode Decomposition) allows for a multi-scale decomposition by successively exploring the different scales of the signal, from the finest (first IMF) to the coarsest (last IMF or residue). Although it offers a discrete scale decomposition, unlike the wavelet transform, the scales of EMD have significant particularities. In fact, the scales are

adaptive, meaning they are determined by the scales present in the signal rather than a predetermined grid. Moreover, the notion of scale in EMD is linked to the spacing between extrema, which differs greatly from the notion of scale relative to a given waveform, as is the case for the wavelet transform. Furthermore, the scale of an IMF is defined locally based on the spacing between extrema, rather than globally. However, adaptivity and locality are also responsible for a flaw in EMD called "mode mixing." This problem occurs when the signal is composed of multiple components, some of which are not present throughout the duration of the signal. In this situation, it may happen that some components that one would like to see grouped in a single IMF are distributed over several IMFs, as shown in the example presented in figure (2.2) (left): a signal composed of three components, a permanent sinusoid (50 Hz) and two sinusoids localized in time, one of higher frequency than the permanent sinusoid (100 Hz) and the other of lower frequency (30 Hz). The representation of the IMFs (Figure 2.2, right) shows that the first IMF captures the highest frequency component at all times and therefore contains the permanent component (50 and 100 Hz), except when the high-frequency component (100 Hz) is present. The part of the permanent component located at the high-frequency component is then shifted to the second IMF.

For fault diagnosis through EMD analysis, mode mixing renders the IMFs devoid of physical meaning and can lead to a false diagnosis. When the mode mixing is founded in EMD method, the EEMD overcomes this problem with a noise-assisted analysis (see figure 2.3). The EEMD calculates an ensemble of trials using the original EMD, and adding to each trial a different composition of white noise of finite variance. This method can be summarized as follow [13-16].

1. A new signal is generated $x^i(t) = x(t) + w^i(t)$, where $x(t)$ is the original signal and $w^i(t)[i = 1 \dots I]$ are different composition of white Gaussian noise.
2. After decomposing $x^i(t)$ by the EMD, different $IMF_k^i(t)$ are obtained, where $k = 1 \dots I$ indicate the modes.
3. Finally, the average of the corresponding IMF is obtained by $\overline{IMF_k(t)} = \frac{1}{I} \sum_{i=1}^I IMF_k^i(t)$, where $\overline{IMF_k}$ is the k -th mode of $x(t)$.

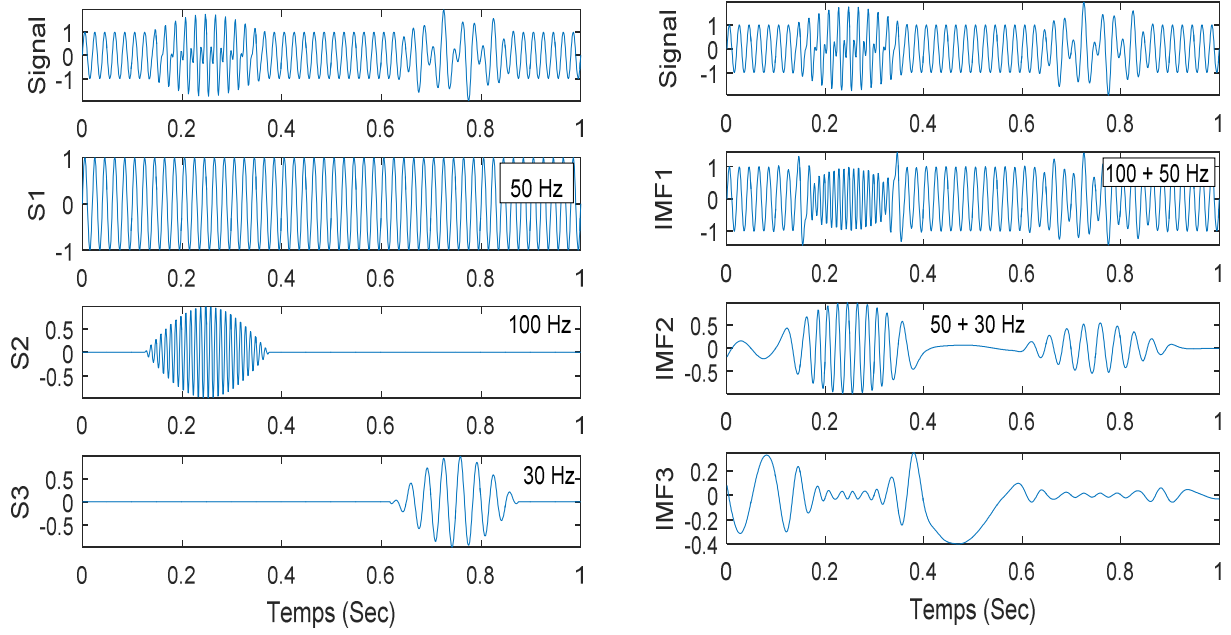


Figure 2.2. Signal sum and its components (left). The IMFs representing mode mixing (right).

The high computing time and the residue of added noise present in the obtained IMFs are the main problems of the EEMD approach (see figure 2.3). To overcome this limitation Torres et al. [17] proposed a new algorithm named CEEMDAN based on adding a white noise in a specific frequency band during the decomposition of the signal. $E_j(\cdot)$ is defined as an operator which, given a signal, produces the j -th mode obtained by EMD, ε_i represents the Signal to Noise Ratio (SNR), the steps of the CEEMDAN algorithm as proposed by Torres are then the following : (see figure 2.4, 2.5):

1. Decompose I realization of $x(t) + \varepsilon_0 w^i(t)$ by EMD to obtain the first \overline{IMF}_1 by averaging:

$$\overline{IMF}_1(t) = \frac{1}{I} \sum_{i=1}^I IMF_1^i(t).$$

2. Calculate the first residue as: $r_1(t) = x(t) - \overline{IMF}_1(t)$.
3. Decompose I realization of $r_1(t) + \varepsilon_1 E_1(w^i(t))$ until their first EMD mode and calculate the second mode: $\overline{IMF}_2(t) = \frac{1}{I} \sum_{i=1}^I E_1(r_1(t) + \varepsilon_1 E_1(w^i(t)))$.
4. For $k=2 \dots K$, calculate the k -th residue: $r_k(t) = r_{k-1}(t) - \overline{IMF}_k(t)$.
5. For $k=2 \dots K$, define the $(k+1)$ -th mode as: $\overline{IMF}_{k+1}(t) = \frac{1}{I} \sum_{i=1}^I E_1(r_k(t) + \varepsilon_k E_k(w(t)))$.

6. Go to step 4 for next k .

The last steps are repeated until the obtained residue is no longer to be decomposed: $r(t) = x(t) - \sum_{k=1}^K \overline{IMF_k(t)}$.

With k is the total number of modes. The original signal $x(t)$ can be presented in the end as:

$$x(t) = \sum_{k=1}^K \overline{IMF_k(t)} + r(t).$$

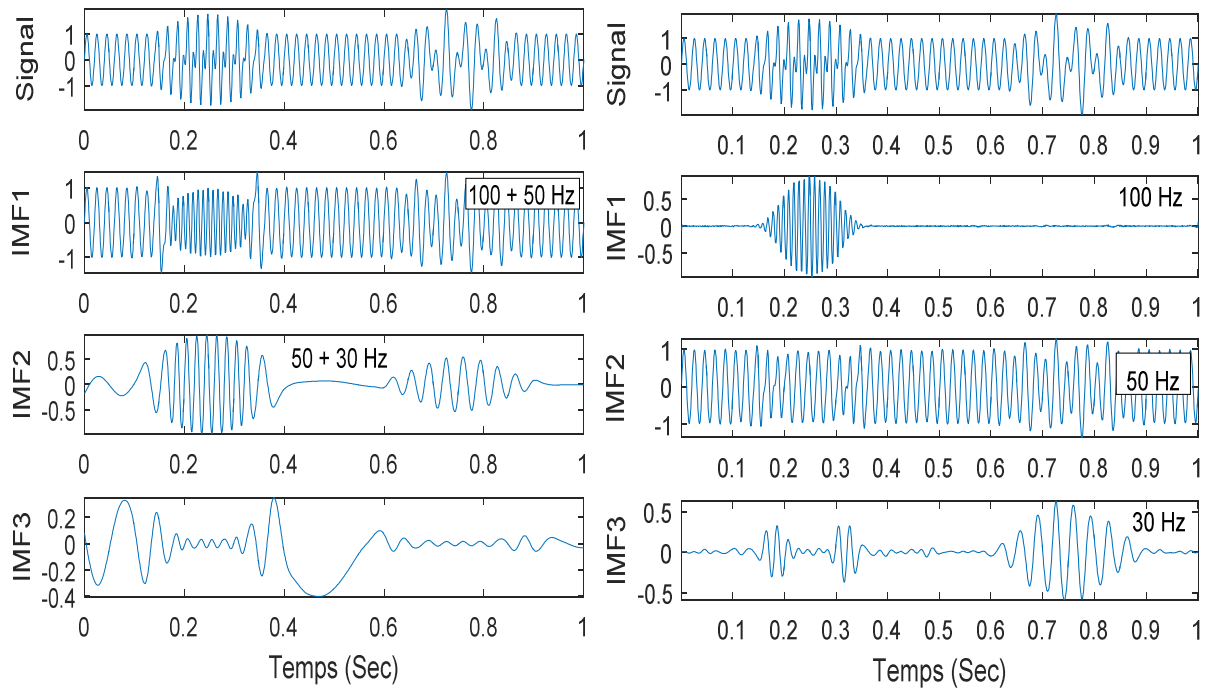


Figure 2.3. Comparison between EMD (left) and EEMD (right) [12].

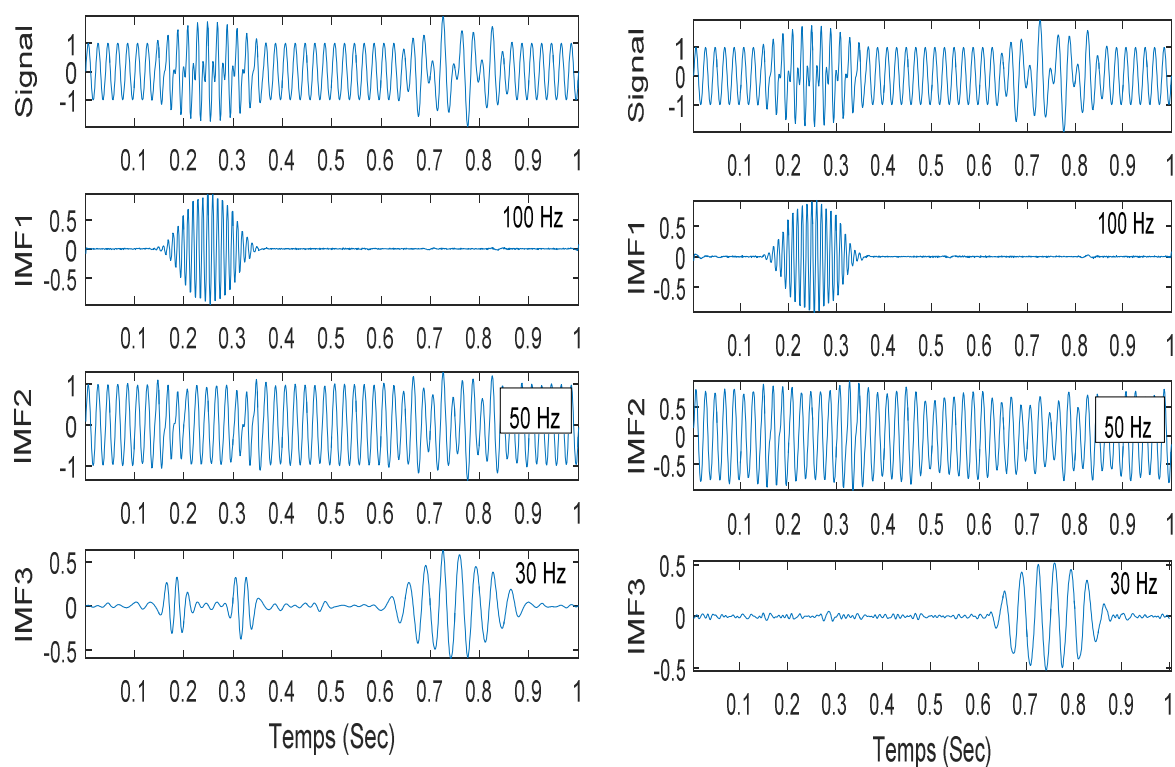


Figure 2.4. Comparison between EEMD (left) and CEEMDAN (right) [12].

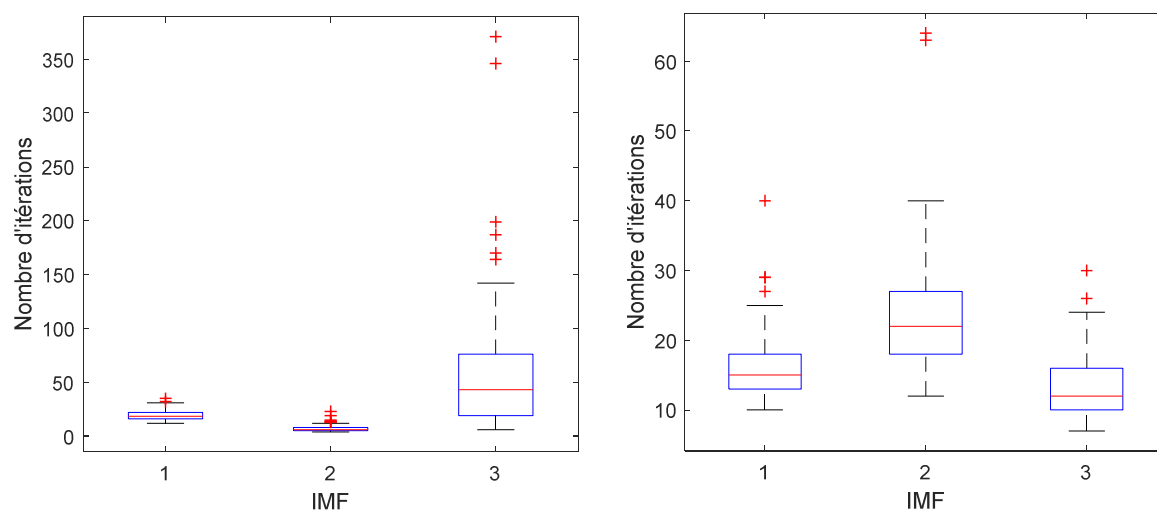


Figure 2.5. Comparison between the number of iterations of EEMD (left) and CEEMDAN (right) [12].

Even with the CEEMDAN algorithm, a little residual noise still exists in the obtained IMFs. Colominas et al. [18] proposed a new improved version of this method applied on theoretical and ECG real signals. It has shown to be more effective than all the previous versions (EMD, EEMD and CEEMDAN).

The improved CEEMDAN algorithm is presented in brief as below (1):

1. Use EMD algorithm to calculate the local means of : $x^i(t) = x(t) + \varepsilon_0 E_1(w^i(t))$

To obtain the first residue: $r_1(t) = (M(x^i(t)))$, where $M(\cdot)$ is the operator which produces the local means of the signal, and w^i a realization of white noise.

2. At the first stage, calculate the first IMF as: $\overline{IMF_1(t)} = x(t) - r_1(t)$.

3. Estimate the second residue as the average of local means of the realization:

$r_1(t) + \varepsilon_1 E_2(w^i(t))$ and calculate the second IMF as: $\overline{IMF_2(t)} = r_1(t) - r_2(t)$.

4. Calculate the k -th IMF: $\overline{IMF_k(t)} = r_{k-1}(t) - r_k(t)$.

5. Go to step 4 for next k .

On the other hand, figure (2.6) shows the number of iterations obtained by the ICEEMDAN. In comparison to that obtained by the CEEMDAN (see figure 2.5), it can be readily observed that ICEEMDAN allows for fewer iterations, thus less computation time, which is a significant factor when dealing with signals with a considerable number of points and a large number of ensembles.

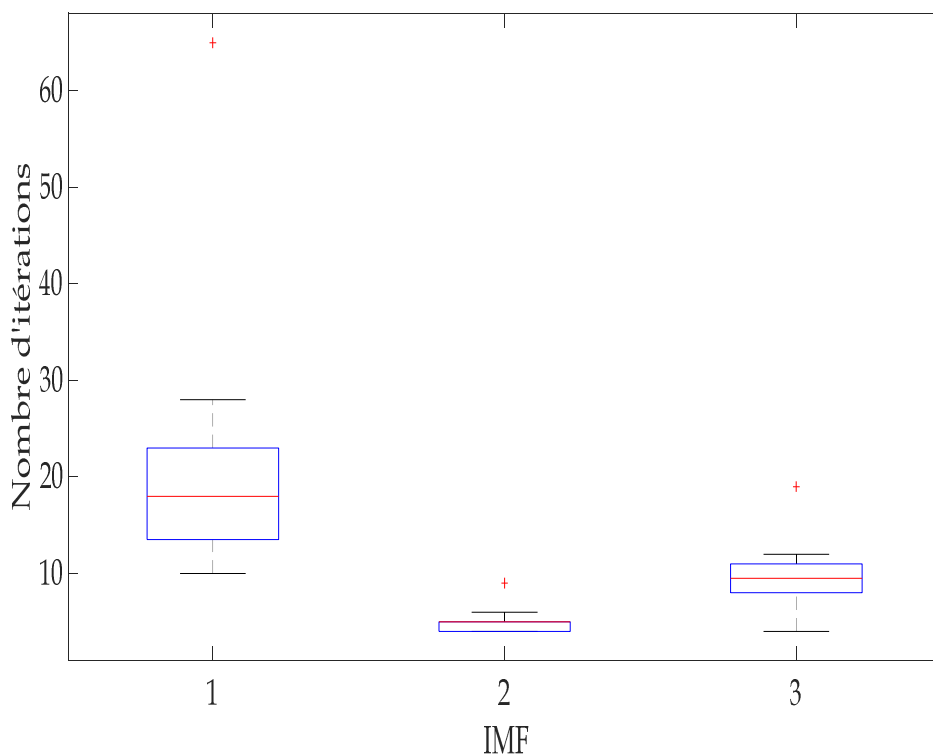


Figure 2.6. Number of iterations obtained by the ICEEMDAN [12].

4. Experimental procedure

The data utilized in this study was gathered from experiments conducted on a test rig located within the Laboratory of Mechanics and Structures at the University of Guelma in Algeria. This test rig primarily consisted of the following components: an electric motor with a power rating of 5 KW and a rotational speed of 1500 rpm, a coupling mechanism, a gearbox (as detailed in Table 2.1), and an electromagnetic brake used to simulate the load, as depicted in Figure 2.7. The gearbox itself comprised three shafts and four spur gears that were typically lubricated. The input and output shafts were each equipped with a gear (gear 1 and gear 4) featuring 42 and 45 teeth, respectively. Additionally, the intermediate shaft hosted two gears (gear 2 and gear 3) with 50 and 65 teeth, respectively. Table 1 provides a comprehensive list of the gearbox specifications. Throughout all the tests, the input shaft rotates at constant speed set equal to 14 Hz. The intermediate and output shafts have rotation frequencies equal to 12 Hz and 17 Hz, respectively.

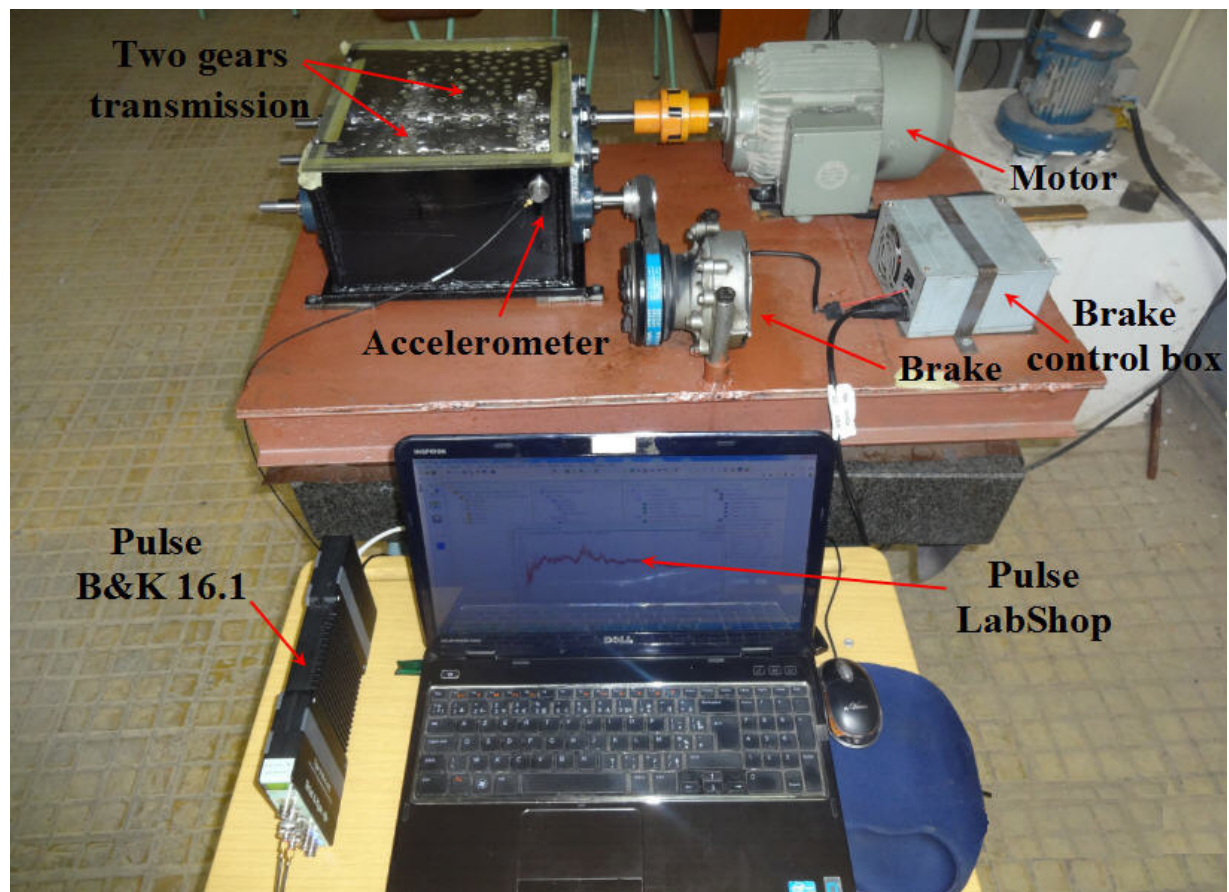


Figure 2.7. Experimental setup.

Gear type	Straight Teeth		
Gear characteristics	Transmission ratios		U1=42/50=0.84 U2=65/45=1.444
	Rotation frequency [Hz]		
	Shaft 1, gear (1)	Shaft 2, gears (2 and 3)	Shaft 3, gear (4)
	14	12	17
Meshing frequency [Hz]	588	761	

Table 2.1. Used gears and characteristic frequencies.

The vibratory signals were measured using a Bruel & Kjaer PULSE 16.1 analyzer along with PULSE LABSHOP acquisition software, as illustrated in Figure 2.7. Subsequently, post-processing and analysis were carried out within the Matlab environment.

Exp	Gear defects	Code	Mode of operation	Maximal frequency
1	Healthy gears	HG	With lubrication and with load	6400 Hz
2	Small defect on gear 2	SDG2		
3	Average defect on gear 2	ADG2		
4	Great defect on gear 2	CDG2		
5	Great defect on gear 2+Small defect on gear 4	CDG2+SDG4		
6	Great defect on gear 2 + Average defect on gear 4	CDG2+ADG4		
7	Great defect on gear 2 + Great defect on gear 4	CDG2+CDG4		

Table 2.2. Experimental plan.

For data acquisition, three accelerometers of Bruel & Kjaer type were strategically positioned in the housing of the gearbox in horizontal direction. The accelerometer 1 is mounted close to

the gear 1 and bearing 2 on the input shaft. The accelerometer 2 was placed adjacent to the intermediate shaft, near gear 2. Lastly, the accelerometer 3 was situated near the output shaft, close to the second gear pair (gear 4 and bearing 4). Consequently, seven signals, denoted as S1 to S7, were obtained. These signals corresponded to various conditions, including single and double gear defects. To cover the meshing frequencies and several of their harmonics, all the signals were measured with the same maximum frequency set equal to 6400 Hz (see table 2.2). For a visual reference, figure (2.8) provides images depicting the simulated defects showcasing different levels of severity.

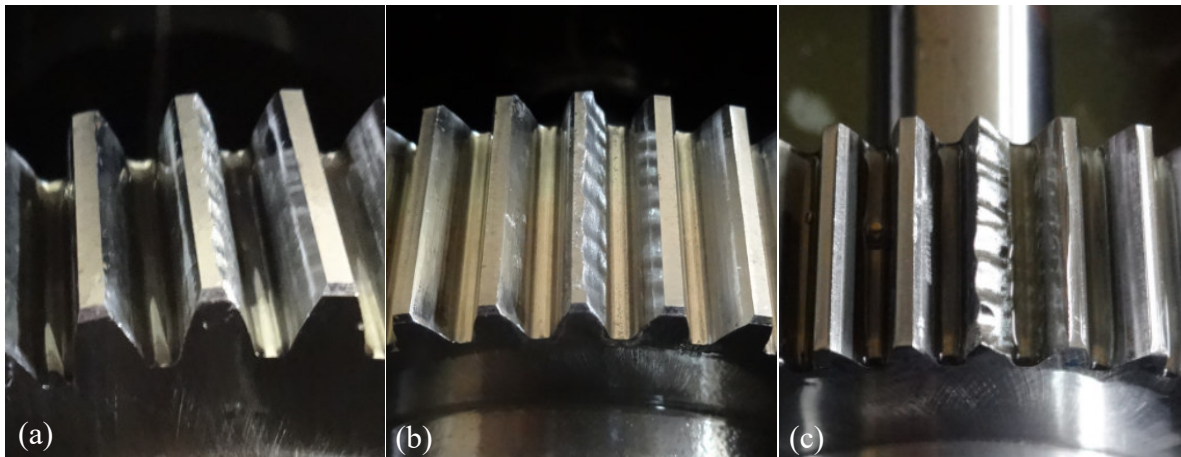


Figure 2.8. Simulated defects for three severities, (a)Small defect, (b)Average defect,(c) Critical defect.

5. Proposed methodology

The proposed methodology aims to integrate both objective and subjective approaches for comparative purposes. The subjective approach centers on sound perception and employs a paired comparison test. Initially, a conversion process was undertaken to transform the vibratory signals into audible sounds, which were then utilized in listening tests. The test interface was developed within the Matlab environment and consisted of two distinct phases. The first phase, termed the learning phase, allowed the listeners to acquaint themselves with the sounds associated with the ongoing test. This phase provided an opportunity for the listeners to become familiar with the test sounds. The second phase involved pairwise comparisons. A total of 31 participants took part in this test, comprising 13 women and 18 men, with ages ranging from 22 to 50 years. Before commencing the test, participants were provided with context and an explanation of how the interface functioned. Each step of the test was elaborated with illustrative examples. Following the completion of the comparisons, a dissimilarity matrix was generated, capturing the assessments made by the listeners. Subsequently, multidimensional analysis was applied to derive the perceptual space. Figure

2.9 offers a summarized representation of the principles underpinning the subjective approach employed in this study.

Three sophisticated signal processing techniques were employed as objective approach for the analysis of vibratory signals captured under various degrees of gear defect severity. These methods include the OWMRA, Cyclostationary analysis, and a hybrid method based on the combination of Improved CEEMDAN and multivariate denoising. As final result, each of these techniques culminates in the generation of an envelope spectrum. Figure (2.10) provides a concise overview, summarizing the three distinct methods employed as part of the objective approach in this chapter.

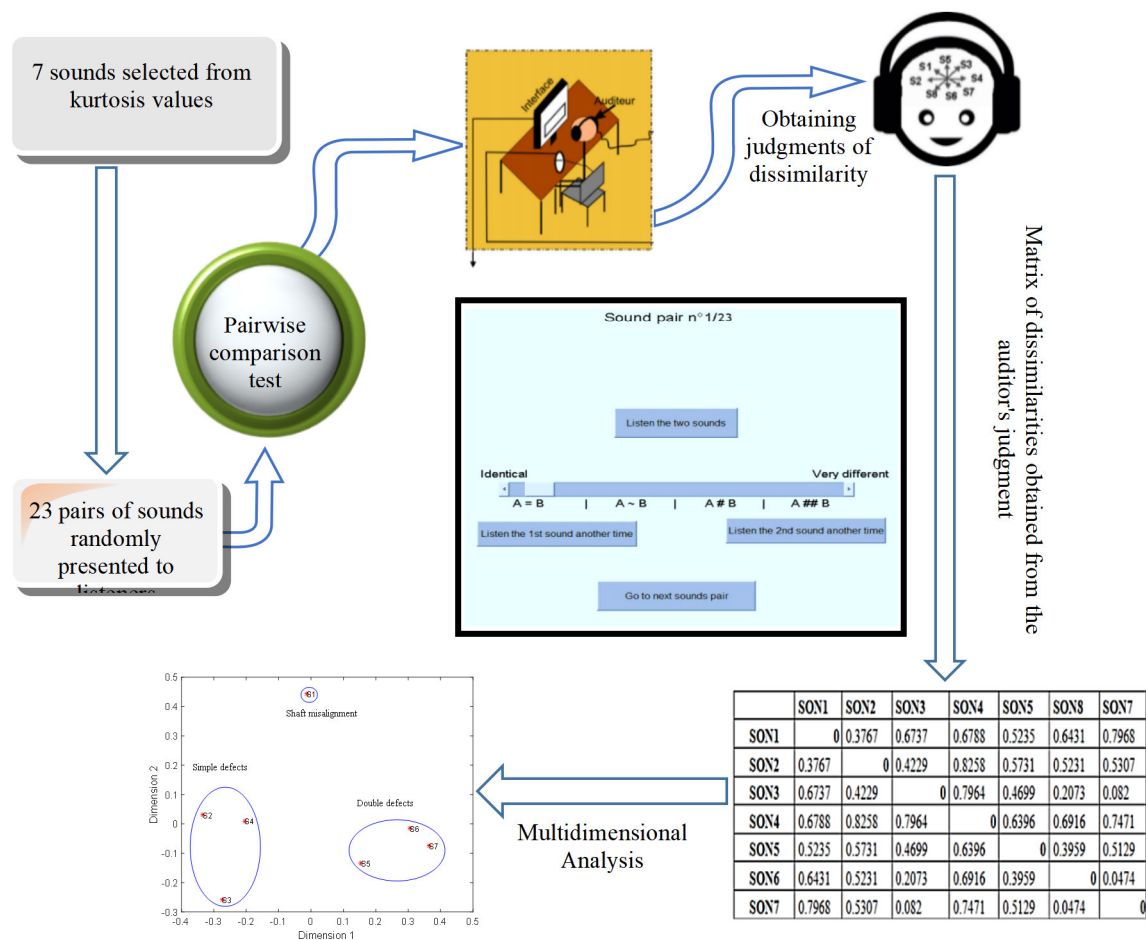


Figure 2.9. The outlined methodology for the subjective approach.

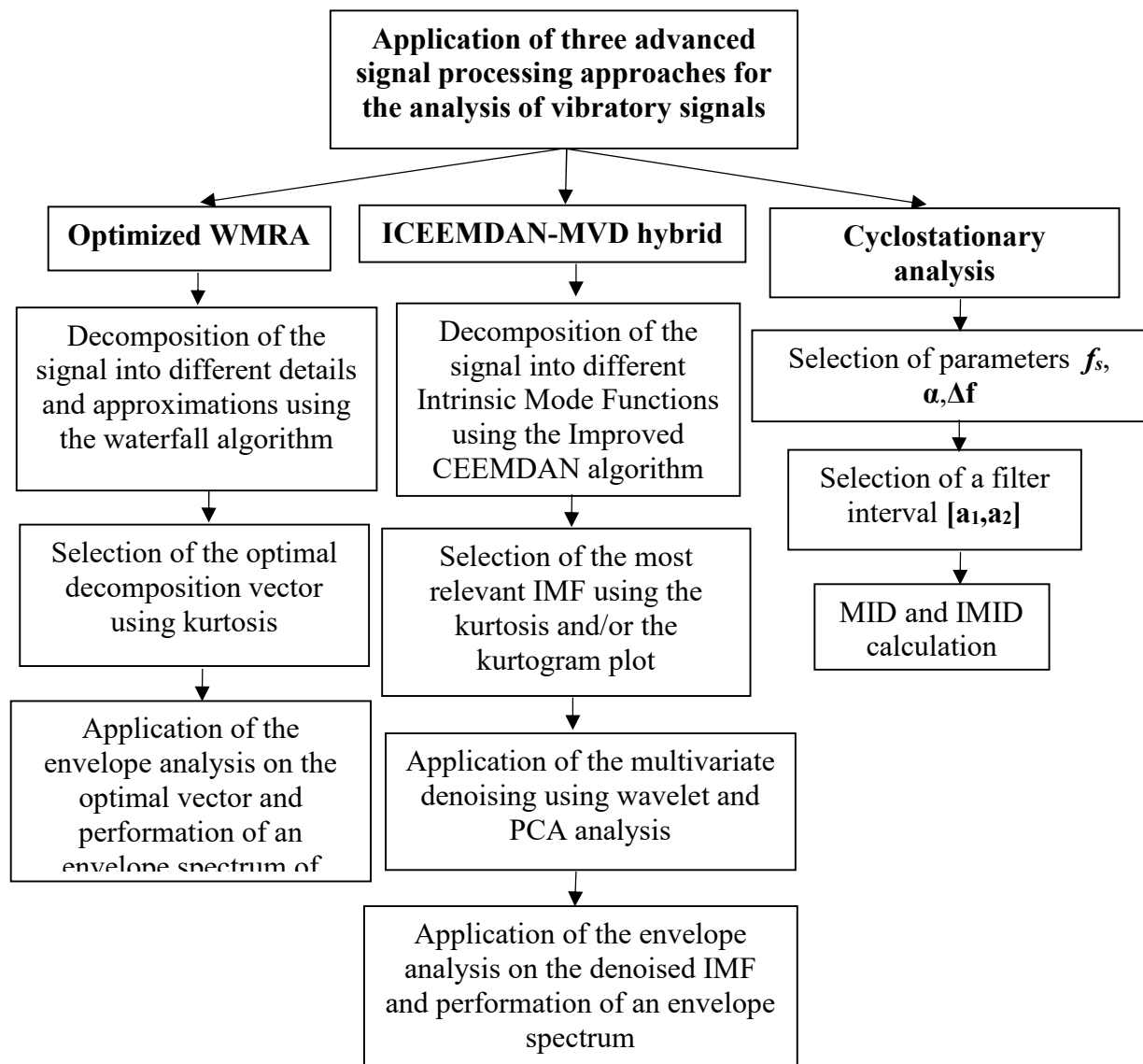


Figure 2.10. The outlined methodology for the objective approach.

6. Results and discussion

6.1. Analysis of the scalar indicators

First a quantitative and statistic evaluation of the seven measured signals is carried out through the use of ten well-known scalar indicators. The primary objective of this study encompasses two aspects: firstly, to establish a mathematical correlation between the calculated indicators and the outcomes of sound perception, and secondly, to conduct a comparative analysis between sound perception, solely based on listening tests (enabling participation from individuals without theoretical expertise in signal processing), and three highly advanced signal processing methods in the realm of mechanical defect diagnosis. These scalar indicators can be categorized into two groups: those sensitive to the energy of the signal and those sensitive to the shape of the signal. Mathematical expressions for these

ten scalar indicators are provided in table (2.3), while table (2.4) offers a summary of the obtained results.

Scalar indicator	Mathematical expression
Peak Value (PV)	$Sup S(t) $
Overall Level (OL)	$\sqrt{\frac{2}{3} \sum_{10}^{1000} (N_i)^2}$
RMS	$\sqrt{\frac{1}{N_e} \sum_{n=1}^{N_e} [x(n)]^2}$
Energy (E)	$\sum_{i=1}^N x_i^2$
Power (P)	$\frac{1}{N} \sum_{i=1}^N x_i^2$
Crest Factor (CF)	$\frac{Sup S_K }{\sqrt{\frac{1}{N} \sum_{k=1}^{N_e} (S_K)^2}}$
Kurtosis (K)	$\frac{\frac{1}{N} \sum_{i=1}^N (x_i - \bar{x})^4}{\sigma^4}$
Skewness (SK)	$\frac{\frac{1}{N} \sum_{i=1}^N (x_i - \bar{x})^3}{\sigma^3}$
K Factor (KF)	$Sup S_K \times \sqrt{\frac{1}{N_e} \sum_{k=1}^{N_e} (S_K)^2}$
Spectral Center of Gravity (SCG)	$\frac{\int f \times L(f)df}{L(f)df}$

Table 2.3. Mathematical expressions of the used scalar indicators.

	RMS	CF	PV	KF	E	OL	K	P	SK	SCG
S1	5.56	5.96	33.1	183.91	506220	5.78	5.08	30.9	0.19	315
S2	4.96	5.92	29.4	145.95	403790	4.92	5.32	24.64	0.20	313
S3	4.61	6.51	30.1	138.98	349320	4.53	5.76	21.32	0.07	315
S4	4.80	6.55	33.6	161.56	378840	4.91	6.12	23.12	0.15	322
S5	4.91	6.35	31.2	153.19	394990	4.96	4.55	24.10	0.12	325
S6	4.85	10.01	48.6	235.77	385650	4.76	10.29	23.53	0.25	337
S7	5.20	10.92	56.9	296.32	444370	5.08	8.52	27.13	0.08	340

Table 2.4. Scalar indicators' values.

Table (2.4) shows that the scalar indicators calculated for the seven signals are significant of measures carried out in a very noisy environment. The RMS, the energy, the power, and the overall level of the healthy case signal (S1), display very significant values, more important than those of defective case (single and double). Actually, these indicators are very sensitive to the signal energy, this is why their values are very important even for the healthy case. Most of these indicators, which should increase with the increase in the severity of the defect, display in certain cases a completely opposite trend. This confirms that the signals are very noisy and the defect signature is embedded into the background noise. The same case is observed for the kurtosis considered as the most sensitive indicator to shock signals. Its value for the healthy signal is very important and exceeds the detection threshold equal to three. In conclusion, most of the calculated scalar indicators don't display correct trend, it is not recommended to use them as indicators for monitoring the gear defect evolution in the case of signals measured in noisy environment.

6.2 Results obtained by sound perception approach

The proximity space of sounds, as depicted in figure (2.11) and derived directly from listeners' judgments, reveals an intriguing pattern. Specifically, the coordinates of DIM1 align remarkably well with the extent of deterioration observed in the tested gears. This alignment spans from single defects (S2, S3, and S4) to double defects (S5, S6, and S7). However, the sound associated with no defects (S1) appears noticeably distinct in this context. To shed light on this anomaly, we subjected the signal (S1) to optimized multi-resolution wavelet analysis. Indeed, the resulting envelope spectrum of detail (D2), as shown in figure (2.12),

highlights a shaft misalignment defect as the dominant feature in this spectrum is the frequency component corresponding to the third harmonic of the input shaft ($3xFr$). We believe that this distinctive spectral characteristic is responsible for the listeners' perception of (S1) as distinct from typical gear defects.

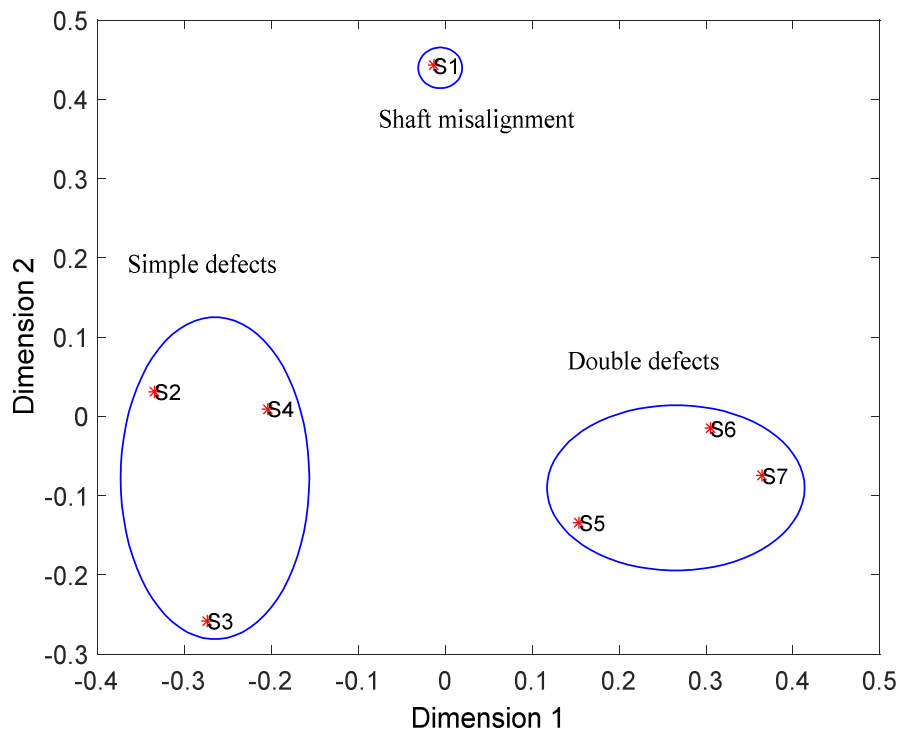


Figure 2.11. Perceptual space.

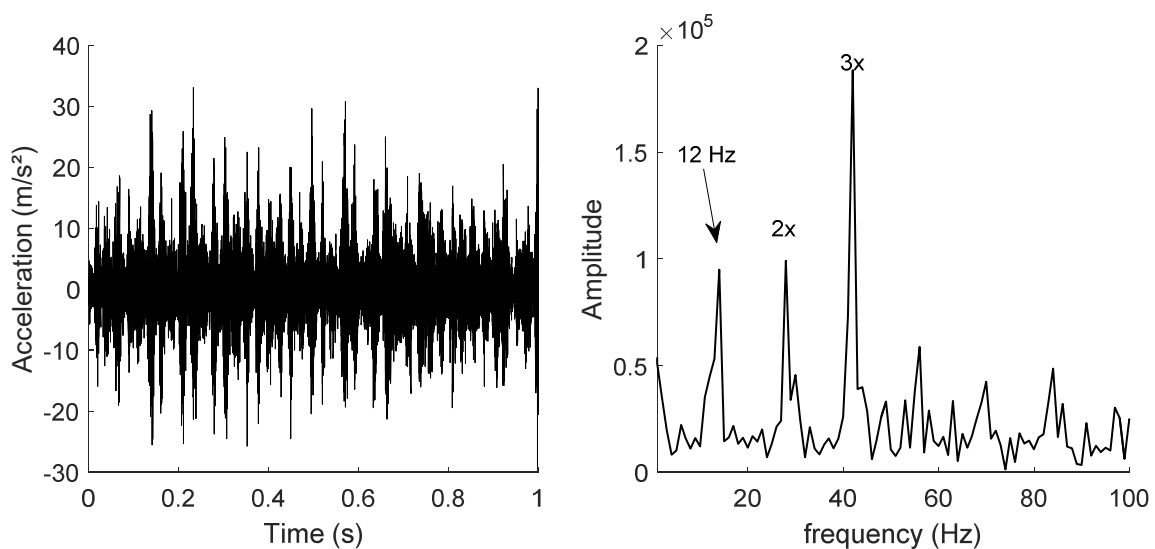


Figure 2.12. Detail D2 and its corresponding envelope spectrum of the healthy case signal (S1) obtained after the application of OWMRA.

Figure (2.13) and Equation (2.12) illustrate the relationship between DIM1 and two key scalar indicators, the Spectral Center of Gravity (SCG) and the Overall Level (OL), which are the most representative of this dimension. However, it's important to note that despite achieving a determination coefficient of $R^2 = 0.90$, this correlation remains modest due to the high level of noise present in the signals. This can be explained by the fact that the adopted scalar indicators are less sensitive to the defect gravity. Moreover, the listeners encountered difficulty in differentiating shaft misalignment from gear defect.

$$DIM1 = 0.223 \times OL + 0.0244 \times SCG - 9.036 \quad (2.12)$$

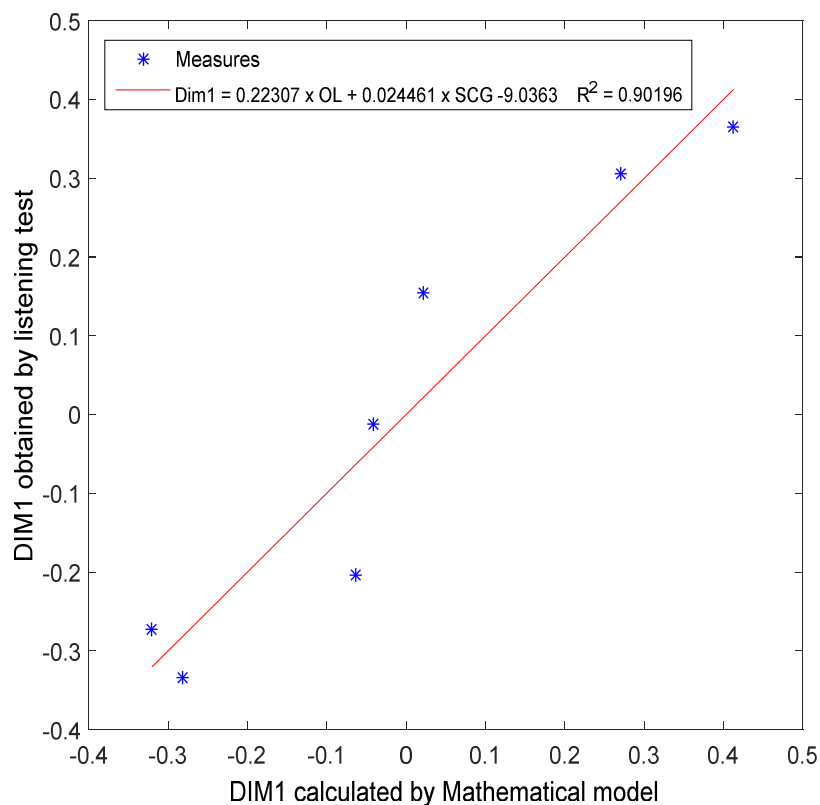


Figure 2.13. Dispersion between the dimension (DIM1) and the scalar indicators.

Figure (2.14) presents the correlation between DIM2 and two scalar indicators, the skewness and the overall level. In this case a much better fit is obtained since the coefficient of determination is $R^2 = 0.94$. The mathematical model representing this relationship is expressed as follows:

$$DIM2 = 0.476 \times OL + 1.116 \times SK - 2.550 \quad (2.13)$$

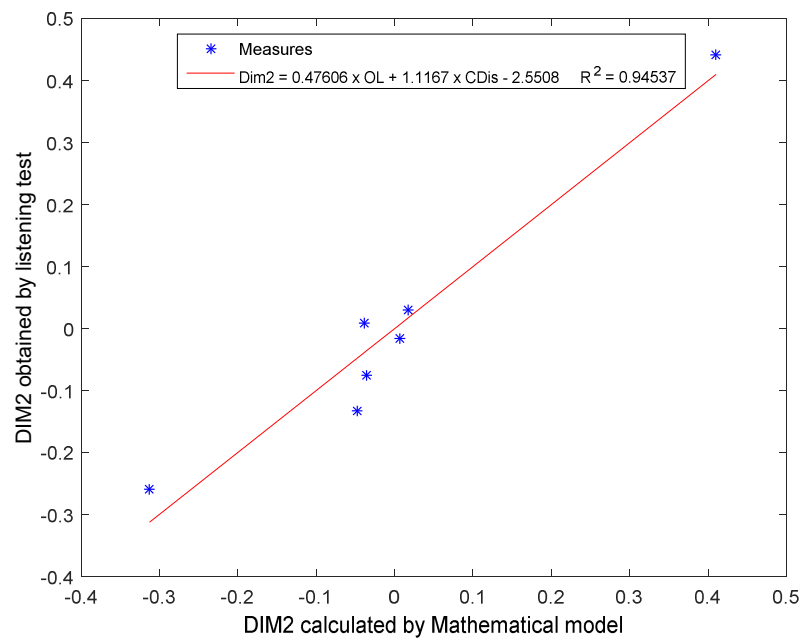


Figure 2.14. Dispersion between the dimension (DIM2) and the scalar indicators.

In the subsequent phases of this research, we will exclude the coordinates associated with the shaft misalignment defect (DIM1, DIM2). Our goal is to refine the mathematical model for DIM1, specifically in relation to gear defects. This enhanced model will have practical applications in machine monitoring, as it directly reflects the progression of defect degradation.

6.2.1. Comparison of DIM1 obtained by sound perception and mathematical model

For six different sounds, figure (2.15) depicts the evolution of the dimension DIM1, both as assessed through sound perception and calculated using equation (2.12). For single defects, the dimension DIM1 displays a negative trend and then increases in function of the defect severity evolution in gear 2. However, these DIM1 values shift to positive territory when double defects are involved. Furthermore, the level of DIM1 increases with the combination of a significant defect on gear 2 and the progression of the defect on gear 4, transitioning from small to critical. The shift of DIM1 values from negative to positive, whether observed through the mathematical model (2.12) or sound perception, signifies a change in defect severity from moderate to severe. This insight can be employed as a decision support tool

regarding whether maintenance operations should be undertaken, or even the complete shutdown of the machine.

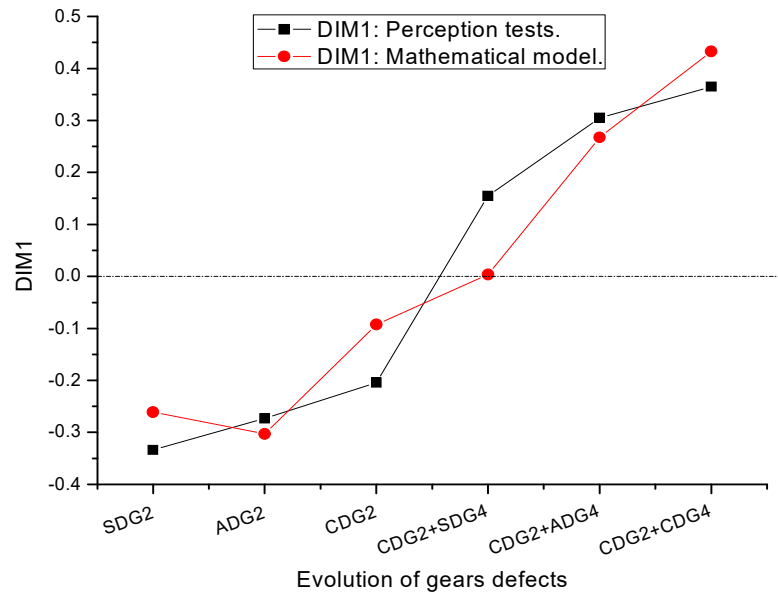


Figure 2.15. Dimension 1 values for the 6 sounds.

In the mathematical model, the DIM1 value for the (CDG2+SDG4) defect becomes positive but remains notably lower than that obtained through sound perception. This difference is primarily influenced by the scalar indicators derived from the signal linked to the shaft misalignment defect, which has a distinct nature compared to gear defects. In [19], large gear defect does not correspond to a total tooth pull-out but rather to the extraction of approximately 50% of the tooth modulus. Consequently, in our research, the DIM1 value for the large defect remains negative, whereas it might become positive in cases involving a complete tooth pull-out in [19-20]. This obtained result agrees perfectly with that found in references [19-20]. Moreover, it gives more accuracy concerning the possible choices of the actions which must be undertaken by the maintenance crew.

6.2.2. Improvement of the DIM1 mathematical model

Under Matlab environment, an experimental approach has been carried out to establish mathematical correlation between the scalar indicators of different signals and the sound perception of different sounds. To enhance the determination coefficient of the mathematical model, the coordinates (DIM1, DIM2) of the signal (S1) obtained through sound perception

were removed, along with their corresponding scalar indicators. The resulting improved mathematical model is represented by equation (2.14) and shown in figure (2.16). Notably, the results indicate a significant enhancement in the coefficient of determination, which increased from 0.90 to 0.94. This refined mathematical model is composed of two scalar indicators: the kurtosis and the spectral center of gravity. Several studies have corroborated that kurtosis is the most sensitive indicator for detecting defects that induce periodic shocks [21].

$$DIM1 = -0.039224 \times K + 0.032729 \times SCG - 10.3825 \quad (2.14)$$

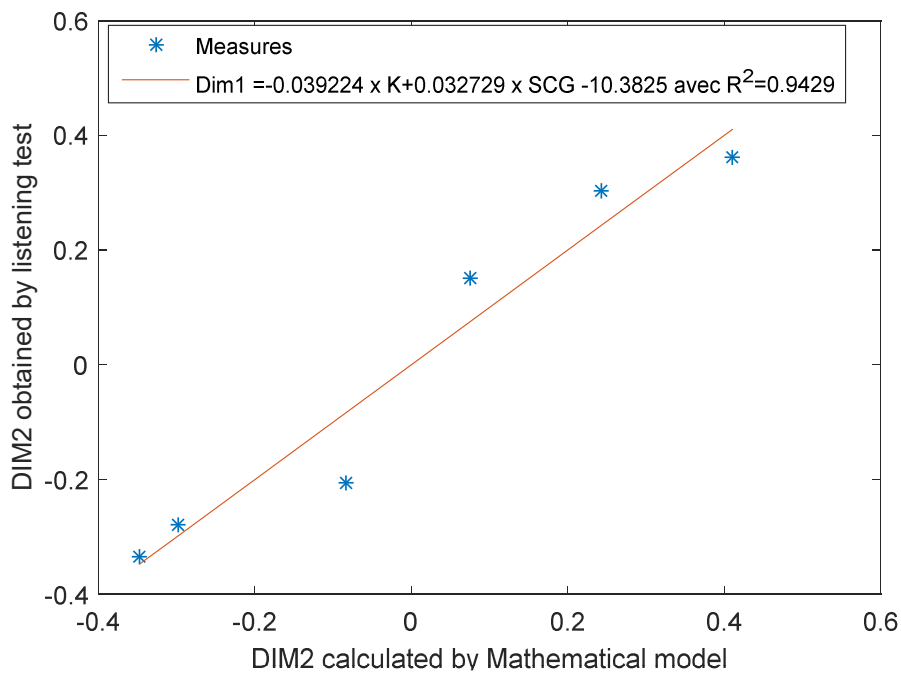


Figure 2.16. Dispersion between the dimension (DIM1) and the scalar indicators.

In figure (2.17), it's evident that the DIM1 values obtained through the mathematical model (2.14) closely align with the DIM1 values derived from sound perception, exhibiting a high determination coefficient of $R^2 = 0.94$. DIM1 emerges as a novel scalar indicator, well-suited for monitoring gear defects in rotating machinery. It combines the outcomes of sound perception with two established scalar indicators. Figure (2.18) presents the results of the sound proximity space generated through sound perception, along with the outcomes of the two new mathematical models. In the DIM1 direction, which corresponds to the progression of defect size, there is a strong concurrence between the two sets of results, except for the case of large defects (S4 and M4). Notably, there exists a considerable disparity between these two outcomes in terms of distance.

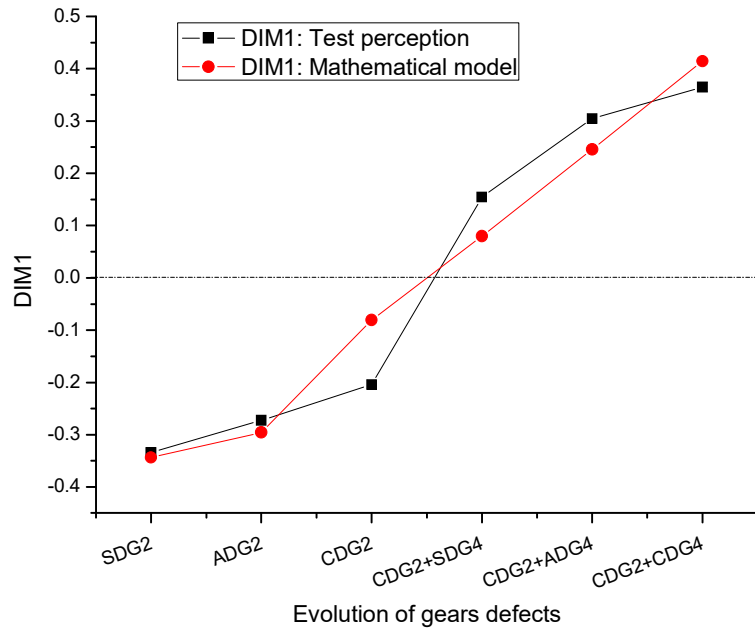


Figure 2.17. Dimension DIM1 values for the 6 sounds.

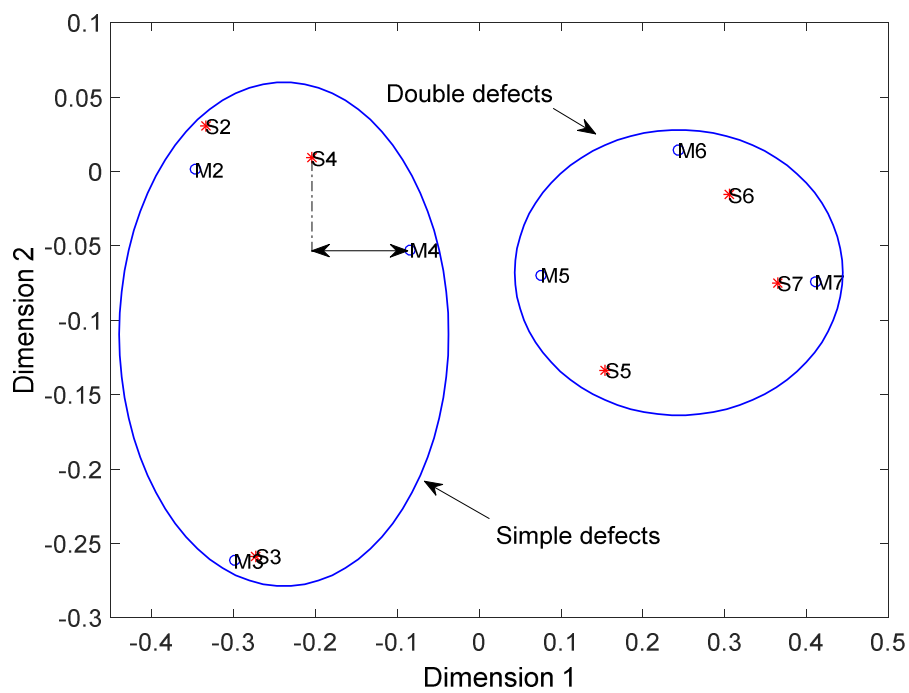


Figure 2.18. Perceptual space, $S(i)$ obtained by sound perception and $M(i)$ obtained by the mathematical model.

6.3. Results obtained by vibratory analysis

6.3.1. Results obtained by OWMRA

Figure (2.19) displays vibratory signals collected under various sizes of gear defects. In the case of simple defects (a-c), the signals exhibit high levels of noise, making it difficult to discern the presence of periodic shocks. However, for double defects (d-f), some periodic shocks become discernible. These shocks are somewhat more pronounced compared to the signals from single defects. Notably, this periodicity exclusively pertains to the large defect on gear 2, rotating at 12 Hz. Regardless of the defect size, no periodicity corresponding to the defect on gear 4, which operates at a frequency of 17 Hz, is observed.

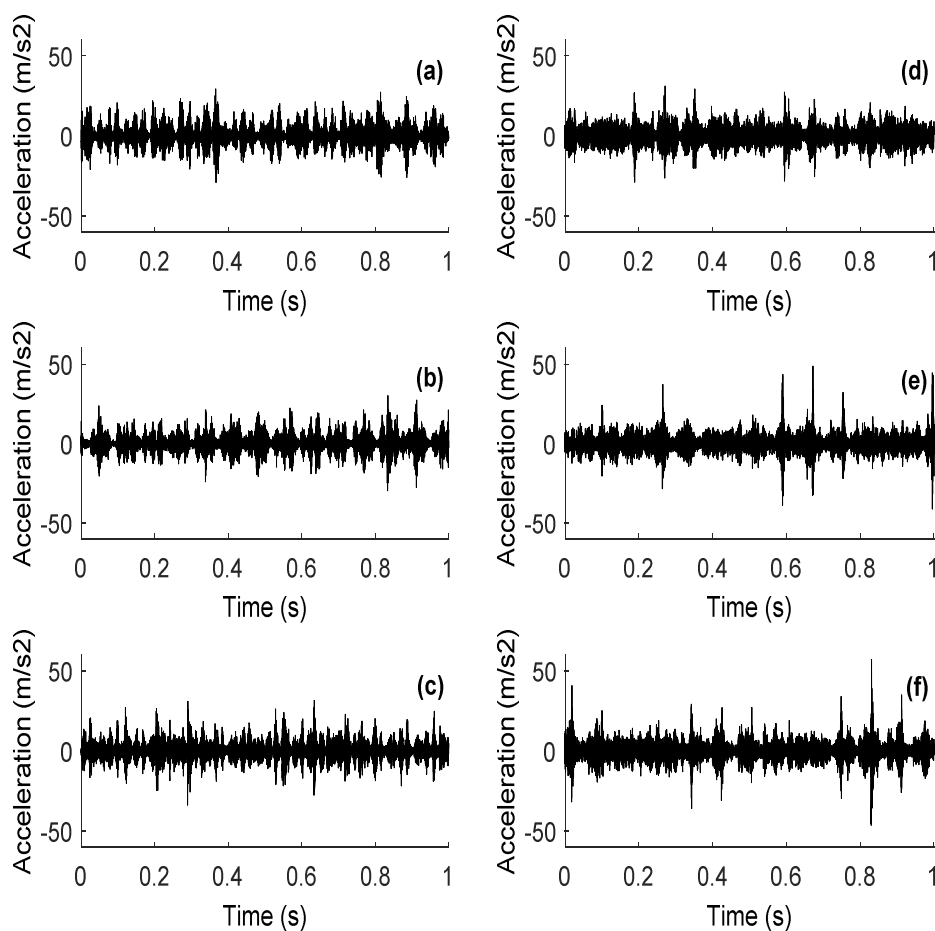


Figure 2.19. Vibratory signals measured for different severity of gear defects
 (a) SDG2, (b) ADG2, (c) CDG2, (d) CDG2+SDG4, (e) CDG2+ADG4 and (f)
 CDG2+CDG4.

Next the OWMRA is applied on the vibratory measured signal according to the methodology developed by Djebala et al. in [21]. The methodology encompasses several sequential steps.

Initially, the measured signal undergoes a decomposition process into multiple details and approximations, facilitated by an appropriately selected wavelet. Following this, the kurtosis values for all these distinct components are computed. Among these components, the one with the highest kurtosis value is singled out as the optimal vector. Subsequently, a demodulation technique utilizing the Hilbert transform is applied to this chosen optimal vector. This multi-step process ultimately leads to the extraction of an envelope spectrum, representing the final outcome of the methodology.

Figure (2.20) displays the envelope spectra obtained after the application of the OWMRA on all the measured signals. For single defect case (figure 2.20. a and b), the component corresponding to the rotation frequency of the defective gear is not identifiable on the spectra.

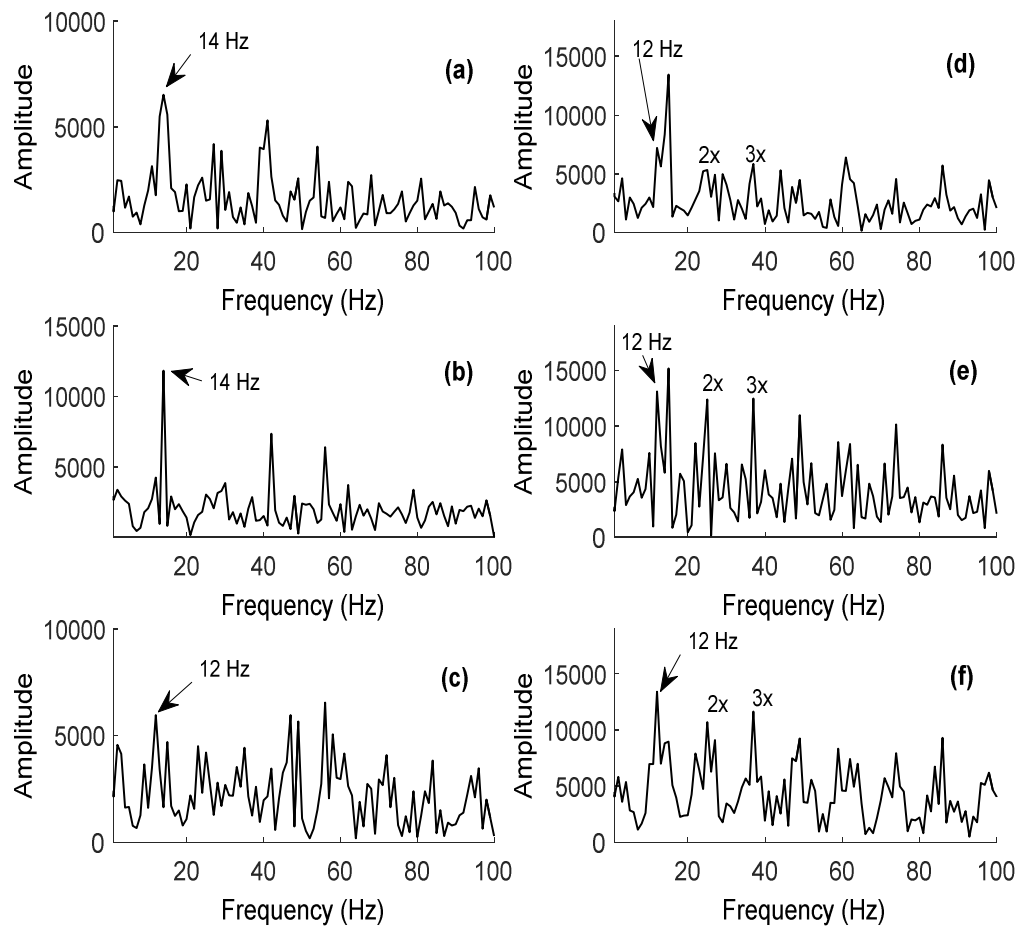


Figure 2.20. Envelope spectra obtained from Optimized WMRA

(a) SDG2, (b) ADG2, (c) CDG2, (d) CDG2+SDG4, (e) CDG2+ADG4 and (f) CDG2+CDG4.

For the case of great defect (figure 2.20. c) and double defect (figure 2.20. d), only the peak corresponding to the rotation frequency 12 Hz is observed (defect on gear 2), the one

corresponding to the small defect on gear 4 (17 Hz) is not obvious. Even for the other double defects (figure 2.20. e and f), only the frequency corresponding to the great defect on gear 2 is detectable. The pronounced noise levels within the measured signals hinder the OWMRA from clearly discerning the distinct gear defects.

6.3.2. Results obtained by cyclostationary analysis

As mentioned earlier, cyclostationary analysis is well-suited for detecting modulation phenomena caused by defects, such as those occurring in rolling bearings and gears. This approach offers two representations: the Modulation Intensity Distribution (MID) and its integrated counterpart, the Integrated Modulation Intensity Distribution (IMID). In the context of defect diagnosis where we seek to identify the modulation frequency (defect frequency), the IMID plot is the preferred choice. It can be interpreted as a simplified envelope spectrum. In contrast, MID provides a 3D representation that displays both the carrier and modulating frequencies on the same plot.

Figure (2.21) provides a representation of the Integrated Modulation Intensity Distribution (IMID) spectra for various defect severities. The results obtained through the Wavelet Multi-Resolution Analysis (WMRA) and the cyclostationary approach are closely aligned. However, it's important to note that the identification of defects proves challenging for small and moderate defects and even more so for large and combined ones. For instance, defects like SDG2 and ADG2, which operate at a frequency of 12 Hz, are obscured by misalignment defects on the shaft rotating at 14 Hz. Consequently, the peaks corresponding to 12 Hz and their harmonics (24 Hz and 36 Hz) are intertwined with those related to 14 Hz and its harmonics (28 Hz, 42 Hz, and 56 Hz). When analyzing signals linked to double defects, only the frequency of the significant defect (CDG2) becomes evident, while no peak corresponding to the defect on the fourth gear (17 Hz) emerges, regardless of the defect size.

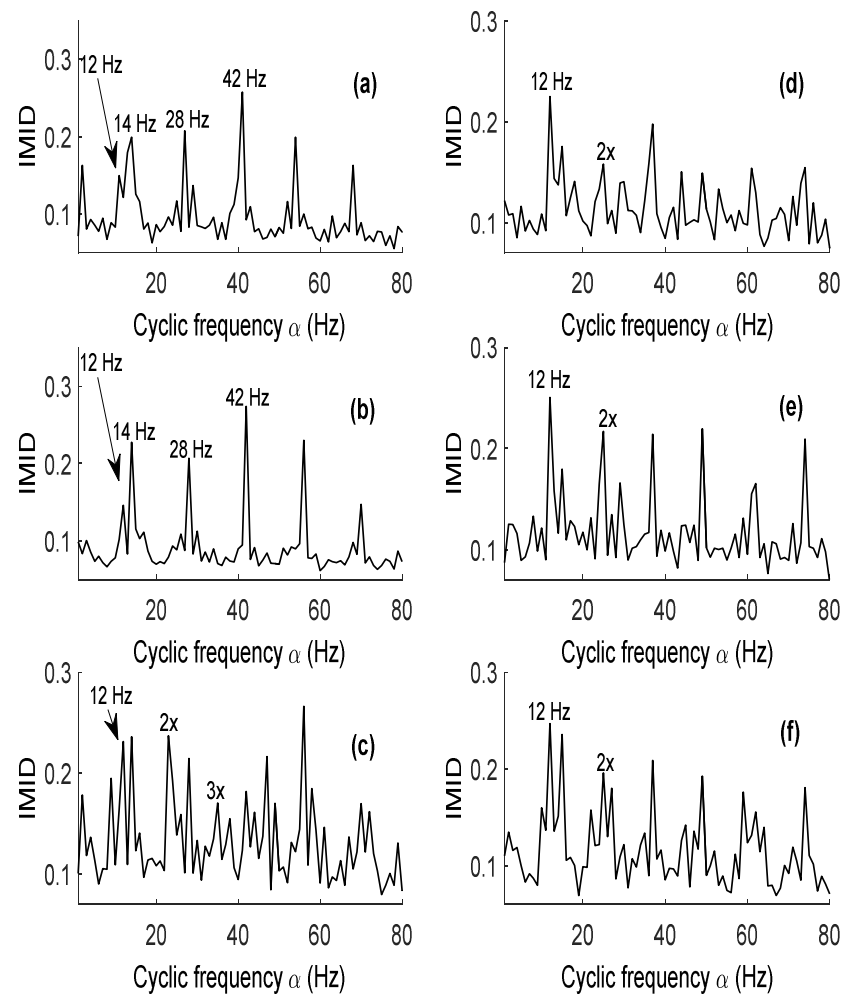


Figure 2.21. IMID spectra obtained by cyclostationary analysis

SDG2, (b) ADG2, (c) CDG2, (d) CDG2+SDG4, (e) CDG2+ADG4 and (f) CDG2+CDG4.

6.3.3. Results obtained by ICEEMDAN-MVD

In this section a hybrid method is applied as developed by Chaabi et al. in [22]. This approach has been developed to detect rolling bearing defects in variable regime. The methodology involves several steps: First, the measured signals are subjected to decomposition using the improved Complete Ensemble Empirical Mode Decomposition with Adaptive Noise (CEEMDAN) method, resulting in several Intrinsic Mode Functions (IMFs). Kurtosis is employed to identify the most pertinent IMF. Following IMF selection, a multivariate denoising technique combining wavelet and Principal Component (PCA) analyses is applied to the chosen IMF. Finally, a demodulation approach is employed on the denoised optimal IMF, leading to the generation of an envelope spectrum. Figure (2.22. a-f)

illustrates the envelope spectra corresponding to various defect severities. Notably, the results obtained through this hybrid approach closely align with those obtained from the two previous methods.

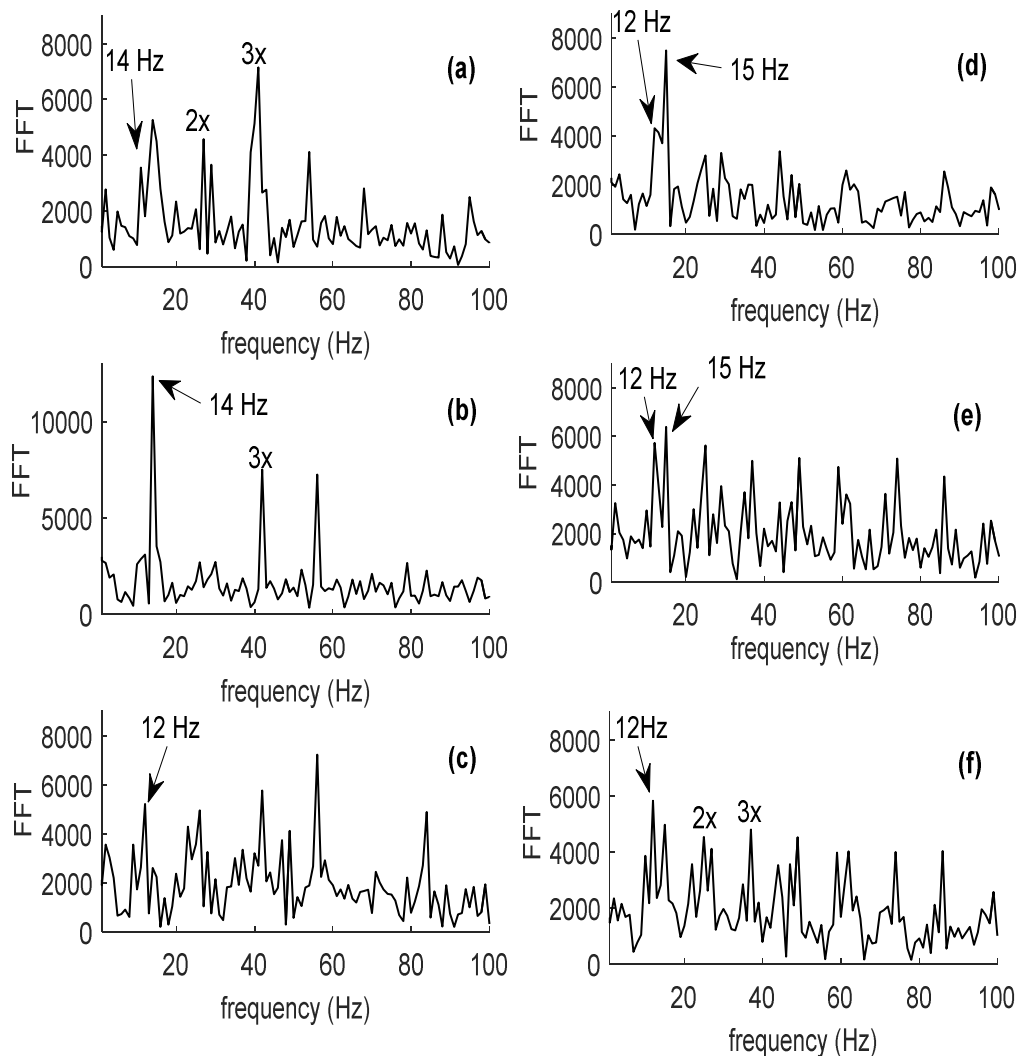


Figure 2.22. Envelope spectra obtained from the ICEEMDAN-MVD hybrid method for (a) SDG2, (b) ADG2, (c) CDG2, (d) CDG2+SDG4, (e) CDG2+ADG4 and (f) CDG2+CDG4.

In the presence of noisy signals and the influence of shaft misalignment, the three methods employed in this study (Wavelet Multi-Resolution Analysis or WMRA, cyclostationarity analysis, and the ICEEMDAN-based approach) encounter difficulty in clearly identifying small and moderate defects on gear 2. However, they are capable of detecting the large defect on the same gear. Conversely, identifying small, moderate, and critical defects on gear 4 proves unattainable, especially when these defects are combined with a critical defect on gear 2. In contrast, the utilization of sound perception allows for the identification and ranking of

defects on both single and double gears in ascending order of severity. Furthermore, the correlation of results obtained through perception with the scalar indicators derived from vibratory signals yields a mathematical model capable of effectively monitoring the condition of gears in rotating machinery.

7. Conclusion

The primary objective of this chapter was to explore the application of the sound perception method for the analysis of gear defects in rotating machinery. This involved the transformation of measured vibration signals into audible sounds, followed by a comprehensive analysis using pairwise comparison tests. The goal was to establish a mathematical relationship between the perception of these sounds and the scalar indicators derived from the measured signals. The results of the perception tests revealed the capability to classify defects based on their level of gear degradation. Additionally, it was possible to distinguish between single defects and double defects within a two-dimensional proximity space with remarkable clarity. The correlation between objective metrics (such as kurtosis, peak value, and spectral center of gravity) and the perceptual differences in gear sounds, as represented by their proximity in the perceptual space, underscored the relationship between these factors. Moreover, the newly obtained indicator, DIM1, from this correlation model proves to be a valuable tool for monitoring the progression of gear defects in rotating machinery. It serves as a decision-making parameter for determining whether to halt the machine's operation. When the value of DIM1 shifts from negative to positive, it signifies the transition of a defect from a moderate to a severe state. This information aids maintenance crews in making informed decisions about machine operation and maintenance.

Furthermore, this chapter sought to compare the outcomes obtained through sound perception, especially in cases involving significantly noisy signals, with the results obtained via vibration diagnosis using three advanced signal processing techniques. The findings revealed that sound perception successfully classifies gear defects in ascending order of severity, whether they are single or double defects. In contrast, the other methods, which are grounded in complex theories, encountered challenges in identifying single gear defects like SDG2 and ADG2. Additionally, they struggled to pinpoint one of the two double defects, CDG2+ADG4 and CDG2+CDG4. The superiority of the subjective approach compared to objective one is due to the fact that the human ear is very sensitive, and can easily differentiate the sounds, thus making it possible to highlight defects in a fairly clear manner.

8. References

1. Wickelmaier, F., Ellermeier W. , Deriving auditory features from triadic comparisons. *Perception & psychophysics*, 2007. 69(2): p. 287-297.
2. Carroll, J.D. ,Chang J. J. , Analysis of individual differences in multidimensional scaling via an N-way generalization of “Eckart-Young” decomposition. *Psychometrika*, 1970. 35(3): p. 283-319.
3. Winsberg, S. and G. De Soete, A latent class approach to fitting the weighted Euclidean model, CLASCAL. *Psychometrika*, 1993. 58(2): p. 315-330.
4. Younes, R., Perception sonore au service de l’optimisation du diagnostic des défauts mécaniques de machines tournantes, 2015.
5. Kanzari, M. and N. Hamzaoui, Diagnostic vibro-acoustique des défauts d’engrenage: Analyse d’une démarche de perception sonore. *Mémoire Master II*, INSA de Lyon, 2009.
6. Mallat, S.G., A theory for multiresolution signal decomposition: the wavelet representation. *IEEE transactions on pattern analysis and machine intelligence*, 1989. 11(7): p. 674-693.
7. Djebala, A., N. Ouelaa, and N. Hamzaoui, Optimisation de l’analyse multirésolution en ondelettes des signaux de choc. Application aux signaux engendrés par des roulements défectueux. *Mechanics & Industry*, 2007. 8(4): p. 379-389.
8. Djebala, A., N. Ouelaa, and N. Hamzaoui, Detection of rolling bearing defects using discrete wavelet analysis. *Meccanica*, 2008. 43(3): p. 339-348.
9. Antoni, J., Cyclostationarity by examples. *Mechanical Systems and Signal Processing*, 2009. 23(4): p. 987-1036.
10. Živanović, G.D. and W.A. Gardner, Degrees of cyclostationarity and their application to signal detection and estimation. *Signal processing*, 1991. 22(3): p. 287-297.
11. Liu, T.-I., Lee J., Singh P. and Liu G, Real-time recognition of ball bearing states for the enhancement of precision, quality, efficiency, safety, and automation of manufacturing. *The International Journal of Advanced Manufacturing Technology*, 2014. 71(5-8): p. 809-816.
12. Tahi, M., Développement d’un système d’aide au diagnostic des machines tournantes par utilisation de l’arbre de décision, 2019.
13. Wu, Z. and N.E. Huang, Ensemble empirical mode decomposition: a noise-assisted data analysis method. *Advances in adaptive data analysis*, 2009. 1(01): p. 1-41.
14. Mahgoun, H., Chaari F., Felkaoui A. and Haddar M. Early detection of gear faults in variable load and local defect size using ensemble empirical mode decomposition (EEMD). in *Advances in Acoustics and Vibration: Proceedings of the International Conference on Acoustics and Vibration (ICAV2016)*, March 21-23, Hammamet, Tunisia. 2017. Springer.
15. Lingli, J., Liman C., Hougchuang T. and Xuejun L.. Fault diagnosis of spiral bevel gears based on CEEMDAN permutation entropy. in *Advances in Asset Management and Condition Monitoring: COMADEM 2019*. 2020. Springer.
16. Huang, N.E., Shen Z., Long S.R. and Wu M. C., The empirical mode decomposition and the Hilbert spectrum for nonlinear and non-stationary time series analysis. *Proceedings of the Royal Society of London. Series A: mathematical, physical and engineering sciences*, 1998. 454(1971): p. 903-995.

17. Torres, M.E., Colominas M. A., Schlotthauer G. and Flandrin P.. A complete ensemble empirical mode decomposition with adaptive noise. in 2011 IEEE international conference on acoustics, speech and signal processing (ICASSP). 2011.
18. Colominas, M.A., Schlotthauer G., Torres M.E. , Improved complete ensemble EMD: A suitable tool for biomedical signal processing. *Biomedical Signal Processing and Control*, 2014. 14: p. 19-29.
19. Younes, R., Hamzaoui N., Ouelaa N., and Djebala A., Perceptual study of the evolution of gear defects. *Applied Acoustics*, 2015. 99: 60-67.
20. Younes, R., Ouelaa N., and Hamzaoui N., Experimental study of real gear transmission defects using sound perception. *The International Journal of Advanced Manufacturing Technology*, 2015. 76(5-8): p. 927-940.
21. Djebala, A., Ouelaa N., Hamzaoui N. , Optimisation de l'analyse multirésolution en ondelettes des signaux de choc. Application aux signaux engendrés par des roulements défectueux. *Mécanique & industries*, 2007. 8(4): 379-389.
22. Chaabi, L., Lemzadmi A., Djebala A., Bouhlais M. L., Ouelaa N., Fault diagnosis of rolling bearings in non-stationary running conditions using improved CEEMDAN and multivariate denoising based on wavelet and principal component analyses. *The International Journal of Advanced Manufacturing Technology*, 2020: 1-15.

Chapter three

Detection of gear defects in variable regime using a new hybrid objective approach

1. Introduction

Machines that operate under variable conditions are those capable of functioning effectively at variable speeds or loads. In contrast to fixed-speed machines, which operate at a constant speed, variable-speed machines are designed to adapt to varying loads, thus rendering them more efficient and flexible. These machines find extensive use across multiple industrial sectors, including aerospace, automotive, energy, shipbuilding, and others. They are particularly well-suited for high-performance and high-flexibility applications such as gas turbines, compressors, pumps, and electric motors. The variable-speed operation of machines is enabled by advanced technologies such as electronic controls, load and speed sensors, and automated control systems. These technologies allow the machines to automatically adjust to load variations, maintain a constant rotational speed, optimize energy efficiency, and prolong machine lifespan. Ultimately, variable-speed machines offer significant benefits in terms of efficiency, flexibility, and performance. They have emerged as an essential element in many industrial processes and continue to play a pivotal role in the successful completion of construction and infrastructure projects.

The objective of this chapter is to propose a new hybrid objective method especially adapted for the detection of gear defects under variable condition.

2. Gear faults detection in variable regime

In the steady state regime, the signal of an undamaged pair of gears is dominated by the meshing frequency and several of its harmonics. Frequency components corresponding to the shafts' rotational speed are also visible. Figure (3.1) shows a typical spectrum of one-stage gear transmission with a wheel and a pinion turning at 25 Hz and 50 Hz, respectively. The meshing frequency is taken equal to 1500 Hz. On the spectrum the meshing frequency and its

harmonics as well as the rotation speeds of the shafts carrying the two gears are normally visible.[1]

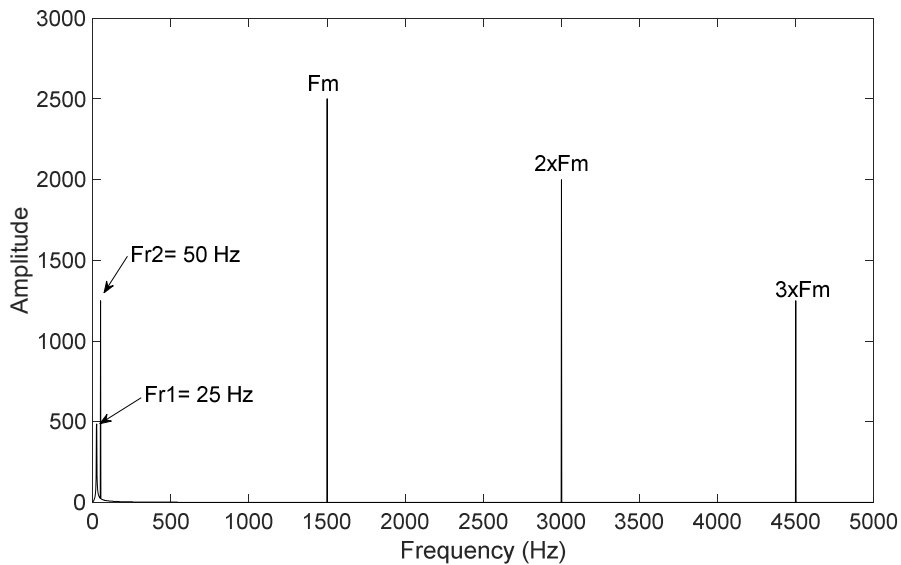


Figure 3.1. Typical spectrum of an undamaged pair of gears.

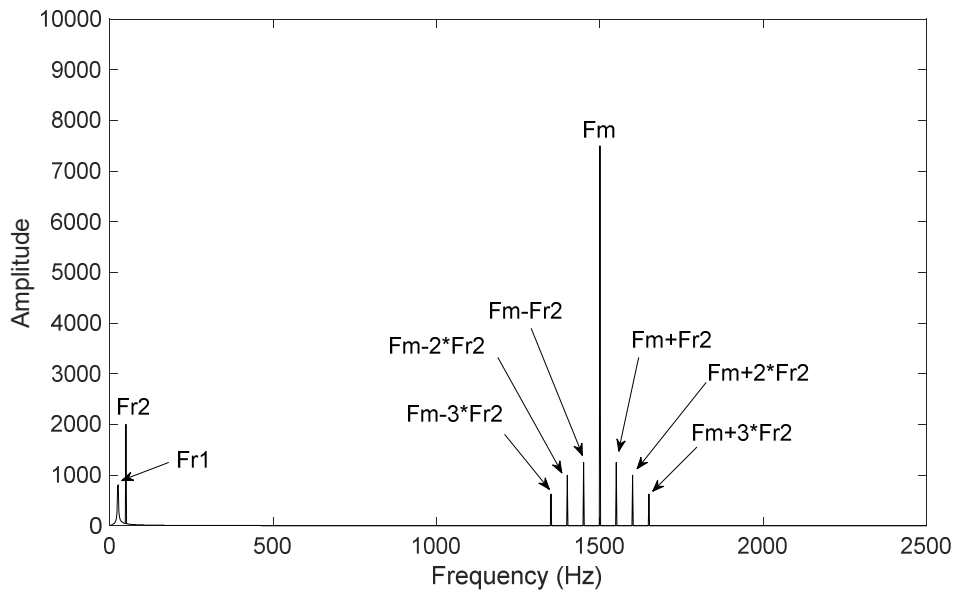


Figure 3.2. Spectrum in the case of small defect located on the gear turning at $Fr_2 = 50$ Hz.

In the case of a damaged gear periodical shocks are produced with each contact of the defective tooth against any other. A modulation phenomenon occurs on the spectrum, this last will show many sidebands around the meshing frequency and its harmonics. These sidebands are spaced by the rotational frequency of the shaft carrying the defective gear. As the previous example, a spectrum corresponding to a small defect on the wheel is highlighted in figure

(3.2). It shows sidebands around the meshing frequency spaced by 50 Hz, which indicates that the gear turning at 50 Hz is the defective one.

Two powerful detection tools are tested on an experimental signal measured in constant regime. Figure (3.3) represents the acceleration signal measured on gear transmission with defective wheel. The rotation speed of the defective gear is taken equal to 14 Hz and the number of teeth is 18, consequently the meshing frequency is equal to 252 Hz. Periodical impacts due to the defect are clearly visible on the signal. The spectrum of figure (3.4) confirms the presence of gear defect since it clearly shows many sidebands around the meshing frequency and its harmonics spaced with the rotation frequency of the defective gear.

Applying cepstrum analysis on the signal of figure (3.3) highlights a main component corresponding to a quefreny of 0.07 s (1/14 Hz) and several of its rhamonics as shown in figure (3.5). This quefreny corresponds perfectly to the rotation frequency of the shaft carrying the defective gear (14 Hz).

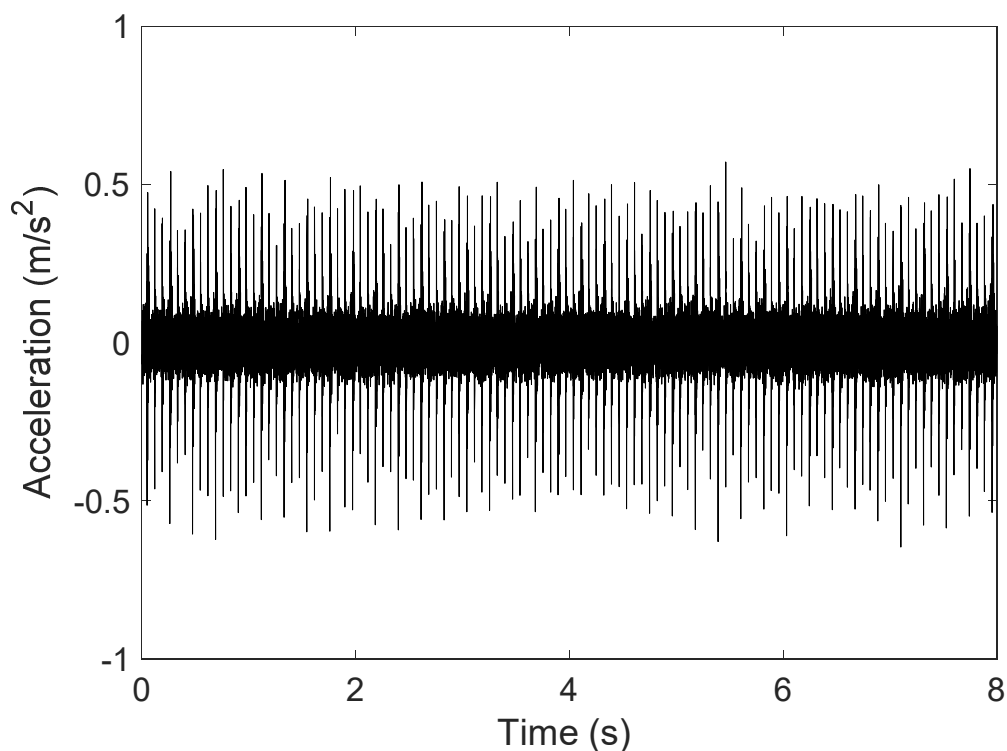


Figure 3.3. Signal of extracted tooth defect.

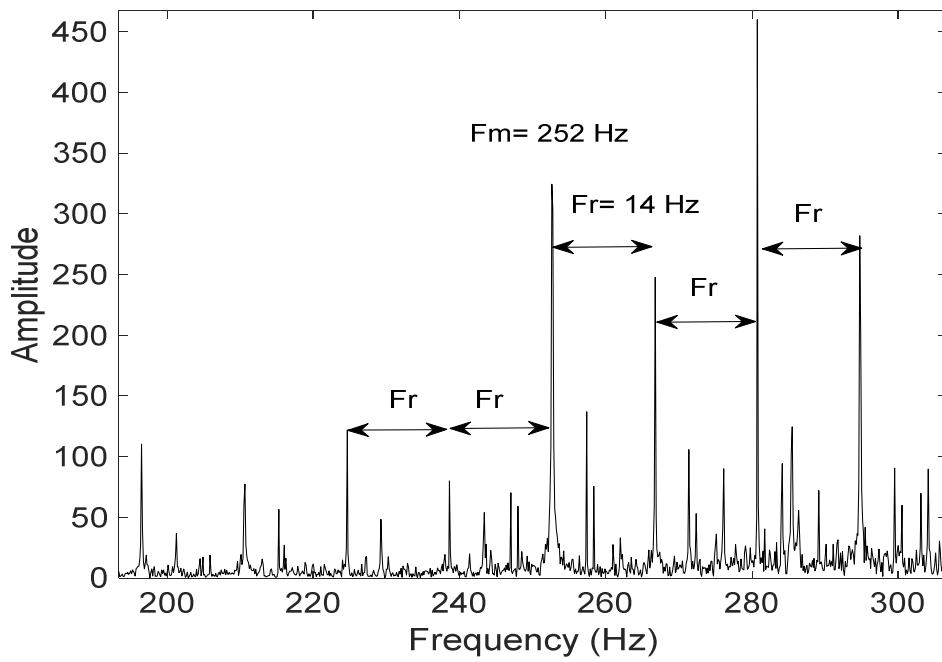


Figure 3.4. Spectrum of an extracted tooth defect.

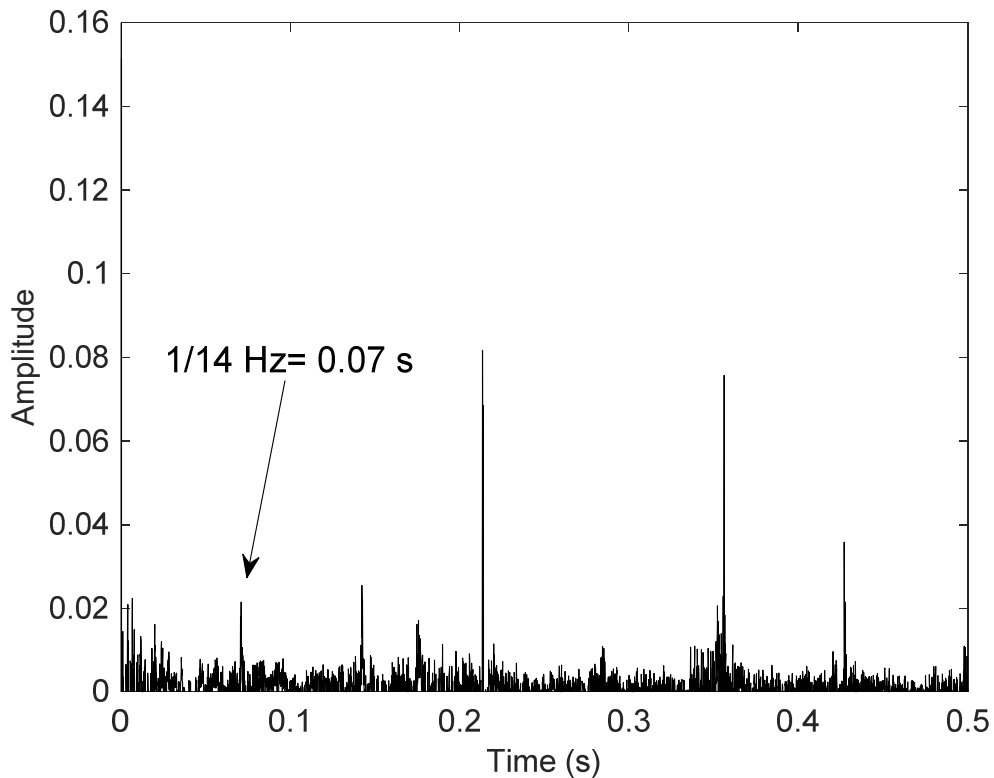


Figure 3.5. Cepstrum in the case of extracted tooth defect.

On the other hand, an envelope spectrum is performed after the application of demodulation approach using Hilbert transform. Figure (3.6) shows a main component corresponding to the

rotation frequency of the gear turning at 14 Hz and several of its harmonics, which means that it is the defective one. In conclusion, on the steady state regime the defect is obviously detected by the two considered tools.

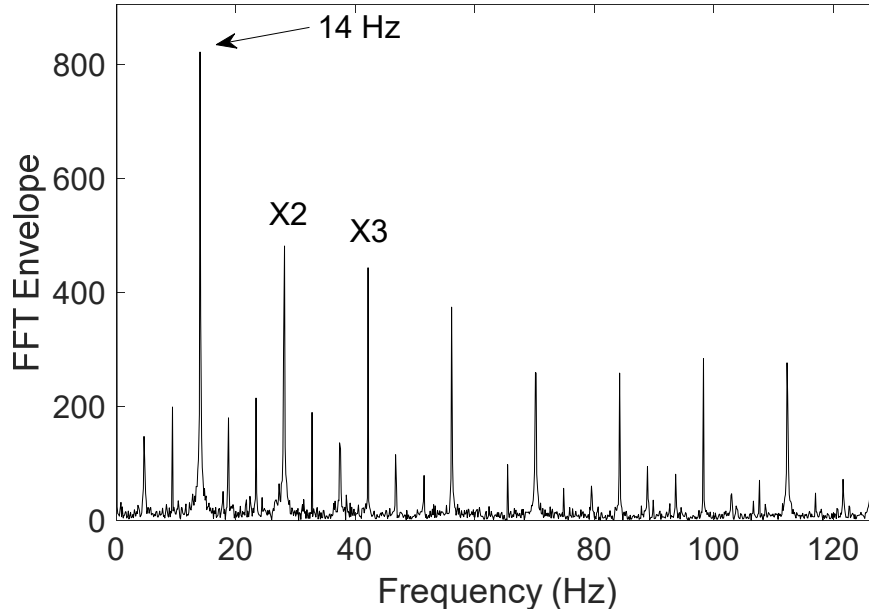


Figure 3.6. Envelope spectrum in the case of extracted tooth defect.

Now, let's consider the same defect but in this case the rotation speed varies by an acceleration mode from 0 rpm to 840 rpm in 10.8 s as shown in figure (3.7). Its corresponding spectrum of figure (3.8) doesn't indicate any information about the defect.

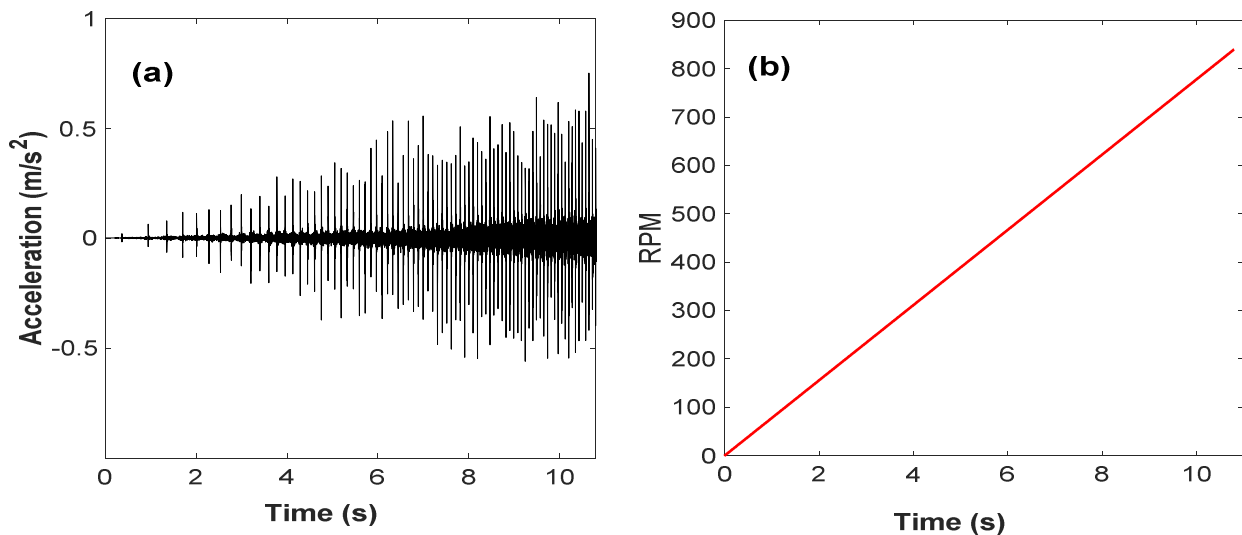


Figure 3.7. Signal of extracted tooth defect measured in acceleration regime: (a) Pure signal and (b) rpm signal.

As the rotation frequency is variable, the meshing frequency is also variable, and in this case the modulations are impossible to detect. Neither the cepstrum nor the envelope spectrum are able to detect the defect, (see figure 3.9.a,b). Consequently, it's very hard, even impossible, to detect gear defect in variable regime by conventional approaches, even using robust methods like the cepstrum and the envelope spectrum.

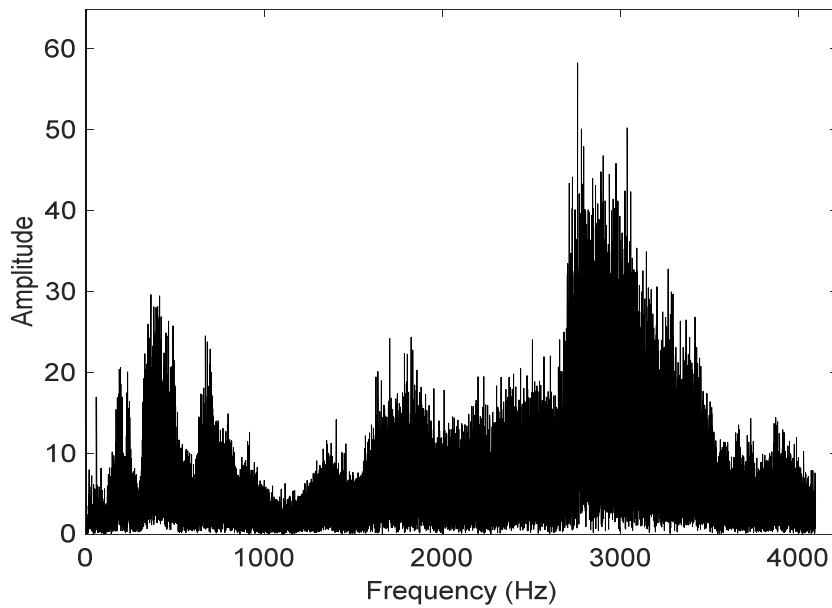


Figure 3.8. Spectrum of the signal in the case of variable regime.

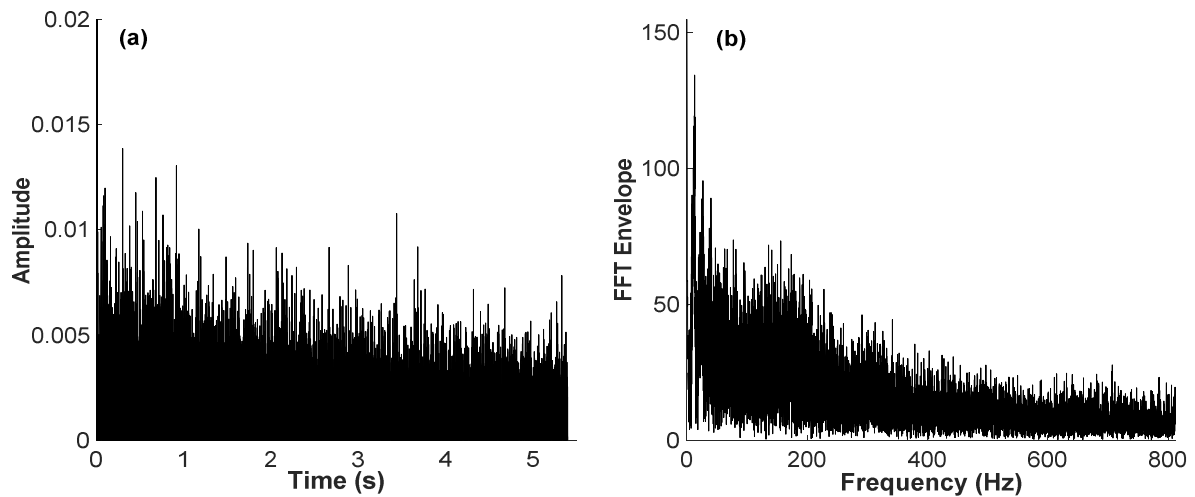


Figure 3.9. (a) Cepstrum and (b) Envelope spectrum of the signal in the case of extracted tooth defect in variable regime.

3. Theoretical background

3.1. Multivariate denoising using wavelet and PCA analysis

Multivariate denoising using wavelet and PCA analysis is a commonly utilized signal processing technique to eliminate noise from multi-dimensional signals or datasets. This involves the application of wavelet transform and principal component analysis (PCA) to a set of observations or measurements to segregate the useful signal or information from the unwanted noise or components. The use of wavelet transform as a mathematical tool decomposes signals into diverse frequency components, allowing them to be used in multi-dimensional signals, such as images or spectra, and resulting in a more efficient representation than traditional Fourier transform. When denoising, wavelet analysis is frequently used to identify and isolate noisy signal components. PCA is a statistical method employed to decrease the dimensionality of a data set while preserving the most significant information. This technique finds principal components, which are linear combinations of the original variables capturing the greatest amount of variation. By holding onto only the most critical components, PCA can aid in noise removal and decrease the complexity of the data set. The new algorithm is summarized as below [2] :

1. Perform the wavelet transform at level J of each column of $x(t)$.
2. For $1 \leq j \ll J$, perform the PCA of the details matrix D_j and select an appropriate number p_j of useful principal component of suppress the detail D_j .
3. Do again the previous step for the approximation matrix A_j .
4. Reconstruct new matrix \check{x} by the inverse wavelet transform from the simplified details and approximations.
5. Perform the PCA of matrix \check{x} and build adequate statistic for statistical Process Control (SPC).

3.2. Order tracking analysis

As shown before, monitoring gear defects is impossible with conventional methods when the operating conditions are variable, especially speed and load. In this case the analysis of vibratory signals must be achieved in order domain rather than frequency domain. For the order analysis, it is necessary to sample the vibration signal at constant angular increments and therefore at a rate proportional to the shaft speed [3].

In stationary regime the characteristic frequency of gear defect is equal to the rotation frequency of the shaft carrying the defective gear:

$$F_d = F_r$$

By analogy with rolling bearing defects this characteristic frequency can then be given by :

$$F_d = C.F_r$$

Where F_r is the rotation speed of the defective gear, and C a constant equal to 1, this constant is named defect order. In rolling bearing defects this constant is calculated from the geometrical characteristics of the bearing and is different from one type of bearing defect to another. As solution to speed variation effect, it is therefore common to look for this constant rather than the characteristic frequency which is variable. For this, an order spectrum must be performed rather than frequency spectrum.

4. Proposed approach

The proposed approach aims to use hybrid method to allow detection of gear defects in variable regime. The most important steps are as follow :

- First, applying the kurtogram [4] on the measured signal allows locating the frequency range that covers the information corresponding to gear defect and having the highest kurtosis value. Indeed, gear defect induces periodical chocks and the kurtosis is the most sensitive indicator to defects inducing periodical impulsive forces.
- In the second step, the Improved CEEMDAN [5-9] is used to decompose the raw signal into different IMFs. This method will isolate the signature of the gear defect in specific IMF.-
- Based on the kurtogram plot, the relevant IMF is selected. This IMF will contain the optimal information about the gear defect.
- After isolating the IMF covering the optimal frequency band selected by the kurtogram and kurtosis value, multivariate denoising based on wavelet and PCA method is applied to remove the residual noise and increase the SNR of the selected IMF to give more effective result.
- Finally, order analysis is performed on the optimal denoised IMF to remove the speed variation effect, then envelope analysis based on Hilbert spectrum is performed to obtain an order envelope spectrum highlighting the defect order and its harmonics.

Figure (3.10) summarizes the global flowchart of the proposed approach.

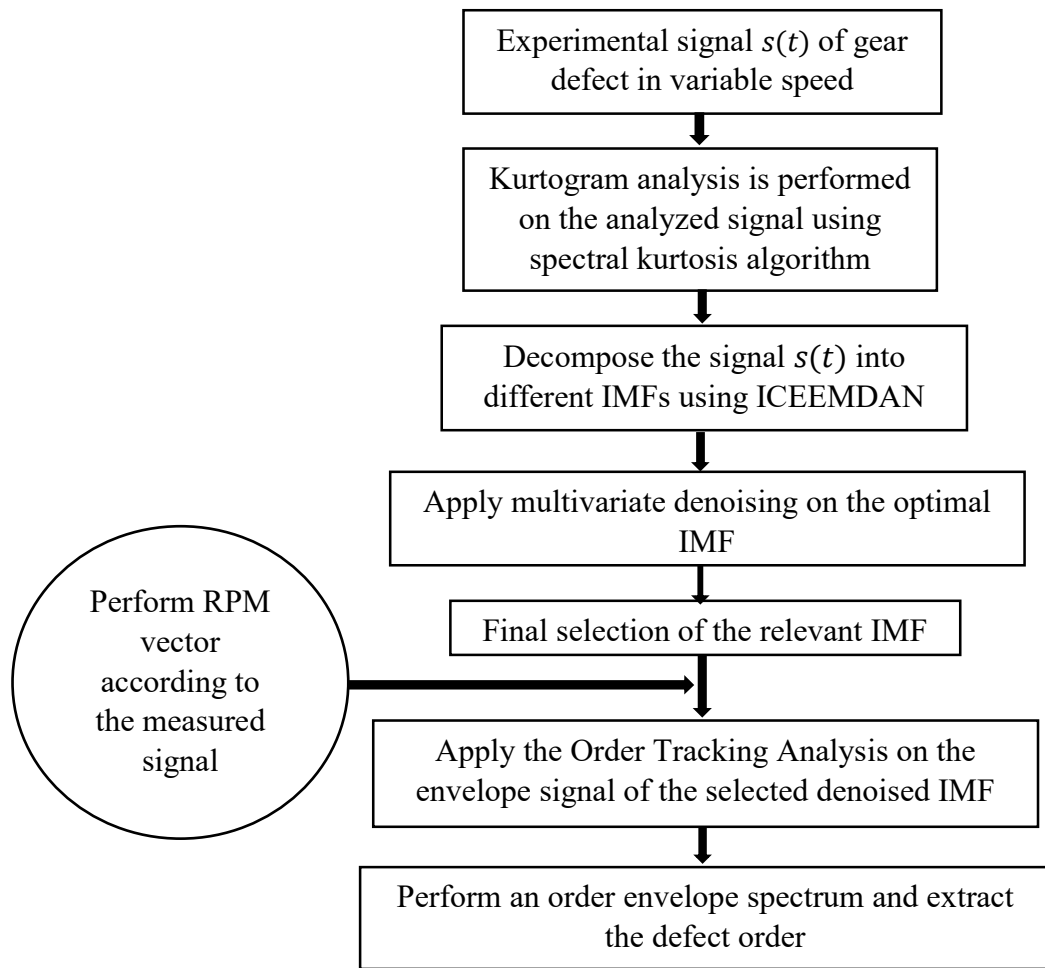


Figure 3.10. Global flowchart of the proposed method.

5. Experimental procedure

The data used in the current study are measured on the Machinery Faults Simulator (MFS) test rig of the university of SoukAhras and using SpectraQuest processing software. The post processing using the proposed approach is carried out under Matlab. The MFS test rig consists mainly of an electric motor with 0.75 KW and a maximum rotation speed of 6000 rpm, coupling, belt transmission ($d_1=51$ mm, $d_2=126$ mm and $L=965$ mm) with transmission ratio equal to 0.4, and finally a gearbox as shown in figure (3.11). The one-stage gearbox contains two wheels of straight cut bevel teeth with 1.5:1 ratio normally lubricated and manually adjustable. A magnetic brake is used to simulate the load. The input and output wheels have 18 and 27 teeth, respectively, the transmission ratio is then equal to 0.67. Two accelerometers were used to measure vibratory signals. The first one is a bidirectional accelerometer placed

on the top of the gearbox reducer (axial, radial), and the second one is mounted horizontally. A tachometer is used to measure the rotation speed of the motor shaft allowing the rpm signal.



Figure 3.11. Experimental setup.

Three different gearboxes are used having each one a different gear defect, half-tooth extracted defect D1 (grey gearbox), generalized defect DG (red gearbox), and extracted tooth defect D2 as illustrated on table (3.1) and figure (3.12). For all the three gearboxes the defective gear is the one having 18 teeth mounted on the input shaft.

Trial	Gear defect	Code	Mode of operation for the three types of defects
1	Half-extracted tooth defect	D1	Acceleration from 0 Hz to 14 Hz
2	Generalized defect	DG	Constant regime at 14 Hz
3	Extracted tooth defect	D2	Deceleration from 14 Hz to 0 Hz

Table 3.1. Experimental plan.

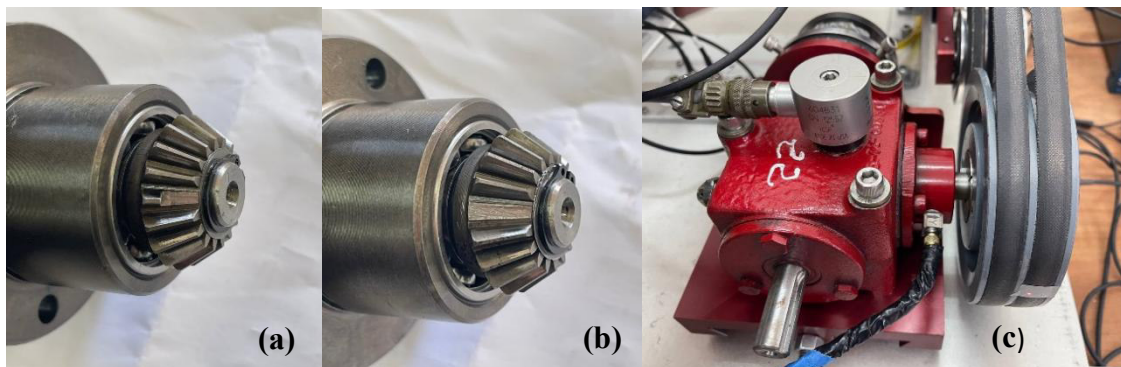


Figure 3.12. (a) Half-extracted tooth defect, (b) Extracted tooth defect, (c) Generalized defect.

A combined regime having three different modes is considered in this study. The first is an acceleration mode from 0 Hz to 14 Hz (0 rpm to 840 rpm) within 10.8 s. The second mode is a steady-state regime at 14 Hz (840 rpm) for 5.4 s, and finally the third mode is a deceleration from 14 Hz to 0 Hz (840 rpm to 0 rpm) for 11.5 s.

6. Results and discussion

6.1. Case of extracted tooth in acceleration mode

6.1.1. Choice of the optimal frequency range

The proposed approach is first applied on the signal shown in figure (3.7). Note that the spectrum, cepstrum and envelope spectrum were incapable to detect the gear defect in variable speed (Acceleration mode). As first step the kurtogram of the signal is calculated indicating the high kurtosis values in the frequency range of [1600 Hz-3200 Hz] (see figure 3.13). This result shows that the highest kurtosis values are located in high frequency range and not usually around the meshing frequency as mentioned in section 2.

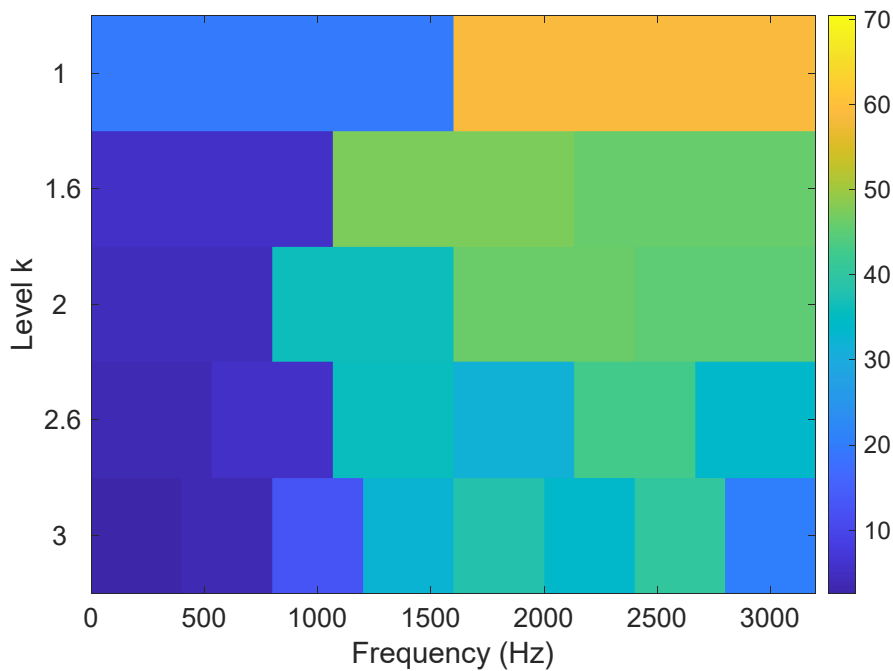


Figure 3.13. Kurtogram of the signal of extracted tooth defect.

6.1.2. Improved CEEMDAN decomposition and selection of the relevant IMF

The Improved Complete Ensemble Empirical Mode Decomposition with Adaptive Noise (ICEEMDAN) is applied to decompose the signal into several Intrinsic Mode Functions (IMF). Only the first four IMFs are retained, the others correspond to low frequency and

consequently don't have significant contribution in the defect detection. The spectra of IMF1 and IMF2 of figure (3.14) show modulation in the frequency band selected from the kurtogram [1600 Hz-3200 Hz]. However, IMF2 has the highest kurtosis value, 73.86 against 58.14 for IMF1, for this reason it will be taken as optimal IMF in the next step.

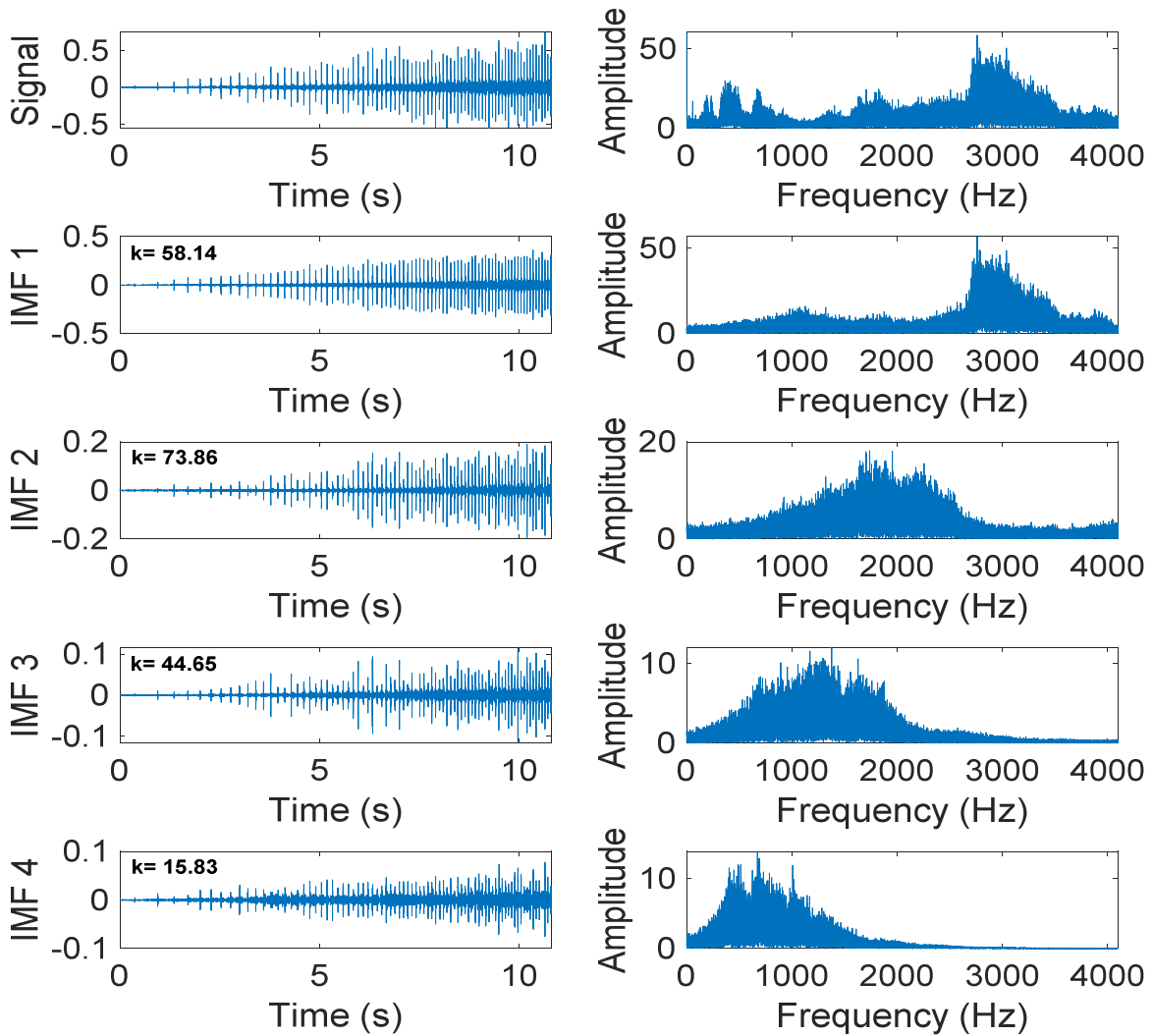


Figure 3.14. IMFs and corresponding spectra obtained after the application of ICEEMDAN.

6.1.3. Wavelet denoising and order tracking analysis

A wavelet denoising is applied on the optimal IMF to remove the residual noise added by ICEEMDAN and improve the Signal to Noise Ratio (SNR), the kurtosis value is increased from 73.86 to 96.81, (see figure 3.15.a, b). Finally, Order Tracking Analysis (OTA) is applied on the denoised IMF to remove the speed variation effect. In this case the rpm signal

corresponding to the gearbox input shaft (carrying the defective gear) is used in the OTA algorithm (acceleration from 0 Hz to 14 Hz). Figure (3.15.c) represents the order envelope spectrum highlighting the order of the defect (order 1 of the rotating frequency) and several of its harmonics, which indicates that the wheel mounted on the input shaft is the defective one.

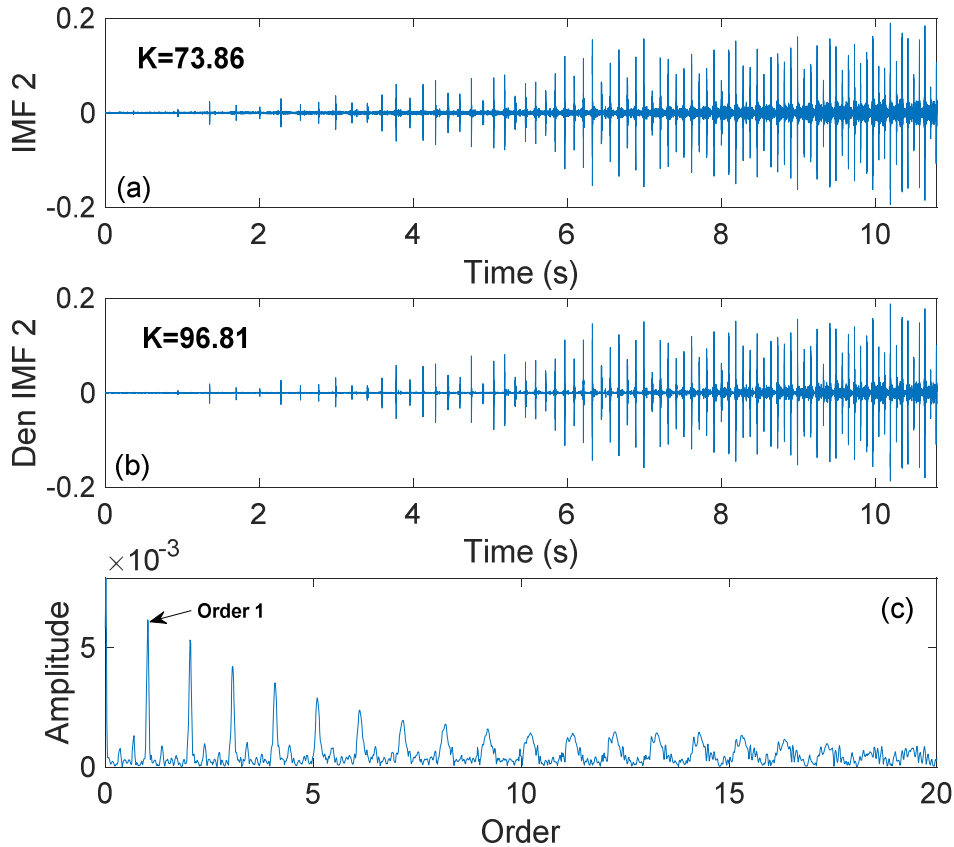


Figure 3.15. (a) Optimal IMF, (b) Denoised IMF, (c) Order envelope spectrum.

6.1.4. Case of non-appropriate rpm signal

In practice the defect is not previously known as in laboratory tests. Both the defective wheel and the shaft carrying it are unknown. Consequently, the rpm signal to be used in the Order Tracking Analysis is also unknown. It is then interesting to test what happens when the OTA algorithm is alimented with the “wrong” rpm signal, i.e., that which not correspond to the shaft carrying the defective wheel. Figure (3.16) shows the order envelope spectrum obtained after the application of the proposed approach on the previous case using rpm signal of the output shaft (acceleration from 0 Hz to 8.4 Hz) instead of the input shaft. In this case the envelope order spectrum shows main order corresponding to 1.71 which means that the defect is not on the wheel mounted on the output shaft.

In practice it is then necessary to test the OTA algorithm with the rpm signals of all the gearbox shafts. The one allowing an envelope order spectrum with a main order equal to 1 is that carrying the defective gear.

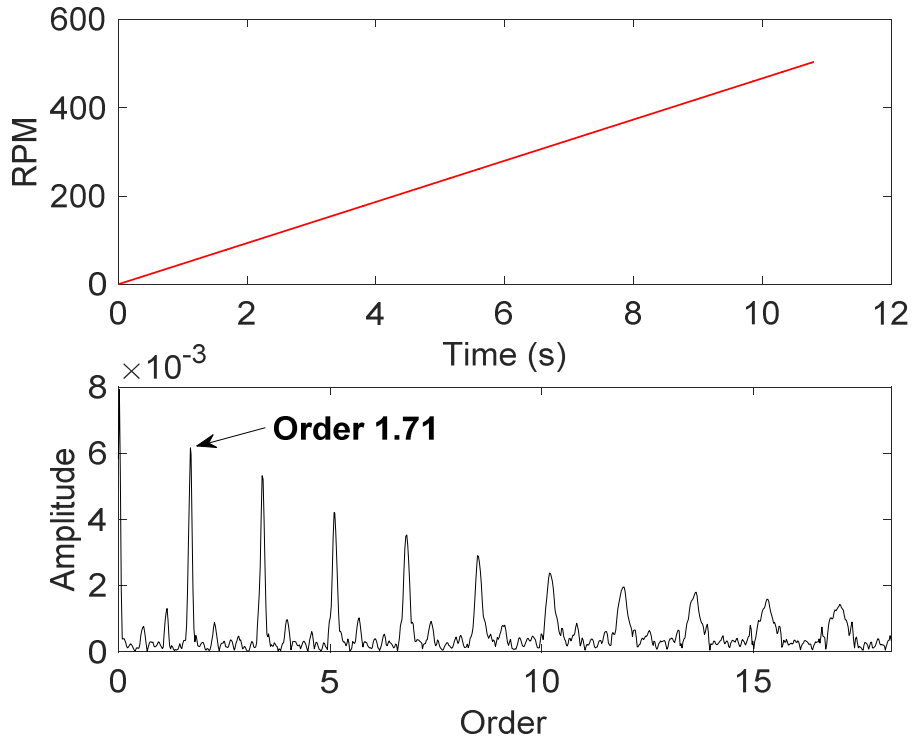


Figure 3.16. Order envelope spectrum with the rpm signal of output shaft.

6.1.5. Case of non-appropriate selection of the relevant IMF

To confirm the validity of the adopted approach for the selection of the optimal IMF, the IMF7 whose frequency band covers the meshing frequency range (from 0 Hz to 252 Hz) is treated as mentioned in the literature for the steady-state regime (cf. section 2). The final result shown in figure (3.17) indicates that the kurtosis value is very weak (8.7) compared to the optimal IMF2 (73.86) taken above. Moreover, the wavelet denoising has apparently no effect since the kurtosis before and after denoising is the same. The order envelope spectrum shows the order of the rotation speed of the defective gear, but the results remain poor compared to those of figure (3.15). This confirms that the kurtogram is the best tool to select the optimal IMF.

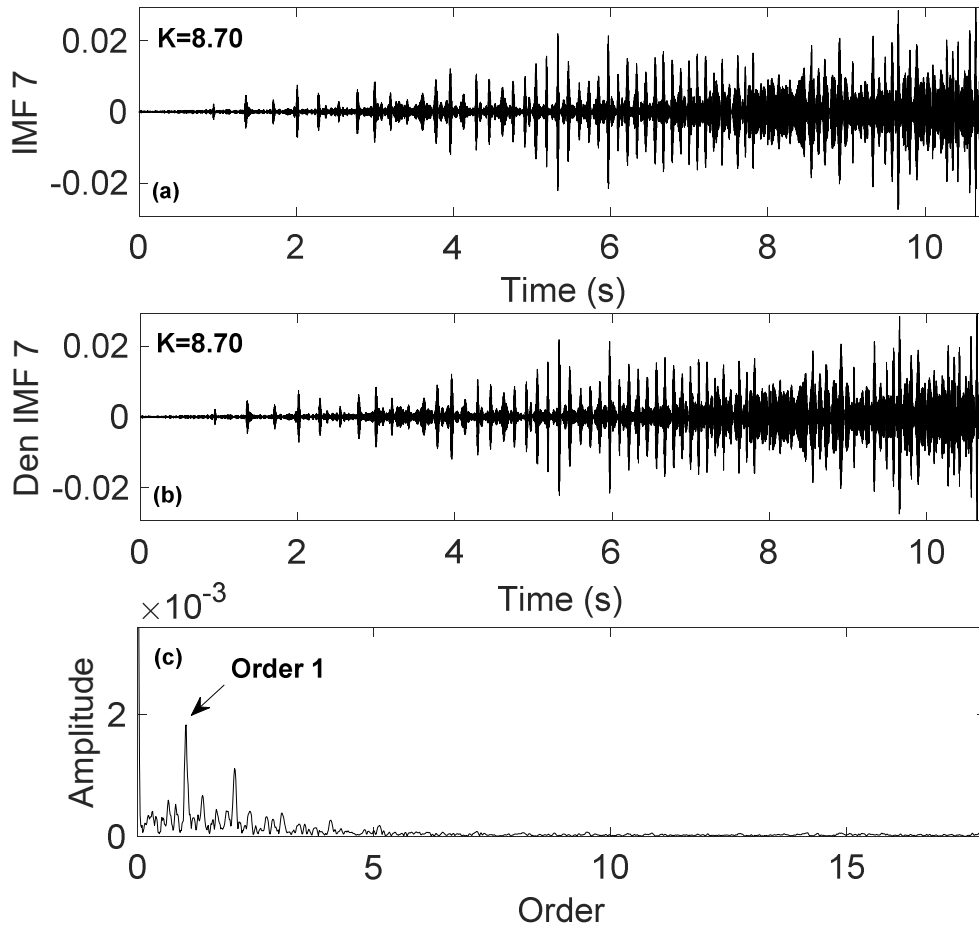


Figure 3.17. (a) IMF7 signal, (b) Denoised IMF7, (c) Order envelope spectrum.

6.2. Case of extracted tooth in deceleration mode

Consider now the same defect in the case of deceleration mode from 14 Hz to 0 Hz. Figure (3.18.a, b) represents the measured signal and its corresponding rpm signal. The final result obtained after the application of the proposed approach is shown in figure (3.18.c). The order envelope spectrum clearly highlights the order 1 corresponding to the rotation frequency of the input shaft and its harmonics.

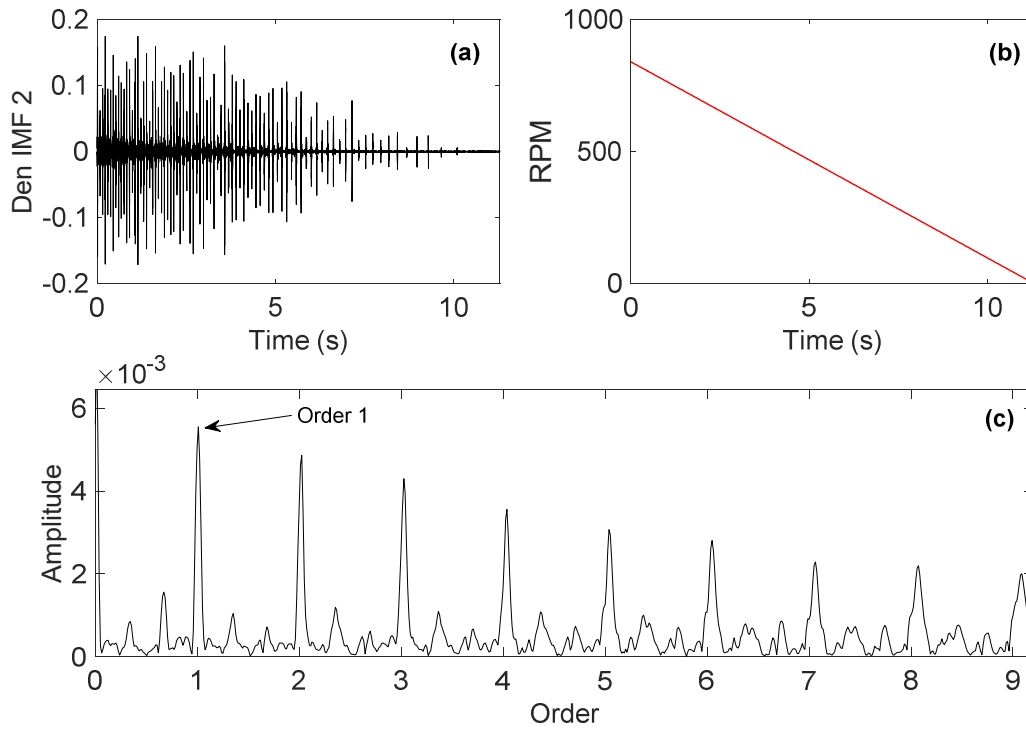


Figure 3.18. (a) Signal of the extracted tooth in the case of deceleration mode (b) rpm signal (c) Order envelope spectrum.

6.3. Case of extracted tooth in combined mode (Acceleration-steady state regime-deceleration)

In this case a more complicated variation regime is considered, three speed variation modes are used, acceleration from 0 Hz to 14 Hz in 10.8 s, constant speed at 14 Hz during 5.4 s, and finally deceleration mode from 14 Hz to 0 Hz in 11.5 s, as shown in figure (3.19.a, b). The proposed method is applied as mentioned before leading to the order envelope spectrum of figure (3.19.c), the order of the rotation speed of the input shaft is clearly visible which confirms another time that the defective wheel is that mounted on the input shaft.

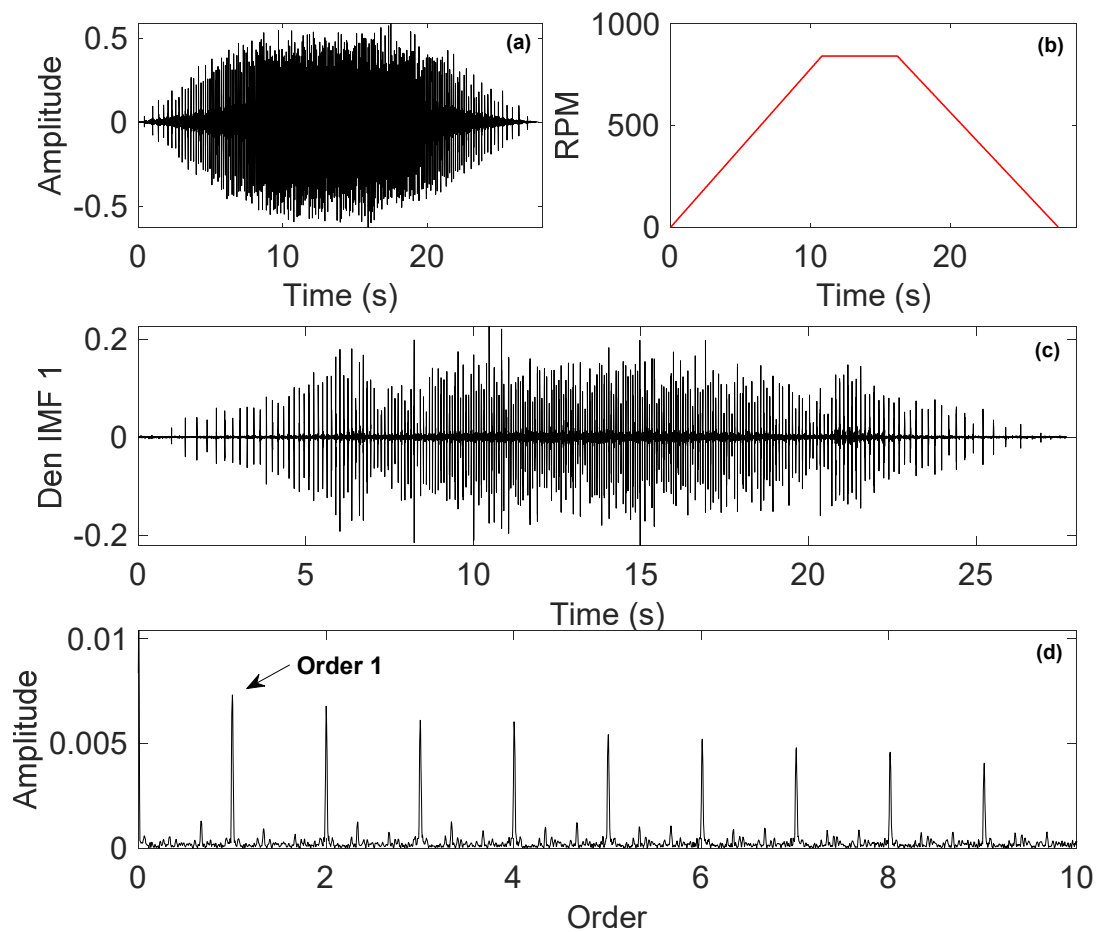


Figure 3.19. (a) Original signal of extracted tooth defect (b) rpm signal (c) denoised IMF (d) Order envelope spectrum in combined mode.

6.4. Case of generalized defect in combined mode

Figure (3.20.a) shows the signal of generalized defect measured in combined mode as mentioned in the rpm signal of figure (3.20.b). In this case the impacts are not visible on the measured signal as in the case of extracted tooth, consequently the detection will be more difficult. As final result and after applying the proposed approach the order 1 of the rotation speed is obtained and some of its harmonics, which confirms the presence of gear defect in the input shaft, (see figure 3.20.c).

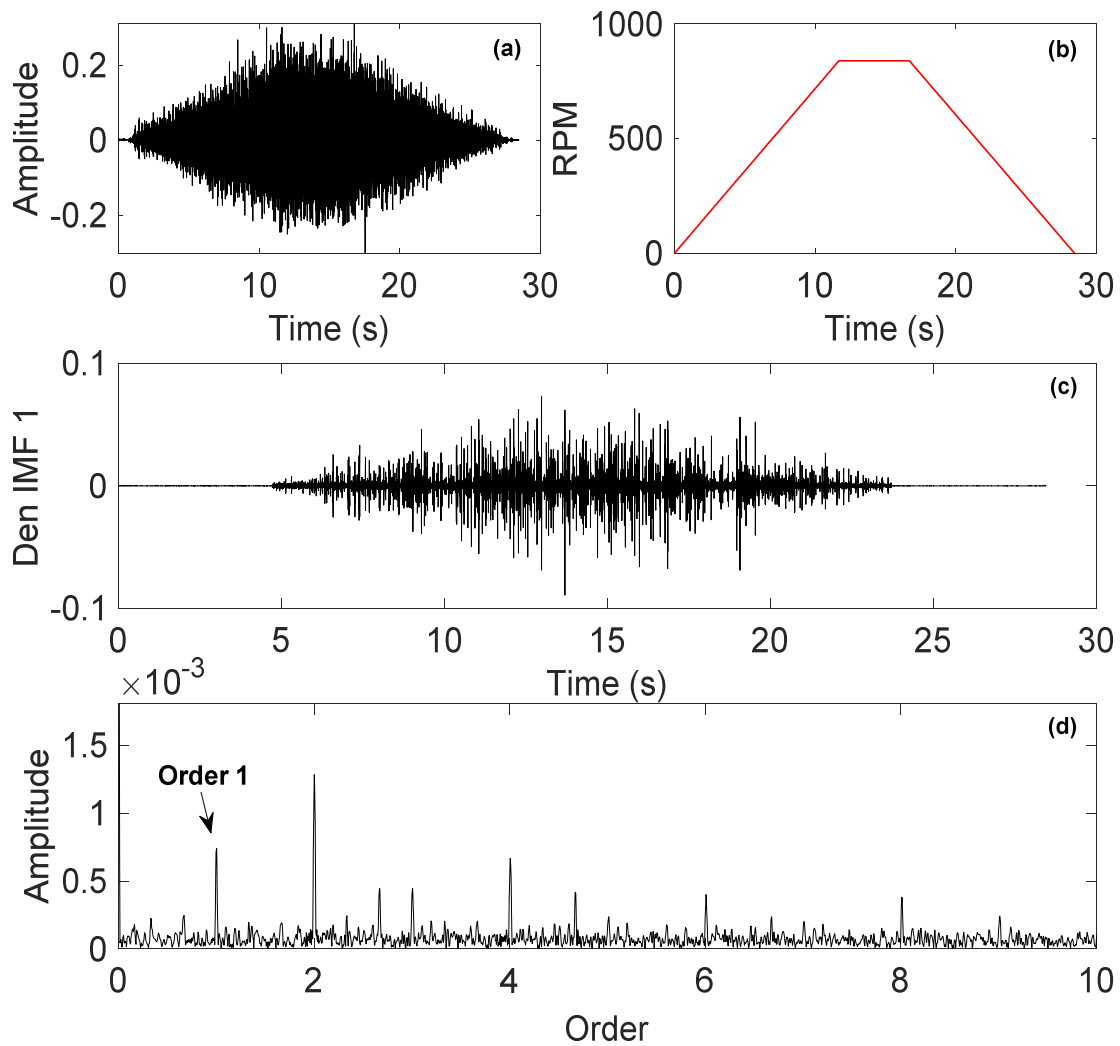


Figure 3.20. (a) Original signal of generalized defect (b) rpm signal (c) Denoised IMF (d) Order envelope spectrum in combined mode.

6.5. Case of half-extracted tooth in combined mode

In this section a half-extracted tooth defect is considered. Figure (3.21.a) represents the measured signal in combined mode as mentioned in the rpm signal of figure (3.21.b). Figure (3.21.c) shows the final order envelope spectrum obtained after the application of the proposed approach; several harmonics of the order defect (order 1) are clearly visible. In addition, sub-harmonics corresponding to almost 1/3 the order 1 are visible. After investigation, these sub-harmonics are due to another defect. Note that this defect was also present in the two previous cases (extracted tooth and generalized defects), however the corresponding sub-harmonics are so weak compared with gear defect. By coincidence, this

result shows that the proposed approach can detect other defects, in addition of gear defect, which is very interesting as perspective in the future.

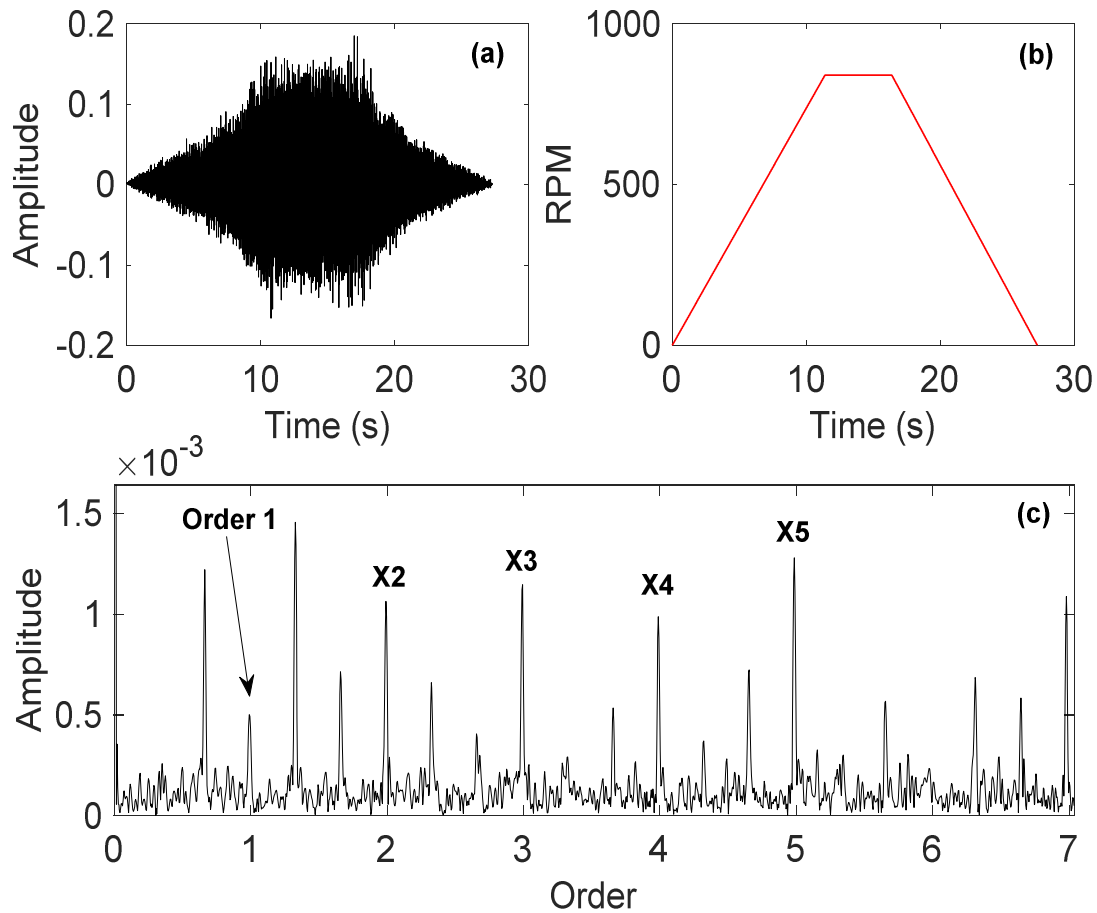


Figure 3.21. (a) Original signal (b) rpm signal (c) order envelope spectrum in the case of half-extracted tooth in combined mode.

6.6. Comments on the obtained results

1. The approach adopted by the proposed method is to isolate the gear defect signature from other machine components. Improved CEEMDAN is then used to decompose the measured signal into several IMFs. In the literature ICEEMDAN was shown to be a more complete decomposition than other methods ie. EMD, EEMD and CEEMDAN. The mode mixing problem and the residual noise are almost completely removed after the decomposition.

2. Gear defect signature is now localized in a specific IMF; it is then essential to look for this IMF and select it as relevant one. As gear defects generate periodical impulsive forces, the best indicator proposed for the selection of the relevant IMF is the kurtosis. For this, the kurtogram plot obtained after the computation of the spectral kurtosis is used. The kurtogram

locates the best frequency band allowing the highest kurtosis values. The IMF covering this optimal frequency band is then selected as relevant one.

3. The results show that the kurtogram is the best way to select the relevant IMF. In this context the IMF covering the meshing frequency range doesn't give such satisfying results. Consequently, the modulations produced from gear defect are not usually located around the meshing frequency and its harmonics, and can excite the system resonances at high frequencies where filtering operation is optimal.

4. The results show that the use of non-appropriate rpm signal in order tracking analysis gave a defect order different from 1, and can lead to false diagnosis. In multiple-stages gearbox it is then necessary to test the order tracking algorithm with rpm signals of all the shafts. The rpm signal allowing an order equal to 1 corresponds to the shaft carrying the defective gear.

7. Conclusion

In this chapter, a hybrid method is proposed for gear defects detection in non-stationary running condition. The proposed approach is based on the Improved CEEMDAN, Multivariate denoising based on Wavelet and Principal Component Analysis, and Order Tracking Analysis. The results show that the proposed approach is proven to be effective with experimental signals measured in variable speed.

The gear defects are very well highlighted for three defect types and in three different speed variation modes. As final result, the defect order is clearly visible on the order envelope spectrum as well as several of its harmonics. Note that this order must be equal to 1 to confirm the presence of the defect and to know the shaft carrying the defective gear, for this we demonstrated that the Order Tracking algorithm must be alimented with the true rpm signal.

The results also demonstrated that the kurtogram is the best tool for the selection of the relevant IMF obtained after the ICEEMDAN decomposition. This step is very important since the gear defect signature is isolated in this relevant IMF, and from which the order envelope spectrum is extracted.

The proposed hybrid approach is very helpful when making decision during the surveillance of gear transmission systems found in almost every rotating machine working under non-stationary condition. This task represented a very hard challenge for engineers.

8. References

1. Djebala A., Ouelaa N., Benchaabane C., Laefer D.F. Application of the wavelet multi-resolution analysis and Hilbert transform for the prediction of gear tooth defects. *Meccanica*. 2012;47(7):1601-12.
2. Ghafari A. M., Cheze N., Poggi J-M. Multivariate denoising using wavelets and principal component analysis. *Computational Statistics & Data Analysis*. 2006;50(9):2381-98.
3. Chaabi L., Lemzadmi A., Djebala A., Bouhalais ML, Ouelaa N. Fault diagnosis of rolling bearings in non-stationary running conditions using improved CEEMDAN and multivariate denoising based on wavelet and principal component analyses. *The International Journal of Advanced Manufacturing Technology*. 2020;107(9):3859-73.
4. Antoni J. Fast computation of the kurtogram for the detection of transient faults. *Mechanical systems and Signal processing*. 2007;21(1):108-24.
5. Ouelaa Z., Younes R., Djebala A., Hamzaoui N., Ouelaa N. Comparative study between objective and subjective methods for identifying the gravity of single and multiple gear defects in case of noisy signals. *Applied Acoustics*. 2022;185:108432.
6. Jing X, Jianmin M, Zhiqiang Z, Chun C. Bearing fault diagnosis based on CEEMDAN and Teager energy operator. *Journal of Physics: Conference Series*; 2019: IOP Publishing.
7. Hu, R.-q., Y.-r. Zhou, et al. (2019). Bearing Fault Diagnosis Based on CEMDAN Energy Weighting Method. 2nd International Conference on Informatics, Control and Automation (ICA 2019), ISBN: 978-1-60595-637-4..
8. Colominas MA, Schlotthauer G, Torres ME. Improved complete ensemble EMD: A suitable tool for biomedical signal processing. *Biomedical Signal Processing and Control*. 2014;14:19-29.
9. Ding F, Li X, Qu J. Fault diagnosis of rolling bearing based on improved CEEMDAN and distance evaluation technique. *Journal of Vibroengineering*. 2017;19(1):260-75.

Chapter four

Application of the perceptive method for the identification of gear fault severities operating under variable conditions

1. Introduction

The use of sound perception in diagnosing faults in rotating machinery is relatively recent. Younes [1] employed this method for detecting faults that result in impacts, such as gears and bearings in a stationary regime. More recently, Laissaoui applied this same technique to a combination of bearing faults and shaft misalignment [2]. Still in a stationary regime, in this thesis's chapter 2, we demonstrated that even in the case of noisy signals, the sound perception method can be highly effective compared to more sophisticated signal processing methods such as , WMRA, Cyclostationarity, and ICEEMDAN for identifying the severity of gear faults [3]. For more details about the perceptive approach and its application for faults detection see references [3-6].

The work carried out in this chapter aims to extend the sound perception method for identifying the severities of gear faults operating under variable conditions, following its successful application in stationary regime. The objective is to utilize the pairwise comparison method and judgments from auditors to identify the severity of gear faults, based on the results of the fault severity evolution indicator DIM1 obtained through the perceptual space. This indicator can also be correlated with the optimal vibration indicators from various measured signals, presented in the form of a mathematical model.

Four vibrational signals corresponding to various gear faults are measured under variable operating conditions on the test bench at Souk-Ahras University. The recording duration for each measurement is quite long, lasting 21 seconds. This duration includes an acceleration phase where the speed varies from 0 to 20 Hz over a period of 6 seconds, followed by a constant speed phase of 20 Hz lasting 12 seconds, and finally, a deceleration phase where the rotational speed decreases from 20 to 0 Hz within 3 seconds. Subsequently, these vibrational signals are converted into four sounds, which will be presented to the listeners for auditory

tests conducted in a semi-anechoic chamber at the Technology Campus of the University of Maine, France. This controlled environment aims to ensure that their judgments are as accurate as possible, isolating them from external environmental influences.

As in chapter 2, the listeners are required to provide assessments of the auditory characteristics for each pair of sounds. The response for each pair of sounds is transformed into numerical values on a scale ranging from 0 to 1, depending on the judgment of the listeners, from very similar to very dissimilar, respectively. Analysis of variance methods is then employed to assess the significance of differences between the mean values for each sound [1-2]. One constraint encountered in the variable regime compared to the stationary regime is the duration of listening for each sound. In the variable regime, the listening duration increases from 4 seconds in the stationary case to 21 seconds. The very lengthy duration of the sound does not allow for a large number of sound combinations in the listening tests. For only 8 sound combinations, the duration of a test exceeds 15 minutes, making it challenging for the listeners to maintain concentration.

2. Experimental study

2.1. Introduction

We will employ the pairwise sound comparison method through the application of the sound perception method to attempt to identify the varying severities of gear faults in variable operating conditions. The simulated faults include simple and severe gear faults, as shown in Table (4.1). After conducting listening tests in the semi-anechoic chamber at LAUM, we will analyze the results and address the question: Can the sound perception method make accurate judgments regarding the different severities of gear faults in variable operating conditions, or not ?

2.2. Vibration measurements

In this experimental setup, we utilized the MFS test bench at the University of Souk Ahras (see figure 4.1) to measure vibrational signals from two variable-speed gearboxes across three phases: acceleration, steady-state, and deceleration. These phases were considered under the following conditions: no faults, half-tooth broken (as shown in figure 3.12.a), broken-tooth (Figure 3.12.b), and generalized wear on the gearbox teeth (Figure 3.12.c). For data

acquisition, we employed a 3D accelerometer (B&K 4524B 33569) and the Pulse 16.1 vibration analyzer software (see figure 4.1).

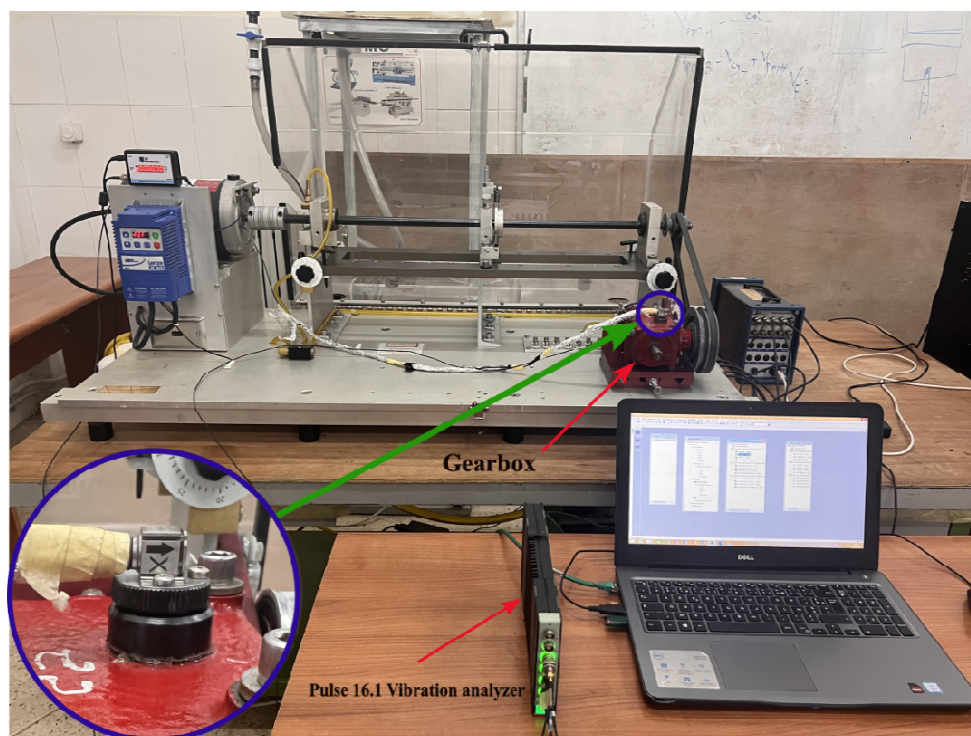


Figure 4.1. 3D accelerometer and the Pulse 16.1 vibration analyzer software.

In table (4.1), we present the designations for four types of gear faults based on a personal judgment of increasing severity. Son1, Son2, and Son4 are derived from the signals measured on the gearbox in figure (4.1), with each corresponding to a different gear configuration after wheel assembly and disassembly. Son1 is associated with the gear assumed to be without faults, although subsequent spectral analysis reveals tooth wear due to frequent use in student practical work. Son2 represents the gear with a half-tooth breakage fault, while Son4 corresponds to the gear with a full-tooth breakage fault. For Son3, we replaced the gearbox from figure (3.11) with the one shown in figure (4.1), which exhibits generalized tooth wear (The red one). While we do not possess precise information on the extent of this wear, the latter gearbox is rarely used in student practical work.

Son1	Healthy Gear	HG
Son2	Half-tooth broken	HTB
Son3	Generalized defect	GD
Son4	Broken tooth	BT

Table 4.1. Various gear defects.

2.3. Structure of the Listening System

The dissimilarity evaluation tests were conducted in the semi-anechoic chamber at the Technology Campus of the University of Maine, France. Sound playback and listening were carried out using a Matlab interface and 'AKG K52' stereo headphones, as shown in figure (4.2).

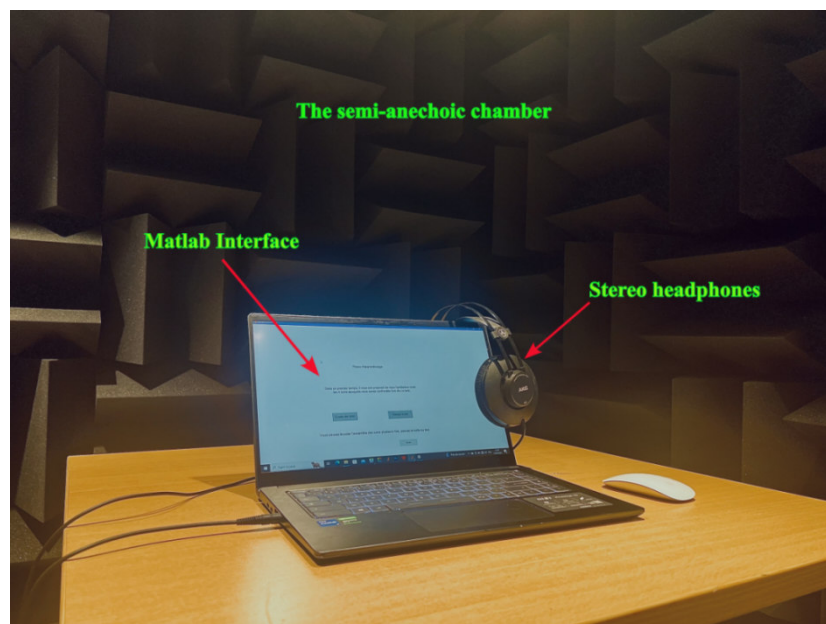


Figure 4.2. Sound listening tests in a semi-anechoic chamber.

2.4. Interface and test subjects

The listening tests interface is developed within the MATLAB environment and consists of two phases: the first phase, known as the learning phase, involves presenting sounds to the participants to help them become familiar with the test sounds. The second phase is a pairwise comparison phase in which participants assess the dissimilarity between sounds. A total of twenty-eight (28) participants took part in the listening tests, comprising 10 females and 18 males, aged between 21 and 45 years. At the beginning of the test, participants are provided with context by explaining how the interface works, with each step of the test detailed for their understanding, as illustrated in the example interface shown in (figure 4.3). Subsequently, using the Rose series, the four sounds generate 8 combinations of sound pairs, which are presented to participants in a random manner, with each test lasting approximately 15 minutes.

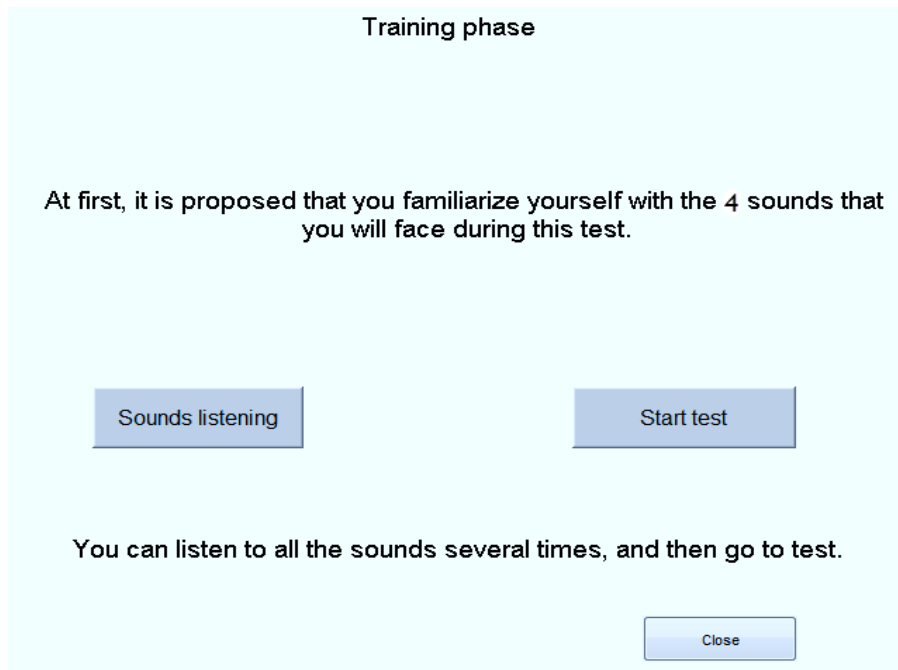


Figure 4.3. Learning phase interface.

3. Results and discussions

In figure (4.4), the scatter plot between measured and reconstructed similarities is presented. A strong correlation coefficient of $R=0.98$ is obtained.

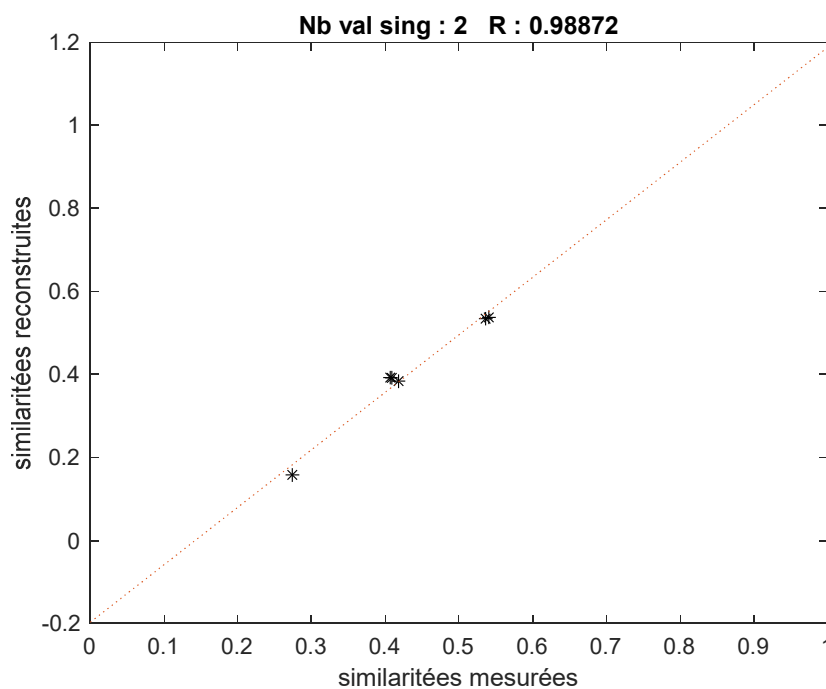


Figure 4.4. Scatter plot between measured and reconstructed similarities.

3.1. Analysis of results obtained by the perceptual method in variable operating conditions

Despite that the machine is operating in variable conditions and the noise generated by the movement transmission belts towards the speed gearbox, the results of the perception tests allowed classifying the sounds in ascending order of degradation.

The naming of the sounds from S1 to S4 for the four sounds corresponding to different gear fault configurations presented in table (4.1) is based on personal judgment, where it was assumed that generalized wear corresponds to a more severe fault condition than the fault corresponding to the loss of half a tooth. However, the analysis of the proximity space of the four sounds presented in figure (4.5) shows the opposite. The generalized wear of the gears teeth (S3) in the gearbox in figure (4.2.c) was judged by the listeners to be a less severe fault condition than the loss of half a tooth (S2) in the gearbox in figure (3.11).

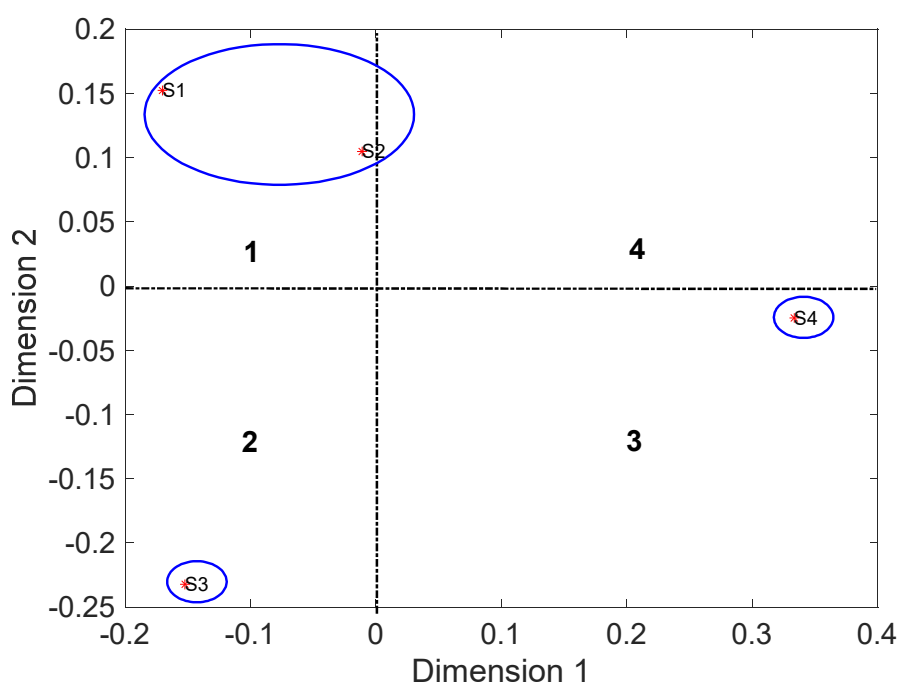


Figure 4.5. Proximity space.

So, according to dimension 1 (DIM1), which represents the evolution of fault severity [3-8], it is observed that the listeners ranked the severities of the defects in the following order: Wheel without defect, generalized wear of the wheel, half-tooth broken, and finally, a full tooth broken. The ranking provided by DIM1 is validated by three classical scalar indicators: Kurtosis (K), Peak-to-Peak Value (PP), and Shape Factor (SF), as shown in table (4.2) below. Another validation of the results will be presented at the end of this chapter, based on the

processing of signals taken from the stationary zone of signals measured under variable conditions, using the ICEEMDAN method, as discussed in chapters 2 and 3.

Sons	DIM1	K	PP	SF	DIM2	CF	IF	MF
S1	-0.170	8.1396	1.6413	1.5445	0.152	5.2600	8.1239	102.9071
S2	-0.011	11.1373	1.8554	1.6611	0.105	8.4080	13.9669	228.0402
S3	-0.152	8.6273	1.8238	1.5743	-0.232	11.0781	17.4400	304.1626
S4	0.334	73.8888	1.9146	2.1089	-0.025	18.8547	39.7633	1728.740

Table 4.2. The various computed indicators for the four sounds, arranged in the order of personal pre-judgment.

In table (4.3), we present the coordinates of the sounds obtained in a two-dimensional space (DIM1 and DIM2). The variable regime's result obtained for dimension DIM1 is in complete agreement with the results of our previous work obtained for the stationary regime. In our earlier work, we observed that the transition of DIM1 values from negative to positive corresponds to the transition from a moderate defect to a severe defect, aiding in the decision to replace the gear.

Sons	DIM1	K	PP	SF	DIM2	CF	IF	MF
S1	-0.170	8.1396	1.6413	1.5445	0.152	5.2600	8.1239	102.9071
S3	-0.152	8.6273	1.8238	1.5743	-0.232	11.0781	17.4400	304.1626
S2	-0.011	11.1373	1.8554	1.6611	0.105	8.4080	13.9669	228.0402
S4	0.334	73.8888	1.9146	2.1089	-0.025	18.8547	39.7633	1728.740

Table 4.3. The various computed indicators for the four sounds, arranged according to the judgments of the listeners (DIM1).

Based on the literature we have reviewed and our previous work, no exact physical interpretation has been given for dimension 2 (DIM2). The results obtained in this study have allowed us to realize that DIM2 actually represents the differences in judgments among the listeners between different sounds (identical, A little different, different, and very different), as shown in figures (4.6) and (4.7). To confirm this analysis, we can observe that the listeners judged S1 and S2 as identical (similar) sounds since they belong to the same gearbox.

However, they classified S1 and S3 as slightly different sounds since they belong to two different gearboxes, despite the fact that the severity of the defect in S3, according to DIM1, is considered lower than that of S2. Based on these results, we can conclude that the physical interpretation of DIM2 expresses the differences in judgments among the sounds generated by the defects.

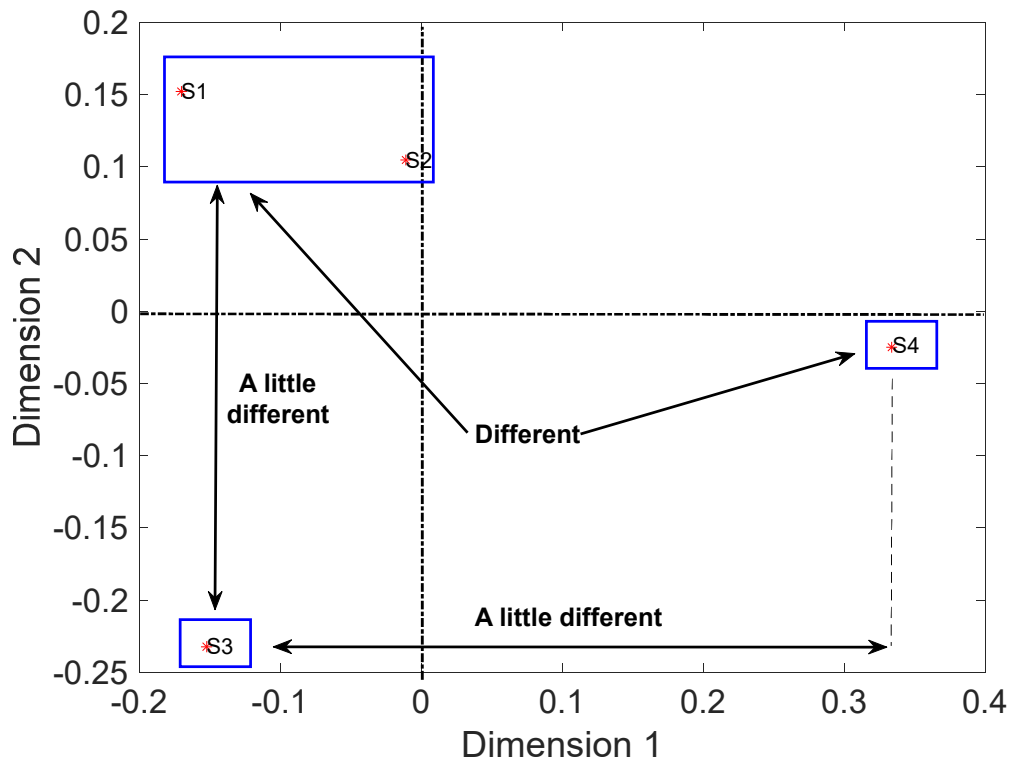


Figure 4.6. Explanation of the proximity space.

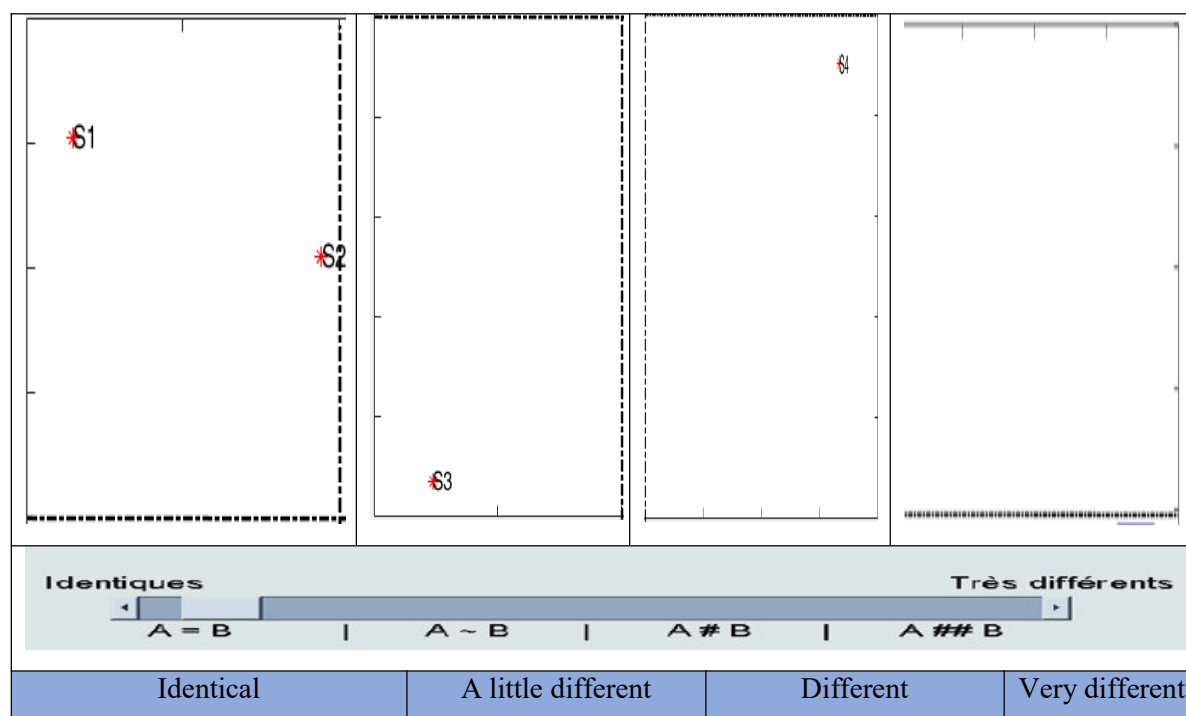


Figure 4.7. New representation of DIM2.

3.2. Scalar indicators analysis

The goal is to find a mathematical correlation between the results of sound perception and these indicators. Based on the values of the scalar indicators in table (4.3), we can observe that the Kurtosis (K), Peak to Peak (PP), and Shape Factor (SF) indicators vary in an increasing manner in good agreement with DIM1, while the Crest Factor (CF), Impulse Factor (IF), Magnetic Factor (MF), Root Mean Square (RMS), and Energy (E) indicators vary in an alternating manner in accordance with DIM2.

3.3. Correlations between scalar indicators and the two dimensions

The search for correlations between the scalar indicators computed from the vibratory signals measured under variable conditions and the two dimensions, DIM1 and DIM2, in the proximity space of figure (4.5) aims to establish mathematical models for machine monitoring. To achieve this, we perform an ascending linear regression, using the vibratory indicators as input and mathematical models with one or two scalar indicators as output. The dimension chosen will be the one that exhibits the highest similarity score, indicating a better alignment of data points on the regression line.

According to figure (4.8), the two physical parameters that best characterize DIM1 are the Shape Factor (SF) and the Margin Factor (MF), with a linear combination yielding a correlation factor $R^2= 0.999$ ($p < 0.001$).

$$\text{Dim1} = 1.4341 \times \text{SF} - 0.00019754 \times \text{MF} - 2.3498 \quad (4.1)$$

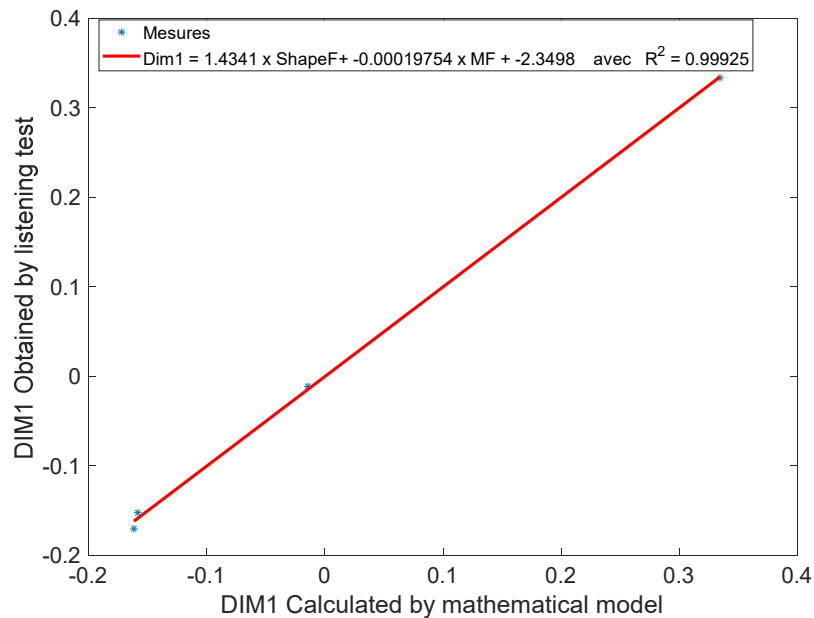


Figure 4.8. Scatterplot between DIM1 and vibratory indicators.

$$\text{Dim2} = -0.074374 \times \text{CF} + 1.4561 \times \text{ShapeF} - 1.6938 \quad (4.2)$$

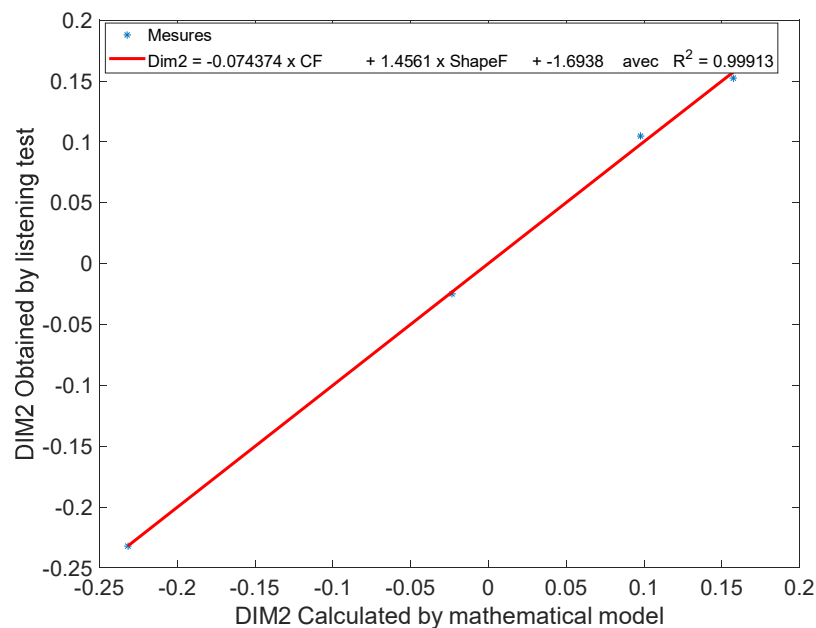


Figure 4.9. Scatter plot between DIM2 and vibration indicators.

According to figure (4.9), the two physical parameters that best characterize DIM2 are the Crest Factor (CF) and the Shape Factor (SF), with a linear combination yielding a correlation factor of $R^2= 0.999$ ($p < 0.001$).

4. Verification of DIM1 and DIM2 mathematical models

In the proximity space of figure (4.10), we present the coordinates of the four sounds based on DIM1 and DIM2, calculated by the two mathematical models (M_i) provided by expressions (4.1) and (4.2), as well as those obtained experimentally through perception tests (S_i). We observe a very good agreement between the two sets of results, indicating the usability of these mathematical models for machine monitoring.

Figure (4.11) displays the DIM1 values of the four sounds calculated by the two mathematical models and those obtained through perception. The results align well, confirming and validating the findings from chapter 2 and other studies conducted in our laboratory [3-8]. In the stationary regime, the transition of DIM1 values from negative to positive corresponds to a shift from moderate to severe defects, such as a fractured tooth in our case. This aids in the decision-making process regarding gear replacement.

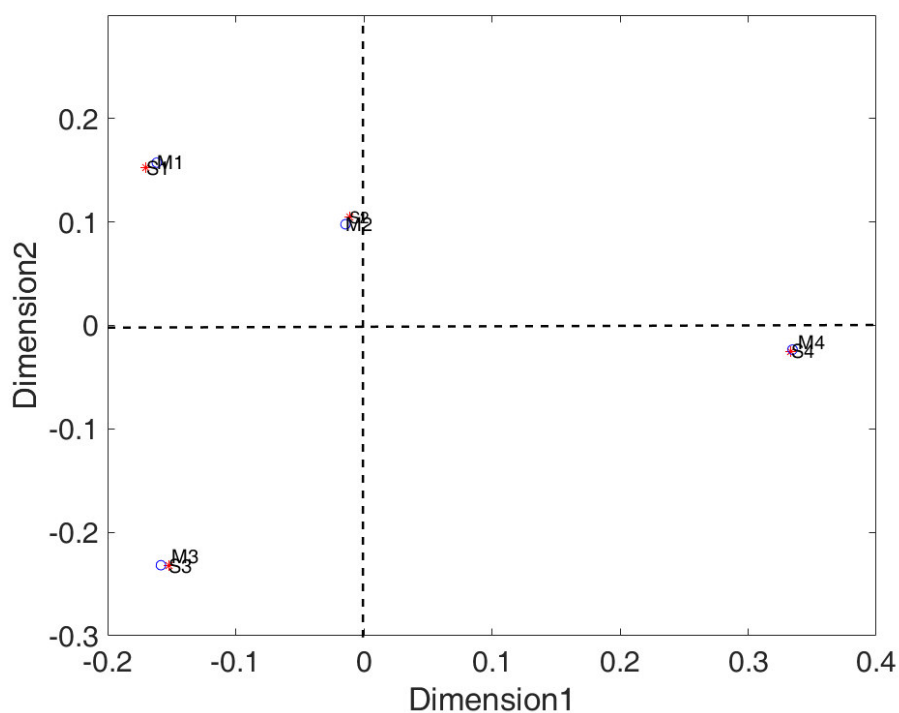


Figure 4.10. Sounds classified by the listeners (S_i) and those calculated by the mathematical models (M_i).

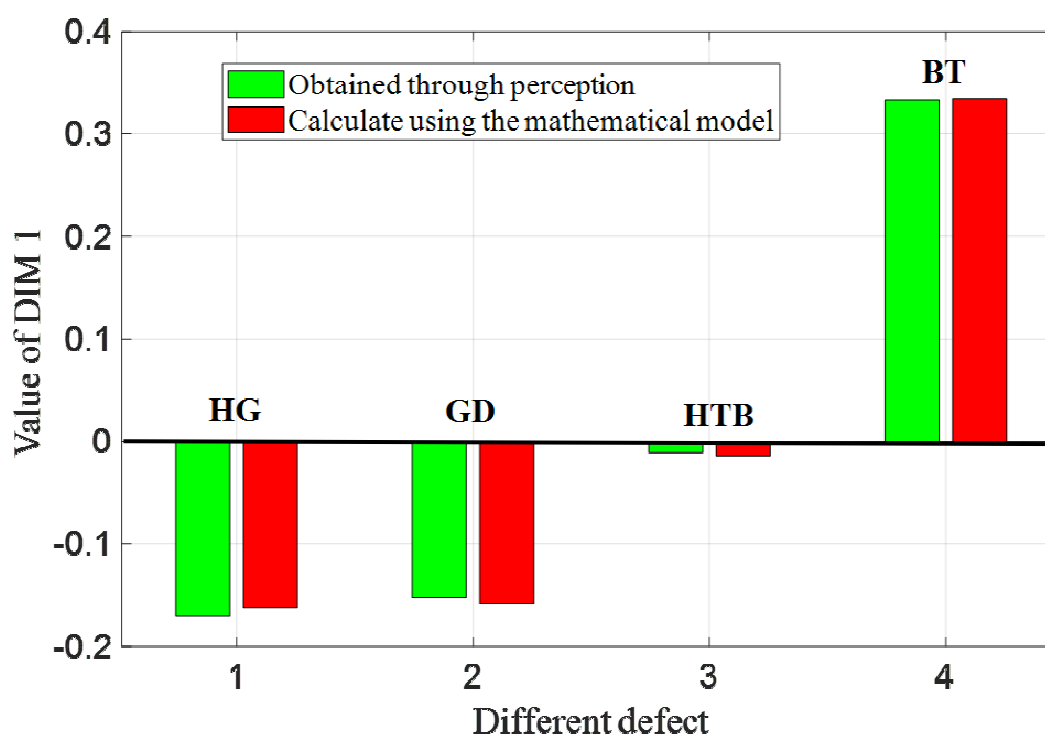


Figure 4.11. Values of DIM1 for the 4 sounds.

5. Faults diagnosis using ICEEMDAN

5.1. Introduction

In order to validate the severity assessments of gear defects based on auditory perception for signals measured under variable operating conditions, we will extract a portion of the stationary zone (constant speed) from each of the four previously processed signals and subject them to ICEEMDAN analysis.

5.2. Signal processing for the healthy state

Based on the spectrum in figure 4.12, the appearance of the meshing frequency $F_m = 138.62$ Hz and its harmonics $2F_m$, $3F_m$, and $4F_m$ is observed. According to the typical spectra of faults, the decrease in amplitudes of the harmonics of the meshing frequency without any modulation corresponding to the rotation frequencies of the input and output shafts indicates that the gear is in good condition. However, on zooms 1 and 2, the appearance of a comb of peaks corresponding to one-third of the rotation frequency of the input shaft of the gearbox

(F_{r_2}) is noticed, with sub-harmonics of the rotation frequency corresponding to the presence of friction or impacts in the rolling bearing of the input shaft of the gearbox ($F_f = F_{r_2}/3 = 2.56$ Hz). After checking the implicated bearing of the gearbox, it was found that there was indeed excessive play between the outer ring of the bearing and the bore of the gearbox. This play is mainly due to the uncontrolled force applied by the belt tensioner on the one hand, and on the other hand, due to the repeated assembly and disassembly of the input shaft of the gearbox each time the type of fault is changed. Initially, we thought of a fault in the belt that transmits the movement from the drive shaft (F_{r_1}) to the input shaft of the gearbox (F_{r_2}), calculated by expression (4.3), $F_b = 3$ Hz, very close to the friction frequency (F_f). These amplitudes are low compared to the amplitude of the meshing frequency and its harmonics. The amplitude of the second harmonic of the impact frequency $2F_f$ is much higher than its fundamental amplitude, indicating the presence of excessive play in the bearing. During perception tests, the noise generated by the presence of impacts in the bearing and that generated by the passage of the belt caused a lot of discomfort for the auditors.

Its characteristic frequency is given by:

$$F_b = \frac{\pi \cdot d_1}{L} \cdot f_{r_1} = \frac{\pi \cdot d_2}{L} \cdot f_{r_2} \quad (4.3)$$

When the details are mentioned in table (4.4)

d_1	F_{r_1}	d_2	F_{r_2}	L	F_b	F_{r_3}	$F_f = F_{r_2}/3$
51 mm	19.5 Hz	126.2 mm	7.63 Hz	970 mm	3 Hz	5.11	2.56

Table 4.4. Belts and friction defects characteristic.

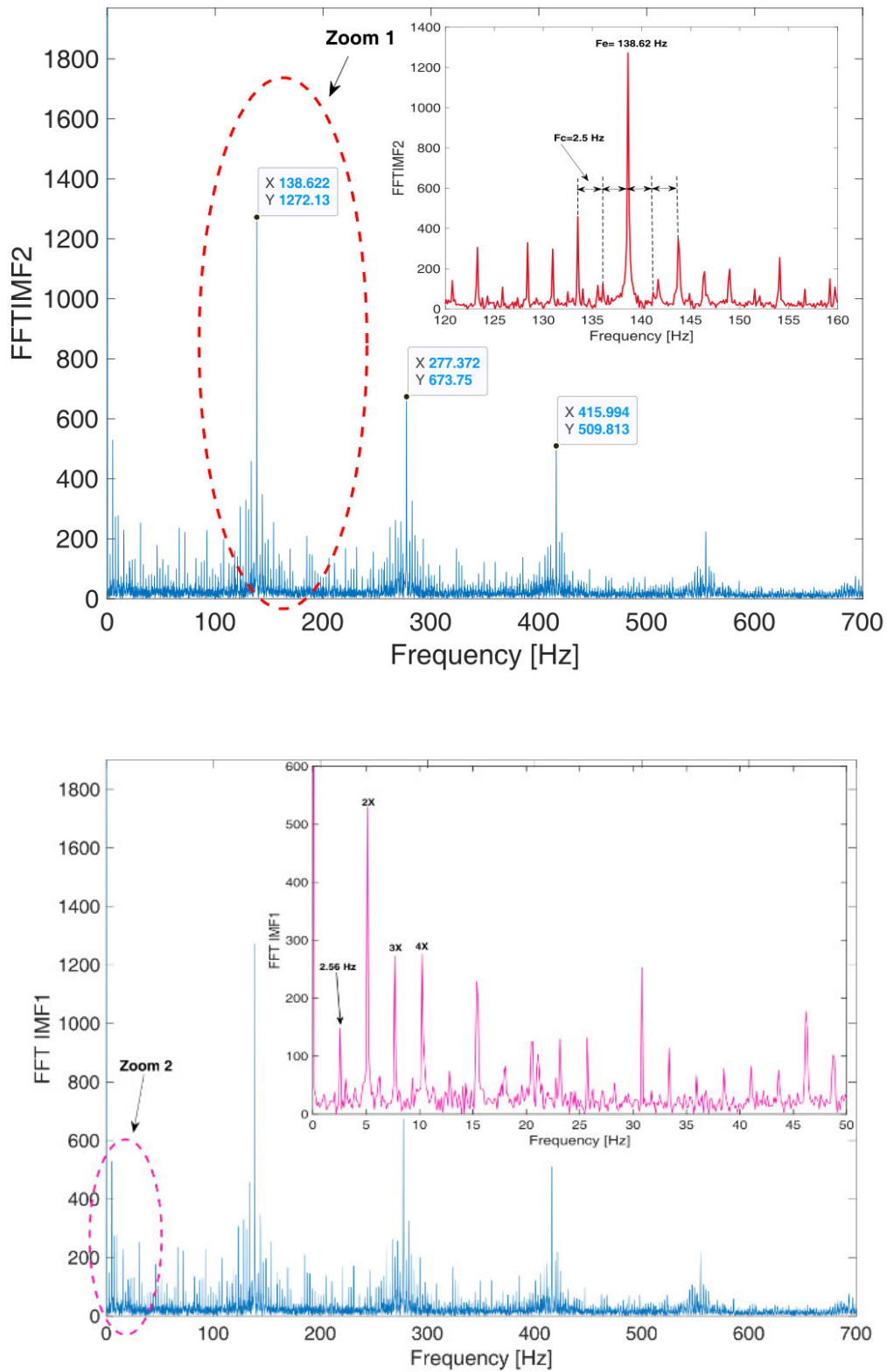
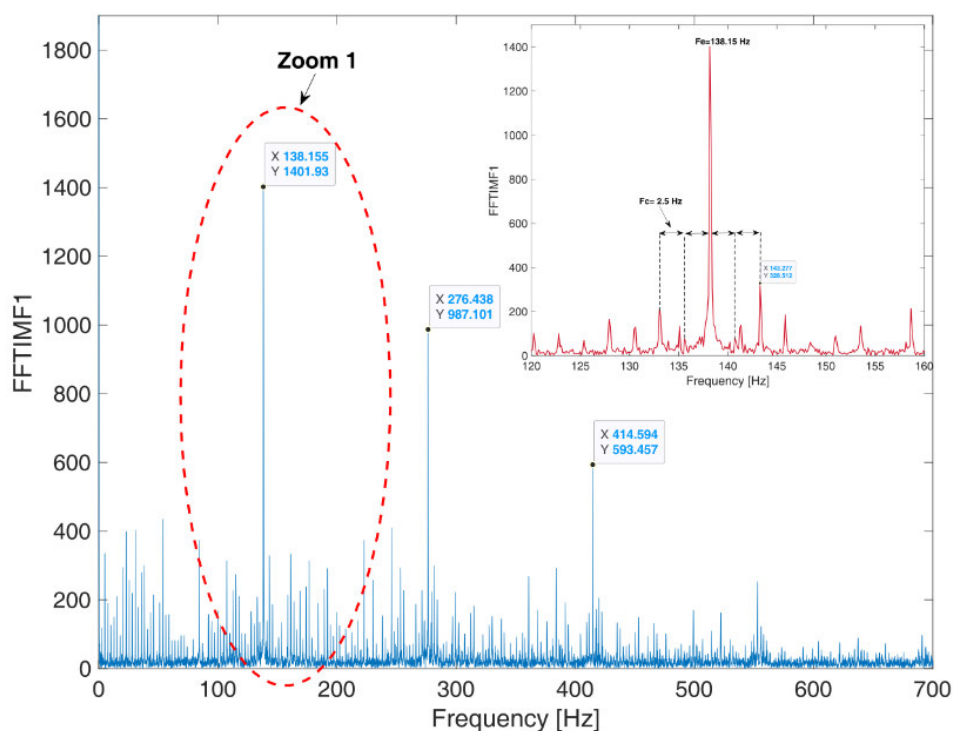


Figure 4.12. Spectrum of a healthy gear measured in the band [0-6400] Hz.

5.3. Signal Processing for half-tooth spalling defect

In figure (4.13), we present the spectrum corresponding to the transverse spalling of a half-tooth. The same observations raised previously are applicable in this case, but with a significant increase in the amplitude of the meshing frequency (a 10% increase compared to the defect-free case) and, more notably, its first harmonic, $2F_e$ (a 46% increase compared to the defect-free case). This increase is attributed to the elevated contact pressure on the half-tooth during engagement. This increase causes a decrease in the amplitudes of the impact frequency and its harmonics (a 36% decrease in the amplitude of $2F_f$). In the case of transverse tearing of half a tooth, the operation of the gear is almost normal, with no play between the teeth during operation. The presence of the gear fault can be distinguished only by comparing the amplitudes of the meshing frequency and its harmonics with the case without faults for the same load and operating conditions.



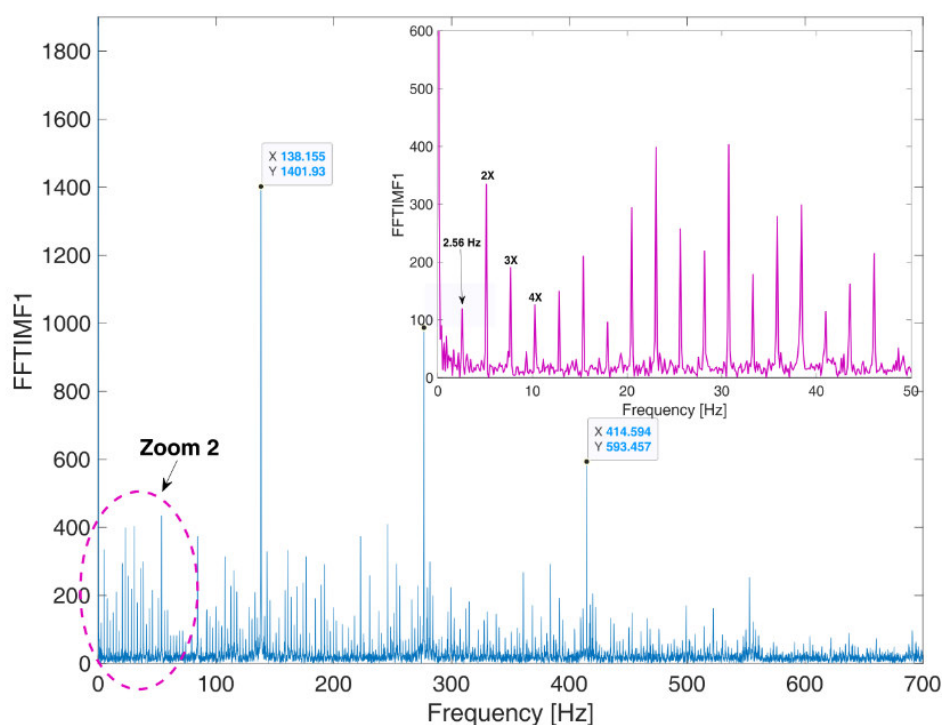


Figure 4.13. Spectrum of a half-tooth spalling defect measured in the band [0-6400] Hz.

5.4. Signal processing for generalized wear defect

In figure (4.14), we present the gear spectrum exhibiting generalized wear. Generalized wear of the tooth profile results in a periodic dull impact at the meshing frequency, generating a comb of decreasing amplitude lines. We observe modulation of the meshing frequency and its harmonics by the rotation frequency of the output shaft of the gearbox, $Fr_2 = 5$ Hz. In this case, the wear is present on the wheel mounted on the output shaft. Zoom 1 shows an asymmetric image of modulations around the meshing frequency, characteristic of degraded meshing. The belt defect is completely masked by the gear defect. Zoom 2, covering the lower frequencies, also reveals that the spectrum is rich in rotation frequency Fr_2 . In the case of generalized wear, the amplitudes of the meshing frequency and its harmonics are significantly lower than those of the half-tooth spalling defect. Therefore, it can be concluded that the generalized wear defect is less severe than the half-tooth spalling defect, confirming the judgments of the auditors obtained through auditory perception under variable operating conditions.

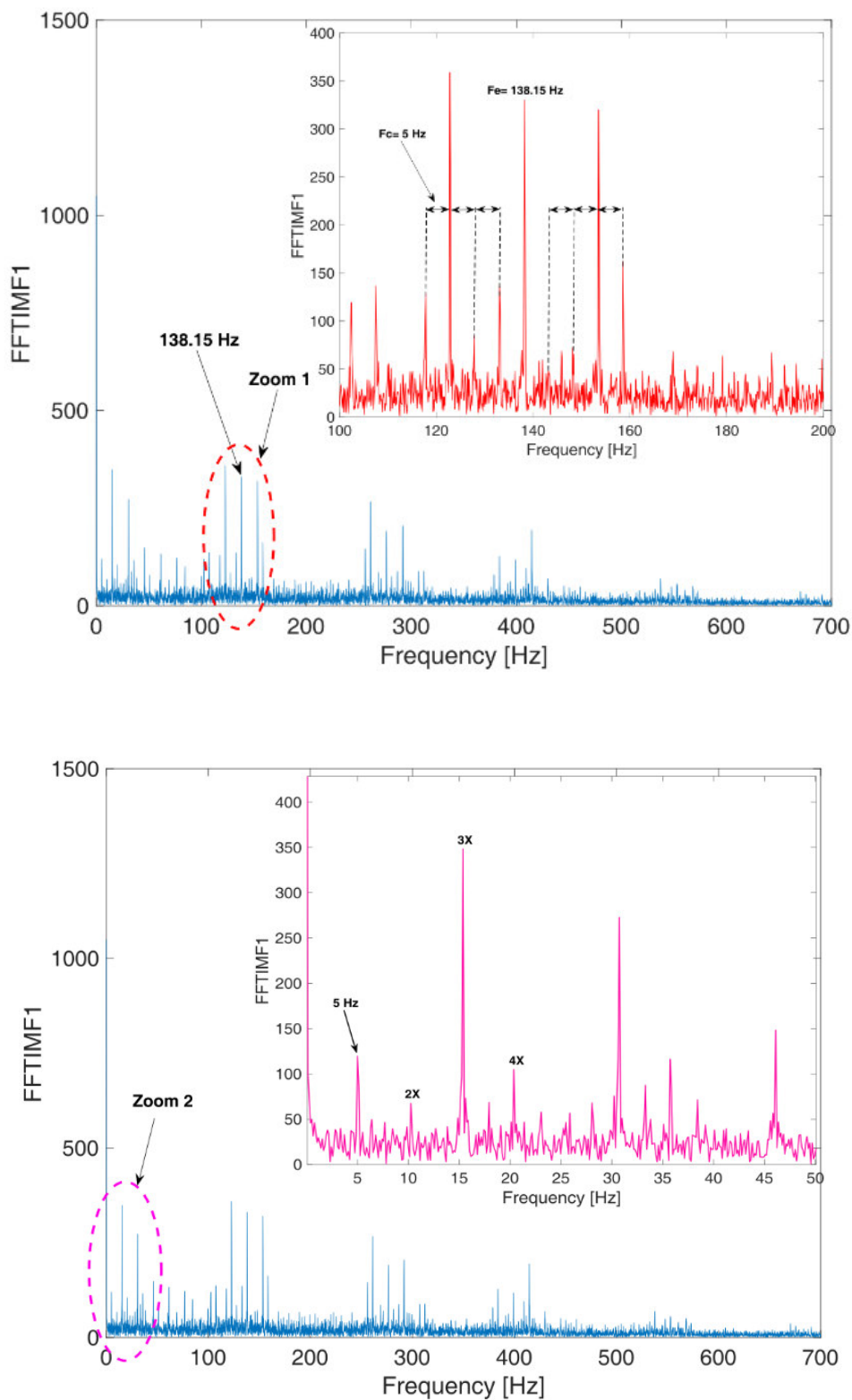


Figure 4.14. Spectrum of gear showing generalized wear measured in the band [0-6400] Hz.

5.5. Signal processing for a broken tooth defect

The spectrum of figure (4.15) is plentiful in harmonics of the input shaft rotation frequency, $Fr1 = 7.63$ Hz, of the gearbox containing a wheel with a completely broken tooth. The amplitudes of the comb of lines corresponding to the rotation frequency are significantly higher than the amplitude of the meshing frequency and its harmonics. Therefore, the defect is considered significant, as illustrated in the zoomed-in spectrum. Once again, The presence of the impact fault in the gearbox bearing is completely masked by the gear fault.

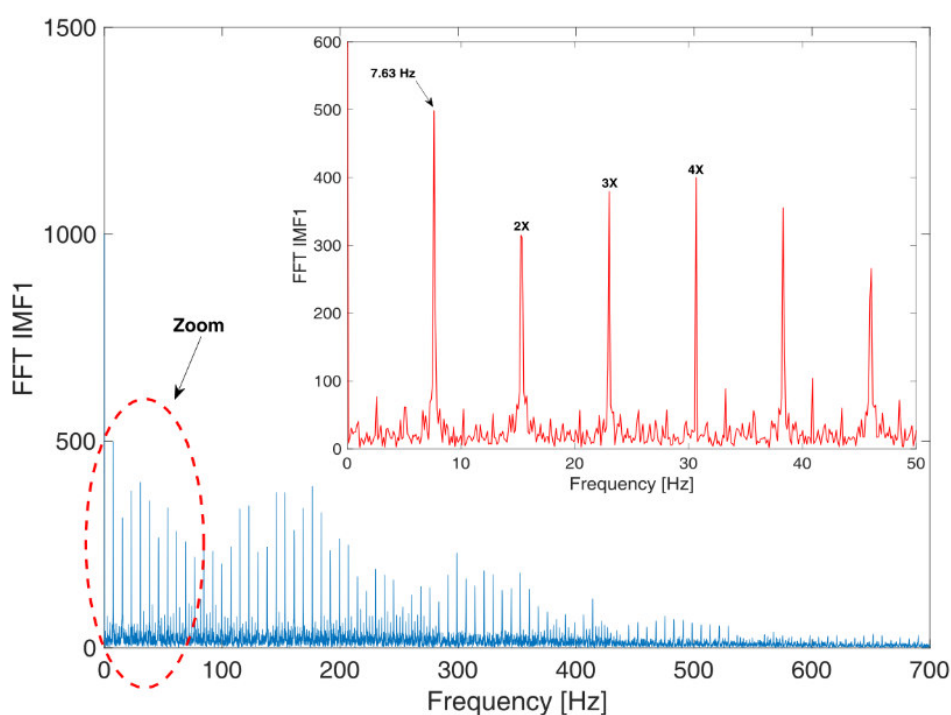


Figure 4.15. Spectrum of a gear with a completely broken tooth measured in the band [0-6400] Hz.

6. Conclusion

The results of the listening tests conducted in the semi-anechoic chamber at LAUM using signals measured under variable operating conditions, reveal the following points:

- Despite the noise generated by the passage of the two transmission belts, which hindered the listeners from focusing on the sound content, and despite the variable operation of the machine, the perceptual tests performed by the listeners successfully classified the defects according to their severity. This classification ranged from the least degraded

condition, S1 (wheel presumed to be defect-free), to the most degraded condition, S4, corresponding to the complete loss of a tooth.

- The results obtained in this study have allowed us to observe that the physical interpretation of DIM2 is to express the differences in judgments between the sounds generated by the defects (identical, slightly different, different, and very different). Listeners judged S1 and S2 as similar sounds (close) since they belong to the same gearbox, whereas they classified S1 and S3 as slightly different sounds since they belong to two different gearboxes, despite the fact that the severity of the defect in S3, as judged from the values of DIM1, is considered to be lower than that of S2.
- The mathematical models for DIM1 and DIM2 have shown a strong correlation between the vibrational scalar indicators and the results of auditory perception, with a correlation coefficient of $R^2 = 0.99$. These models can be used as diagnostic tools and decision support for assessing the evolution of the defect's degradation under variable operating conditions.
- The results of the spectral analysis using ICEEMDAN in steady-state conditions confirm the findings obtained through the auditory perception method under variable operating conditions.

7. References

1. Younes R. Perception sonore au service de l'optimisation du diagnostic des défauts mécaniques de machines tournantes 2015, Doctoral thesis ,University of Guelma.
2. Laissaoui A., Bouzouane B., Miloudi A, Hamzaoui N. Perceptive analysis of bearing defects (Contribution to vibration monitoring). *Applied Acoustics*. 2018;140:248-55.
3. Younes R., Hamzaoui N., Ouelaa N., Djebala A. Perceptual study of the evolution of gear defects. *Applied Acoustics*. 2015;99:60-7.
4. Younes R., Ouelaa N., Hamzaoui N., Djebala A. Perceptual study of simple and combined gear defects. *Applied Mechanics, Behavior of Materials, and Engineering Systems: Selected contributions to the 5th Algerian Congress of Mechanics, CAM2015, El-Oued, Algeria, October 25–29; 2017: Springer.*
5. Ouelaa Z., Younes R., Djebala A., Hamzaoui N., Ouelaa N. Comparative study between objective and subjective methods for identifying the gravity of single and multiple gear defects in case of noisy signals. *Applied Acoustics*. 2022;185:108432.
6. Hamzaoui N., Younes R., Ouelaa N. Indicators of real gear transmission defects using sound perception. *Congress and Conference Proceedings; 2015: Institute of Noise Control Engineering.*
7. Younes R., Ouelaa N., Hamzaoui N., Djebala A. Experimental study of real gear transmission defects using sound perception. *The International Journal of Advanced Manufacturing Technology*. 2015;76:927-40.
8. Younes R., Ouelaa N., Hamzaoui N., Djebala A. Experimental study of combined gear and bearing faults by sound perception. *Advances in Acoustics and Vibration: Proceedings of the International Conference on Acoustics and Vibration (ICAV2016), March 21-23, Hammamet, Tunisia; 2017: Springer.*

Chapter five

General conclusion

This thesis aims to make a significant contribution in the field of fault detection in rotating machinery, with a primary focus on gears. Throughout the different chapters, we have explored various objective and subjective approaches to enhance the reliability of fault detection, even under variable and noisy operating conditions.

The effectiveness of the sound perception method in classifying gear faults based on their severity has been demonstrated. The correlation between this auditory perception and scalar indicators derived from vibration signals has been established. For highly noisy signals, the subjective approach proves to be more effective in assessing the severity of gear faults compared to objective methods, thanks to the heightened sensitivity of the human ear in detecting and evaluating faults. It even surpasses the most advanced objective signal processing techniques, which have limitations in the case of highly noisy signals.

For the objective approach, an innovative hybrid method, combining Improved CEEMDAN (Complete Ensemble Empirical Mode Decomposition with Adaptive Noise), wavelet denoising, and order tracking analysis for gear fault detection under non-stationary conditions. The results showcased the effectiveness of this approach in detecting gear faults, providing a promising alternative to traditional methods. This novel approach not only demonstrated its ability to identify gear faults in challenging operational conditions but also underscored its potential to enhance the field of machinery fault detection and diagnosis.

The results of the listening tests reaffirmed the auditory perception's ability to classify gear faults based on their severity, even in the presence of noise and speed variations. Furthermore, mathematical models were developed to correlate the auditory perception results with objective measurements, thereby providing valuable diagnostic tools for assessing the fault progression. These findings not only validated the subjective auditory approach but also established a bridge between human perception and quantitative data, enabling more accurate and comprehensive fault assessment in gear systems.

Overall, this thesis opens exciting new prospects for the industry in terms of predictive maintenance and machine reliability. The advancements made here have the potential to significantly reduce unplanned downtime, optimize maintenance operations, and lower costs for businesses. This research represents a crucial step towards the path of continuous improvement in monitoring and maintaining mechanical systems, highlighting the importance of combining both objective and subjective approaches and fully leveraging the strengths of each for more effective fault detection in complex and dynamic environments.